

U.S. DEPARTMENT OF THE INTERIOR
U.S. GEOLOGICAL SURVEY

Proterozoic Geology of the Western and
Southeastern Needle Mountains, Colorado

Field Trip Guidebook

by

David A. Gonzales¹, Clay M. Conway¹, Jack A. Ellingson², and John A. Campbell²

Open-File Report 94-437

This report is preliminary and has not been reviewed for conformity with U.S. Geological Survey editorial standards or with the North American Stratigraphic Code. Any use of trade, product, or firm names is for descriptive purposes only and does not imply endorsement by the U.S. Government.

¹ United States Geological Survey
2255 N. Gemini Drive
Flagstaff, AZ 86001

² Fort Lewis College
Department of Geology
Durango, CO 81301

CONTENTS

	Page
Field Trip Road Log - Day 1.....	2
Field Trip Road Log - Day 2.....	17
The Needle Mountains Proterozoic Complex: A Summary by David A. Gonzales and Clay M. Conway.....	31
Are There Other Precambrian Conglomerates in the San Juan Mountains? by John A. Campbell	51
APPENDIX I - U-Pb Isotopic Data for Samples of Proterozoic Rocks in the Needle Mountains	55
APPENDIX II - Sm-Nd Isotopic Data for Samples of the Electra Lake Gabbro	69
References Cited	73
PLATE 1 - Geologic Map of the Electra Lake Area, Western Needle Mountains, Colorado	
PLATE 2 - Geologic Map of the Vallecito Creek-Lake Creek area, LaPlata and Hinsdale Counties, Colorado	

Field Trip Road Log

Day 1

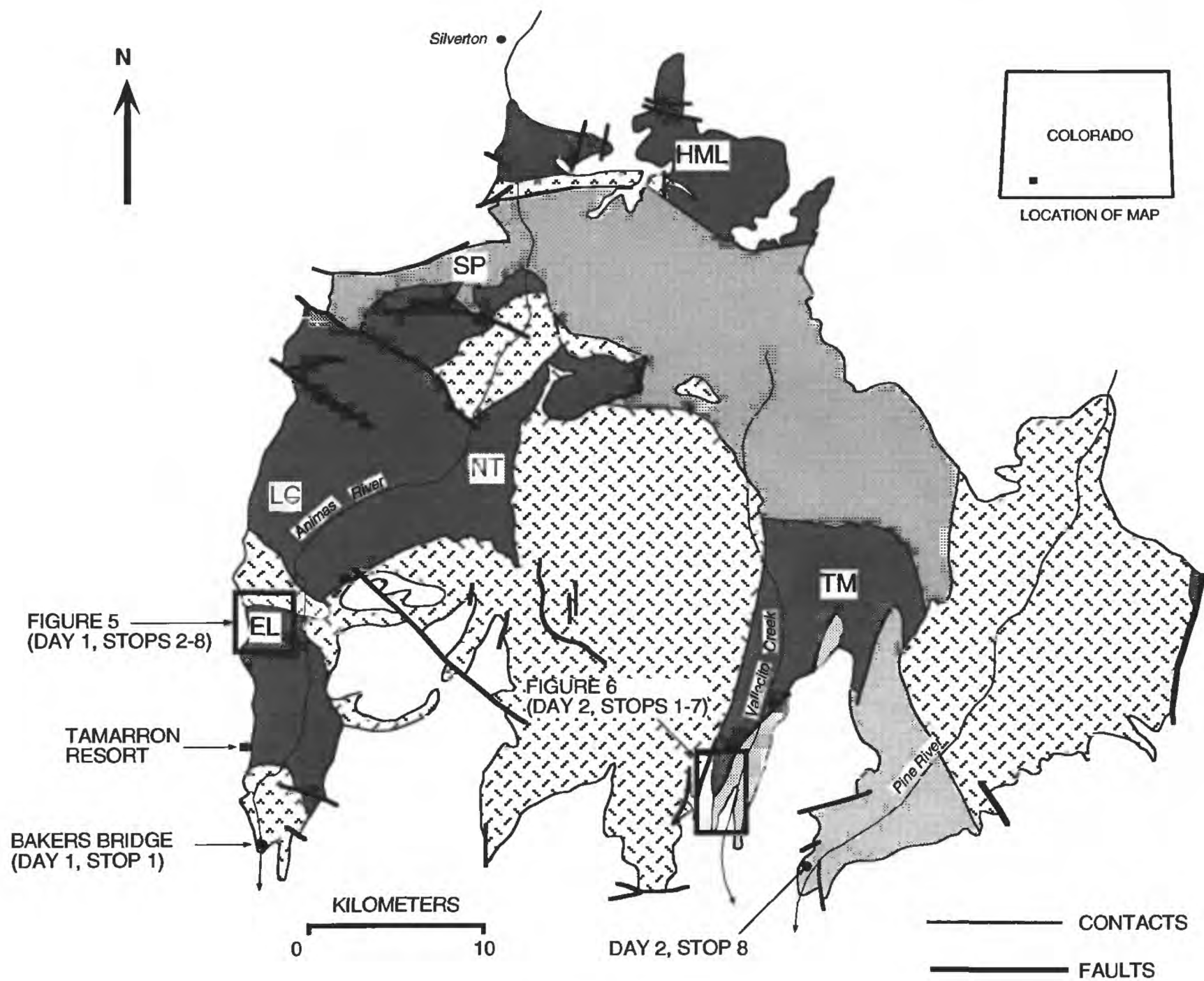
Western Needle Mountains

INTRODUCTION (FIRST DAY)

This two day field trip presents both new and previous interpretations regarding the nature and timing of Proterozoic events in the Needle Mountains Precambrian complex. These rocks were the subject of reconnaissance and detailed studies at the turn of the century and again in the late 60's and early 70's. More detailed field studies and analytical work over the past 10 years have given further insight into the history of Precambrian rocks in southwestern Colorado. This contemporary work has also raised new questions, and some of the ideas and hypotheses brought forth in these studies contradict earlier conclusions. There are still some important questions regarding the history of the Needle Mountains complex that remain unanswered. The relationships and features of several of the Proterozoic units will be examined at various stops in the western and southeastern Needle Mountains, and some new geochronologic and geochemical data that relate to these rocks will be introduced.

The first day of the trip will focus on the Early and Middle Proterozoic rocks exposed in the area between Bakers Bridge and Electra Lake in the western Needle Mountains (Figure 1). Discussions will concentrate on new and previous interpretations that: 1) the 1805-1790 Ma Irving Formation is a volcanic arc assemblage that was intruded by 1770-1755 Ma trondhjemitic-tonalitic plutons of the Twilight Gneiss; 2) both the Irving Formation and Twilight Gneiss were intruded by swarms of gabbroic sills and dikes during extension prior to multi-phase compressional deformation and amphibolite facies metamorphism; 3) syn- and post-deformational granitoids cut the Irving and Twilight rocks between 1735-1695 Ma; and 4) emplacement of the ~1435 Ma Electra Lake Gabbro was accompanied by deformation and partial melting of surrounding Precambrian crystalline rocks.

Cumulative Mileage	Interval Mileage	
0.0		Road log begins at the entrance to Tamarron Resort (Figures 1-2) and continues south on U.S. Highway 550. Road cut directly west of the entrance exposes beds of the Mississippian Leadville Limestone (Figures 3-4).
0.8	0.8	The highway is constructed on a bench of the Leadville Limestone that forms part of the south-dipping limb of the Laramide San Juan dome.
1.9	1.1	Outcrops of the Leadville Limestone to the west (right).



EXPLANATION



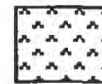

-  1440-1350 Ma GRANITIC TO GABBROIC PLUTONIC ROCKS
-  FLUVIAL AND MARINE SILICICLASTIC SEDIMENTARY ROCKS
(MULTIPLY DEFORMED & METAMORPHOSED TO GREENSCHIST FACIES)
-  1735-1695 Ma SYN- & POST-DEFORMATIONAL GRANITOID INTRUSIVE ROCKS
-  ca. 1800-1750 Ma VOLCANIC & PLUTONIC ROCKS
(MULTIPLY DEFORMED & METAMORPHOSED TO AMPHIBOLITE FACIES)

Figure 1: Generalized geologic map of the Needle Mountains Proterozoic complex showing the major time- and litho-stratigraphic subdivisions. The general locations of sites referred to in the text are indicated by: EL - Electra Lake; LC - Lime Creek; SP - Snowdon Peak; NT - Needleton; HML - Highland Mary Lakes; TM - Table Mountain.

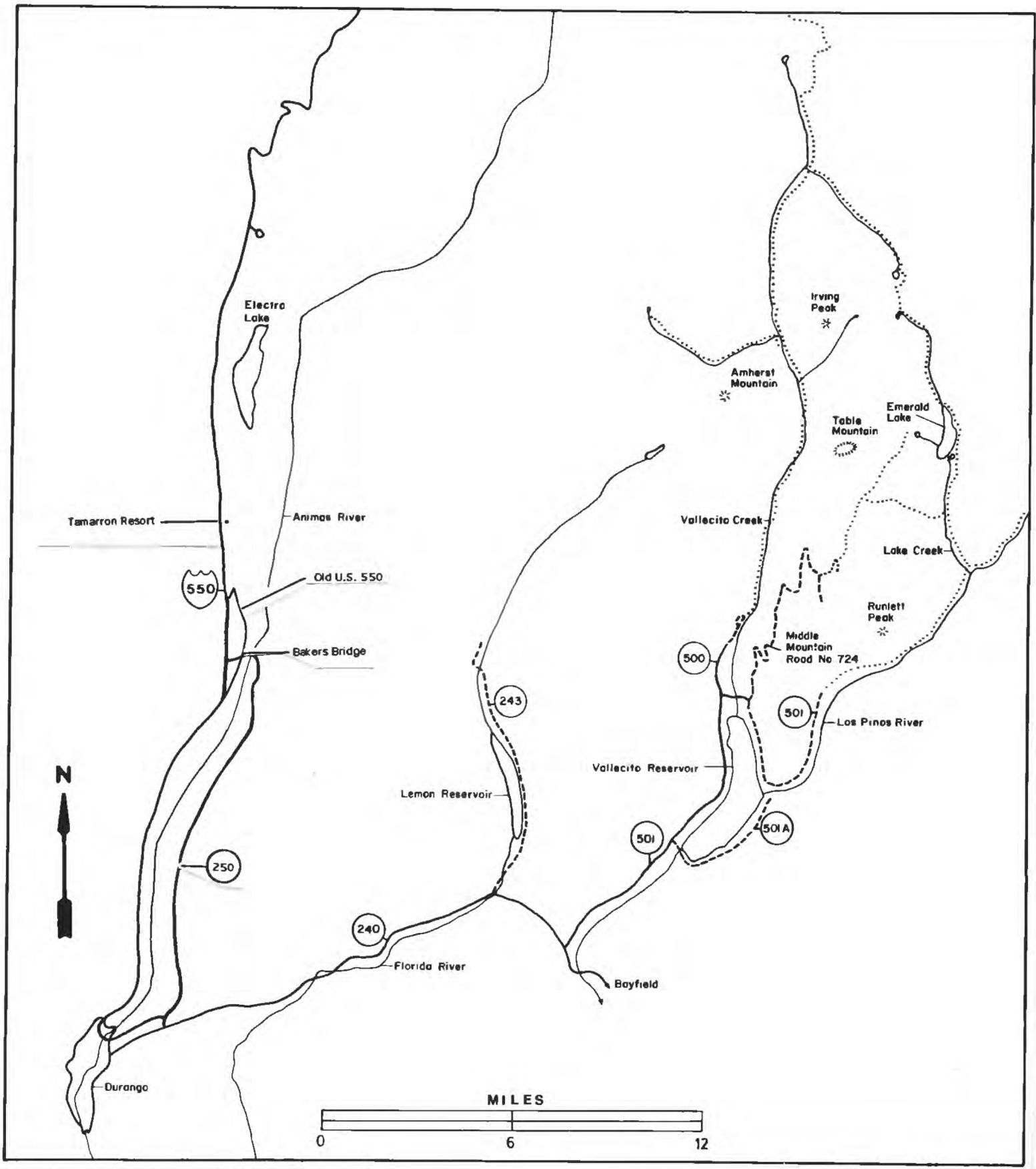


Figure 2: Access map; solid lines are paved roads (shield - U.S. Highway; circle - County Road). Long dashed lines are maintained roadways, short dashed lines signify unmaintained roadways, and dotted lines represent maintained trails.

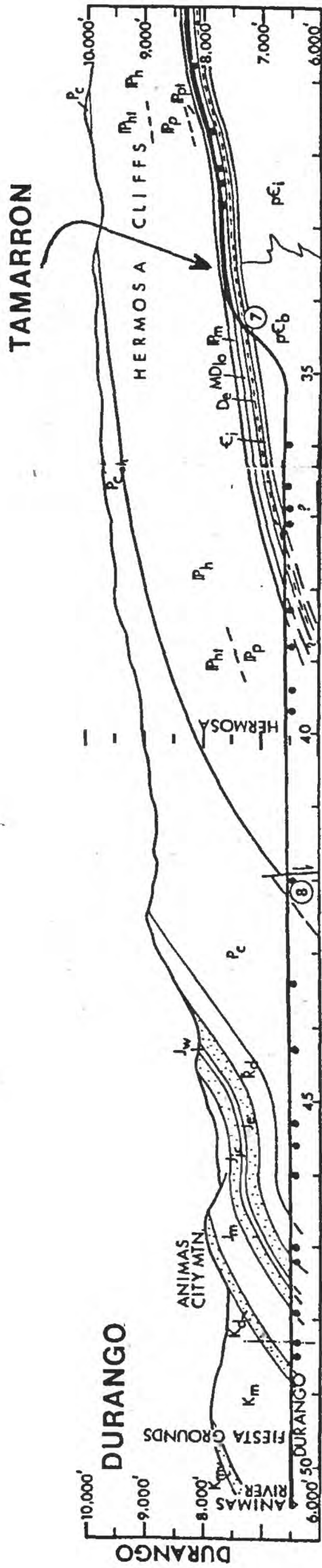


Figure 3: Road Section; DURANGO - - TAMARRON

Scale: 1 in. - 2.5 mi.

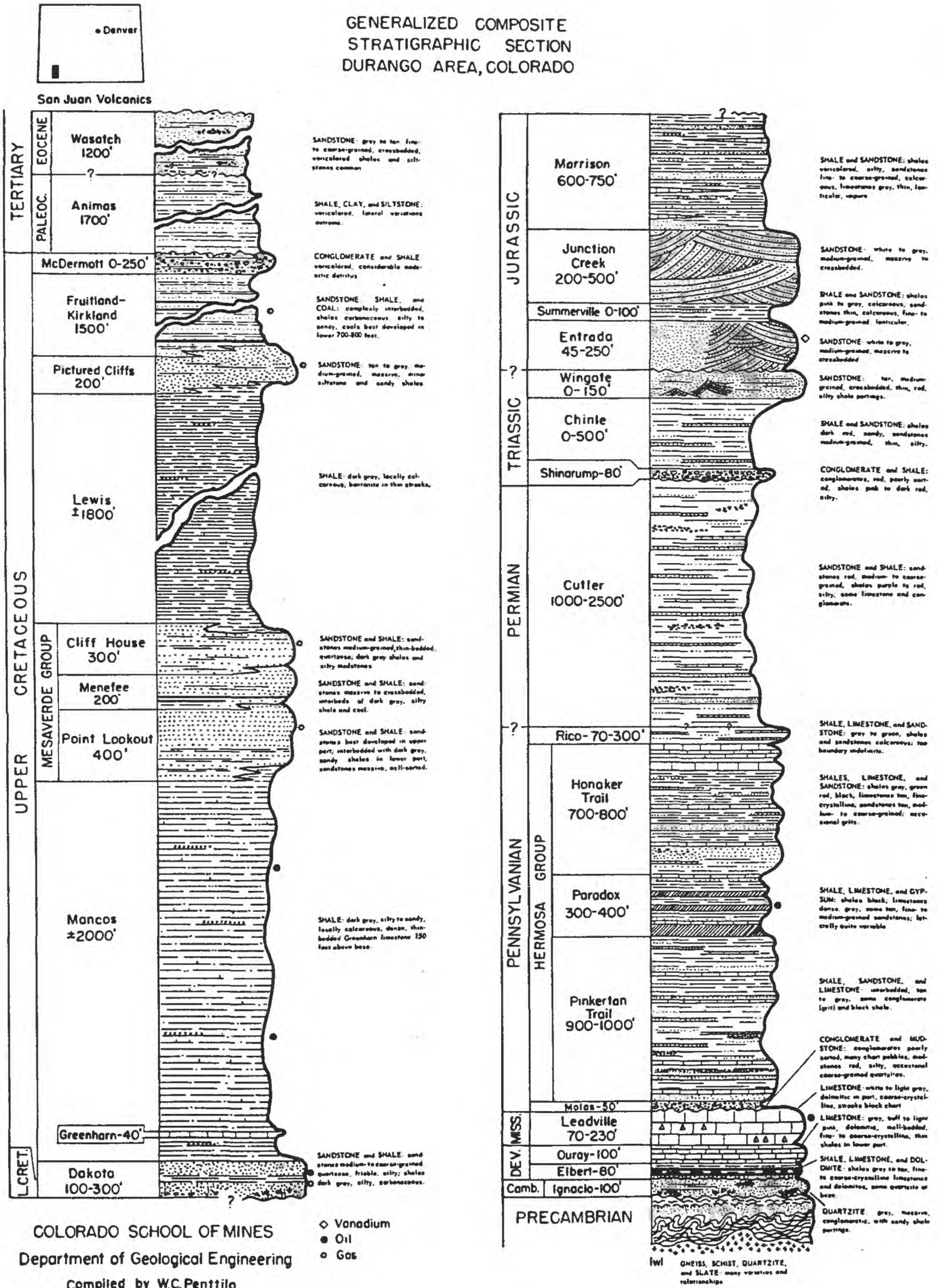
From: CSM, No. 8

KEENAN LEE - 1976

- Je Entrada Ss.
- Rd Dolares Fm.
- Pc Cutler Fm.
- Ph Hermosa Gp.
- Phr Honaker Trl. Fm.
- Pp Paradox Fm.
- Ppr Pinkerton Trl. Fm.
- Pm Malas Fm.
- MDlo Leadville-Ourray
- De Elbert Fm.
- Ei Ignacia Fm.
- Kmv Mesaverde Gp.
- Km Mancos Sh.
- Kd Dakota Gp.
- Jm Morrison Fm.
- Jjc Junction Ck. Ss.
- Jw Wanakah Fm.
- qc Quartzite congl.
- pCb Bakers Brg. Gran.
- pCu Uncompahgre Fm.
- pCj Twilight Gneiss
- pCi Irving Fm.

4X vertical exag.

GENERALIZED COMPOSITE
STRATIGRAPHIC SECTION
DURANGO AREA, COLORADO



COLORADO SCHOOL OF MINES
Department of Geological Engineering
Compiled by W.C. Penttila

Figure 4.

- 2.4 0.5 Durango and Silverton Narrowgauge Railroad overpass. Outcrops to the west (right) are of the Leadville Limestone and Devonian Ouray Formation (Figures 3-4).
- 3.5 1.1 Turn left on LaPlata County Road 250, cross cattle guard, and continue east to intersection with old section of U.S. Highway 550.
- 3.7 0.2 Cross old U.S. Highway 550; continue on County Road 250, past the KOA campground (Figure 2).
- 3.9 0.2 Outcrop on the north (left) is composed of either the Devonian McCracken Sandstone or Upper Cambrian Ignacio Formation (Figures 3-4).
- 4.1 0.2 **STOP 1: Bakers Bridge over the Animas River (Figures 1-2).**

On the west side of the Animas River the Bakers Bridge Granite is unconformably overlain by the Ignacio/McCracken formations. Compositionally the Bakers Bridge Granite is relatively homogeneous, and the granite exposed at this location is representative of the dominant lithology. It contains phenocrysts of perthitic microcline set in a coarse-grained groundmass dominated by perthitic microcline, plagioclase, quartz, biotite, hornblende, and magnetite. Biotite-muscovite granite crops out at the southernmost exposed part of the pluton, about 1 kilometer south and east of Bakers Bridge (Bickford and others, 1969). Except for localized ductile or brittle deformation along faults that cut the Bakers Bridge Granite, it appears undeformed in outcrop. Previous U-Pb zircon and Rb-Sr work gave ages of about 1700 Ma for the Bakers Bridge Granite (Silver and Barker, 1968; Bickford and others, 1968, 1969). These data are supported by a new U-Pb zircon age of 1699 ± 7 Ma obtained by Gonzales (Appendix I, NMGC6).

The Bakers Bridge Granite is a post-orogenic granite similar to many other ~1700 Ma granites in the Southwest (Conway, 1991). These granites, especially those emplaced at hypabyssal levels, are typically oxidized (red) and have high silica and alkali contents (Barker, 1969; Conway and others, 1987; Silver and others, 1986).

The first mining camp in southwest Colorado was established at Bakers Bridge in 1861, on the east bank of the Animas River, by a group of about 100 people led by Charles Baker. Little gold was found, however, and the Indians were a constant hazard. When the Civil War started, the party disbanded and returned east. Baker later returned and was killed by Indians as he was preparing to lead an exploring party into the Grand Canyon.

- 4.5 0.4 Retrace route to the intersection of County Road 250 and old Highway 550 (Figure 2).
- 5.0 0.5 Roadcut in the Ignacio/McCracken formations.
- 5.2 0.2 Bakers Bridge Granite forms the glaciated surface to the east (right). Outcrop of the Devonian McCracken Sandstone and Cambrian Ignacio Formation to the west (left).
- 5.5 0.3 Roadcuts expose Bakers Bridge Granite that is capped by glacial till. Note several diabase dikes in roadcut to the east (right). The absolute age of these dikes is unknown, but they are pre-Ignacio. Undeformed diabase dikes also cut Proterozoic rocks in the Table Mountain area, and near Highland Mary Lakes (Figure 1).
- 6.8 1.3 Cross railroad tracks.
- Durango and Silverton Narrowgauge Railroad. This narrowgauge line runs 45.2 miles (72.7 km) from Durango to Silverton. It was completed in 1882 to serve mining industry at Silverton. At present it is operated primarily for tours.
- North along the railroad tracks, the Precambrian-Cambrian nonconformity is exposed with Ignacio Formation on Bakers Bridge Granite. North of the highway-railroad intersection (1 o'clock) is the abandoned Rockwood Quarry, dug in the Leadville Limestone. The underlying Ouray Formation crops out in the cliffs below and east of the quarry. The McCracken Sandstone is exposed along the railroad. The uppermost part of the Leadville Limestone in the rim of the quarry is a coarse regolithic breccia.

It is composed of fragments of Leadville Limestone embedded in red clay of the overlying Molas Formation (Figures 3-4). Molas red clay fills deep solution channels and cavities in the limestone.

Road is constructed on the Lower Paleozoic sedimentary rocks. Outcrops of the oolitic and fossiliferous Leadville Limestone.

- 7.3 0.5 Continue west on old Highway 550 to stop sign; turn right and proceed north on U.S. 550.
- 9.0 1.7 Entrance to Tamarron Resort (Figures 1-2). The self-guided hiking tour at set up at the meeting site provided an opportunity to examine the Lower Paleozoic section in the area, and the intrusive contact between the Bakers Bridge Granite and 1805-1790 Ma (based on new U-Pb zircon data from Gonzales; Appendix I, NMGC25) multiply deformed and amphibolite facies mafic igneous rocks in the Irving Formation.
- 11.1 2.1 Intersection of Haviland Lake road and U.S. Highway 550. At 9 o'clock is a view of Engineer Mountain that exposes the upper portion of a Tertiary (?) laccolith that intrudes Permian red beds of the Cutler Formation. You may be able to make out the columnar jointing on the sheer southern face. The laccolith consists principally of sanidine-phyric trachyte. The rock type, textures, and form of this intrusive suggest that it and similar bodies in the Lime Creek-Cascade Creek area are related to Cretaceous-Tertiary laccolithic intrusive activity on the Colorado Plateau, rather than the Oligocene activity in the San Juan Mountains. For those willing souls, the climb to the +12000-foot summit of Engineer Mountain provides a magnificent view of the Animas River valley and surrounding area.
- View of Pigeon Peak (13,972 ft; 4259 m) at 2 o'clock in the central mass of the Needle Mountains which is composed mostly of the ~1435 Ma Eolus Granite (Figure 1; Appendix I, NMGC7). At 1 o'clock is a view of Twilight Peak (13,158 ft, 4011 m) and the West Needle Mountains. Rocks of the 1805-1755 Ma Irving Formation and Twilight Gneiss, and deformed granitoids of the ~1720 Ma Tenmile Granite, are exposed in the West Needle Mountains (Figure 1).

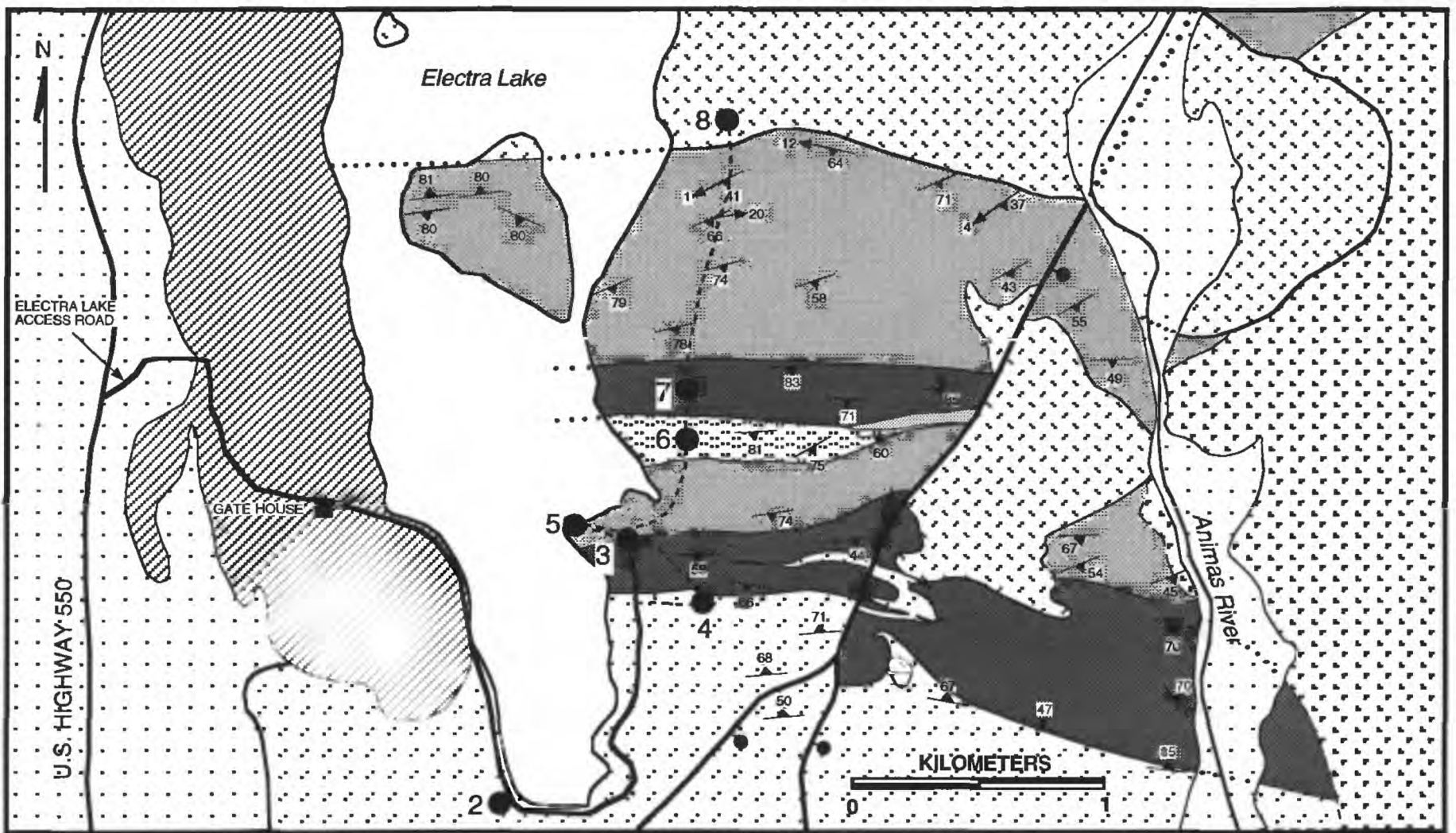
13.2 2.1 Turn right on Electra Lake access road. (Figures 2 and 5). Roadcuts expose the Leadville Limestone and Ouray Formation (Figures 3-4).

14.0 0.8 Gate house on road (Figure 5).

Electra Lake is the source of water for the hydroelectric plant at Tacoma in the Animas River canyon. A dam across Elbert Creek forms the lake, which is supplied chiefly by a flume from Cascade Creek about 5 miles (8.0 km) to the north. The water from the lake drops about 153 m to a penstock, then plunges 61 m to the turbines with a 450 lb. (204.5 kg) pressure at the plant.

Type sections for the Ignacio and Elbert formations are exposed along Elbert Creek, which enters Electra Lake from the northwest. The 1435 ± 2 Ma (Appendix I, NMGC27) Electra Lake Gabbro is exposed along the northern half of the lake, and farther east in the Animas River canyon where it intrudes the Early Proterozoic Twilight Gneiss and Irving Formation, and Middle Proterozoic Eolus Granite (Figure 1). The Electra Lake Gabbro is one of only several ~1400 Ma mafic intrusive bodies that are exposed in the United States.

15.0 1.0 **STOP 2 (Figure 5):** Intermediate to mafic gneiss and schist of the Irving Formation cut by numerous granitoid and quartz stringers trending subparallel to S_1 and S_2 tectonic foliation. The foliation and stringers define multiple phases of folding. Attenuation and detachment of the stringers locally imparts an augen-like structure to these rocks. The outcrop at this point is typical of many of the rocks seen in the Irving Formation in the Electra Lake area, farther south near Haviland Lake, and the Highland Mary Lakes area (Figure 1). A U-Pb zircon age of 1731 ± 10 Ma (Appendix I, NMGC23) was obtained for a strongly foliated granitic sill that cuts similar rocks in the Irving Formation at Four Base Lake, about 3 miles east of Haviland Lake. These deformed sills are slightly older than the 1720-1715 Ma Tenmile Granite (Figure 1) (Appendix 1, NMGC21). Granitoids with a weak to strong tectonic foliation also make up the Tenmile Granite which cuts rocks of the Irving Formation and Twilight Gneiss.



EXPLANATION

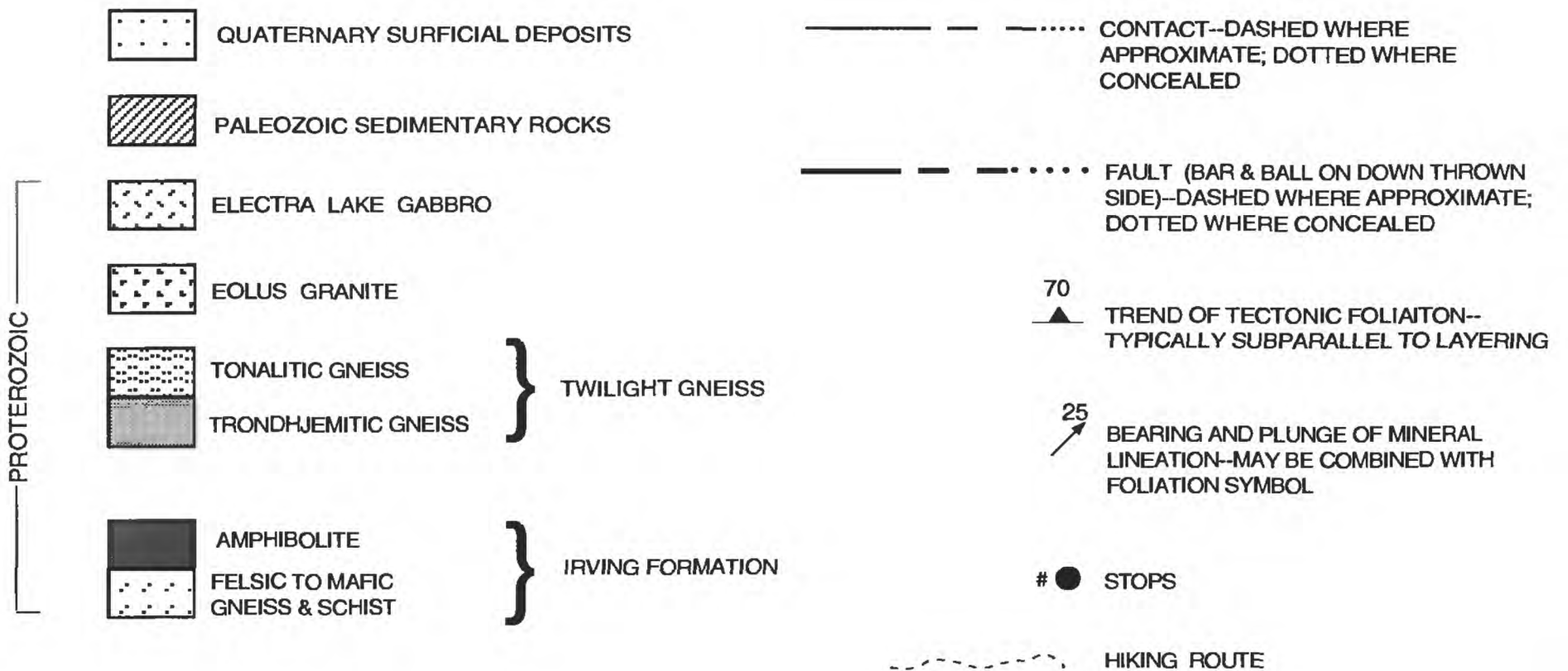


FIGURE 5: Generalized geologic map showing field trip route for day 1, stops 2-8.

In contrast, the Bakers Bridge Granite does not show the ductile deformation that is recorded by the Tenmile Granite and granitoid sills in the western Needle Mountains. This evidence argues for syn-deformational granitoid plutonism between about 1735-1710 Ma in the western Needle Mountains.

Deformed rocks at this stop are cut by an undeformed mafic dike that locally contains reddish (imparted by iron-rich inclusions) phenocrysts of plagioclase. This dike is most likely an offshoot of the Electra Lake Gabbro. Both the deformed rocks of the Irving Formation and undeformed mafic dike in this outcrop are cut by an aplite dike that is probably part of the widespread suite of granitoid intrusives related to the ~1435 Ma Eolus Granite.

Drive east across dam of Electra Lake; at east side of dam turn left (north) and proceed to Edison public parking area.

16.5
1.5

STOP 3 (Figure 5): Edison public parking area. Begin hiking part of trip. Total hike distance about 3-4 miles (5-7 kilometers).

The parking area is located near the steeply south dipping contact of the Twilight Gneiss and Irving Formation. Interlayered trondhjemitic gneiss and amphibolite in the Twilight crop out to the north and east side of the parking area (Figures 1 and 5). Amphibolite layers in this unit are typically < 2 m thick and continuous along strike for hundreds of meters. They are texturally and compositionally homogeneous, and show primary cross-cutting relationships with other rocks in the Twilight Gneiss in the Electra Lake and Lime Creek areas (Figure 1). From this evidence amphibolite layers of the Twilight Gneiss are interpreted as gabbroic intrusives that were emplaced during an extensional event before compressional deformation and metamorphism of the Twilight Gneiss and Irving Formation (Gonzales and others, 1993). However, the tectonic regime in which this proposed extensional event occurred is not well constrained.

Thin amphibolite layers in the Twilight Gneiss were not observed in the Irving Formation in this area. However, petrologically and chemically similar metamorphosed sills and dikes of gabbro cut the Irving Formation in the Highland Mary Lakes area (Figure 1).

From Edison parking area, hike 300-400 meters south on the road across the contact of amphibolite and felsic to intermediate gneiss and schist in the Irving Formation. Felsic to intermediate lithologies are interpreted as metamorphosed rhyolitic to dacitic volcanic rocks. Turn east and hike 500-600 meters along strike of foliation .

STOP 4 (Figure 5): Felsic schist in the Irving.

The Irving Formation in the Needle Mountains consists of interlayered mafic to felsic gneiss and schist. Locally, well-preserved relict features, such as pillow lavas and volcanic breccia structures, reveal that these rocks are predominantly volcanic in origin. However, in most areas (including this site), evidence of the protolith is masked by a strong and pervasive tectonic overprint. Note the numerous deformed granitoid stringers that cut the rocks at this stop. An absolute age for rocks in the Irving Formation has not been previously reported. New U-Pb zircon data for a sample of granitoid stringer-free felsic schist collected near this stop gives an age of 1805-1790 Ma (Appendix I, NMGC25). The precision of this age varies depending on the fractions used. The four best zircon fractions from the sample yield an age of 1801 ± 6 Ma; analyses on additional fractions were made to confirm this age. Collectively, the data gives an imprecise age of 1803 ± 20 Ma.

From stop 4, hike northwest across amphibolite of the Irving Formation, and then into interlayered amphibolite and trondhjemitic gneiss of the Twilight Gneiss. Discuss units along the way.

Amphibolites in the Irving Formation locally contain a pronounced compositional layering and relict volcanic features, and commonly form layers that are tens to hundreds of meters thick. There are general petrologic similarities between amphibolite of the Irving Formation and amphibolite layers in the Twilight Gneiss. This was used by early workers (Cross and others, 1905) to suggest that all mafic layers in the Twilight Gneiss were pieces of the Irving Formation that were incorporated into the intrusive complex of the Twilight Gneiss. However, as mentioned above, the form and spatial distribution, primary intrusive relationships, and homogeneity of amphibolite layers in the Twilight Gneiss argues that they originated as swarms of

gabbroic sills and dikes (Gonzales and others, 1993). Along with new ages for rocks of the Twilight Gneiss, this implies that the mafic intrusives in the Twilight were emplaced after about 1760-1755 Ma (Appendix I).

Walk to stop 3 at Edison parking area. Pick up lunches and hike west about 200-300 meters to the east shore of Electra Lake, near the Irving-Twilight contact (Figure 5). A good view of the thick succession of Paleozoic rocks exposed in Hermosa Cliffs is seen on the western skyline.

STOP 5 (Figure 5): Interlayered trondhjemitic gneiss and amphibolite in the Twilight Gneiss. At this locality amphibolite layers have undergone brittle deformation. They are cut by numerous tension fractures that locally become ductile shear zones in adjacent trondhjemitic gneiss layers. Tension fractures and shear zones are dominated by NE and NW trending arrays that typically record sinistral and dextral sense of movement, respectively. Undeformed granitoid stringers that extend from adjacent layers of trondhjemitic gneiss commonly fill the tension fractures, and some of the shear zones. Brittle deformation of amphibolites in the Twilight Gneiss was interpreted by Cross and others (1905) as evidence for intrusion of trondhjemitic to tonalitic rocks of the Twilight Gneiss into the Irving Formation. Barker (1969) suggested that the massive granitoid stringers and brittle deformation were generated during high grade metamorphism. He proposed that partial melting of trondhjemitic gneisses in the Twilight Gneiss produced the undeformed granitoids that then intruded the amphibolite layers along "tensional fractures." The granitoid-filled fractures and shear bands cut all tectonic fabrics and structures in the Twilight Gneiss (and locally in Irving Formation), and are concentrated in an aureole around the Electra Lake Gabbro. We interpret this as evidence for deformation and anatexis of Early Proterozoic crust during emplacement of the ~1435 Ma Electra Lake Gabbro at mid- to upper-crustal levels (Gonzales and others, 1993; Gonzales and others, 1994). Deformation involved N-S contraction and related E-W extension that is reflected by boudinage defined melt-filled amphibolite layers in the Twilight Gneiss, and E-W tectonic foliation in rocks of the Eolus Granite.

Excellent view of brittle deformation and partial melting is seen on the island to the west.

About 20 meters south, amphibolite of the Irving Formation is in contact with the Twilight Gneiss. At this site, the contact appears gradational and no constraint on the relative ages of these units is provided. However, in the Needleton area (Figure 1) metamorphosed and deformed sills and dikes of trondhjemite extend from the main mass of the Twilight Gneiss and cut relict compositional layering in the Irving (Gonzales and others, 1993). These relationships and U-Pb zircon ages for both units (Appendix I) suggest that the Irving Formation is the oldest unit in the Needle Mountains.

Lunch break at lake.

After lunch, hike back to Edison parking area and follow hiking trail north. Examine more exposures of interlayered trondhjemitic gneiss and amphibolite in the Twilight Gneiss along the way.

STOP 6 (Figure 5): Examine tonalitic gneiss in the Twilight Gneiss. Note that this lithology is exposed in a macroscopic boudin that pinches out to the east (Figure 1 and Plate 1). A U-Pb zircon age of 1759 ± 6 Ma was obtained for a sample of the gneiss in this area (Appendix I; NMGC13).

Continue hiking north to **STOP 7 (Figure 5):** Examine a 60-m-thick layer of amphibolite within the Twilight Gneiss. Layers of amphibolite that are tens of meters thick are uncommon in the Twilight Gneiss in the Electra Lake-Lime Creek area (Figure 1). The thick amphibolite layer exposed at this stop may be a pendant of Irving Formation that was incorporated in intrusive rocks of the Twilight Gneiss during their emplacement. This is supported by a local crude compositionally banding in the amphibolite that is similar to primary bedding and lamination in intermediate to mafic volcanic rocks in the Irving Formation. Similar isolated pendants of Irving Formation occur in the Twilight Gneiss between Snowden Peak and Needleton (Figure 1; Harris and others, 1987; Gibson, 1987; Gibson and Simpson, 1988; Gibson and Harris, 1992; Gonzales, recent unpublished mapping). Gibson (1987) suggests that some of these pendants define upright, subhorizontal F_2 folds. Pendants of Irving Formation within the Twilight Gneiss provides additional evidence that the Irving is the older unit.

At this point continue hiking north across more interlayered trondhjemitic gneiss and amphibolite of the Twilight Gneiss to the contact of the Twilight and the Electra Lake Gabbro. Examine and discuss features in the Twilight Gneiss during hike.

STOP 8 (Figure 5): Electra Lake Gabbro.

The Electra Lake Gabbro is mostly a hypersthene-bearing gabbro (norite) with minor diorite and granodiorite. Pegmatitic gabbro collected at station G27 yields a U-Pb zircon age of 1435 ± 2 Ma (Plate 1; Appendix I, NMGC27). This is supported by isochron ages from new Sm-Nd whole-rock and mineral-separate analyses (Appendix II), and previous Rb-Sr data (Bickford and others, 1968, 1969). Sm-Nd whole-rock data suggest that the Electra Lake Gabbro formed by partial melting of slightly depleted mantle (relative to chondritic uniform reservoir) (Gonzales and others, 1994; Appendix II).

In the Electra Lake and Highland Mary Lakes areas (Figure 1), compositional layering and subparallel S_1 and S_2 tectonic foliations in rocks of the Irving Formation and Twilight Gneiss trend roughly east-west. Between these areas, the layering and tectonic fabrics in these units strike northeast. This is reflected in a regional sigmoidal pattern of S surfaces in basement rocks in the western and northern Needle Mountains. The timing and origin of this structure are uncertain, but could be related to post-1700 Ma deformation in the Uncompahgre Formation and Vallecito Conglomerate (Figures 1). The Electra Lake Gabbro is located in the southern bend of this older regional structure which may have had some control on emplacement of the gabbro (Gonzales and others, 1994).

Retrace hike back to Edison parking area.

- | | | |
|------|-----|---|
| 19.8 | 3.3 | Drive back to U.S. Highway 550. Turn left (south) on highway and return to Tamarron Resort. |
| 24.0 | 4.2 | Turn left (east) into Tamarron Resort. |

End of day one.

Field Trip Road Log

Day 2

Southeastern Needle Mountains

INTRODUCTION (SECOND DAY)

During the second day of the field trip we will examine exposures of major Precambrian units in the southeastern Needle Mountains. Controversy over the time- and litho-stratigraphic succession in the Needle Mountains complex has arisen because of different interpretations of the: 1) nature of contacts between the Irving Formation (southeastern Needle Mountains) and Vallecito Conglomerate; and 2) stratigraphic relationship between Irving Formation in this area and similar rocks in the western and northern parts of the Needle Mountains complex (Figure 1). We will look at outcrops and contacts of the Eolus Granite, Vallecito Conglomerate, conglomerate of Fall Creek, and Irving Formation. New geochronologic data that bears on the controversies involving these rocks will be presented.

Discussions will focus on ideas that: 1) the Irving Formation in the southeastern Needle Mountains is a metamorphosed basaltic-rhyolitic-andesitic volcanic arc suite that appears to have formed at about the same time as similar rocks in the western and northern Needle Mountains; 2) fluvial siliciclastic sedimentary rocks of the Vallecito Conglomerate were deposited unconformably on deformed and metamorphosed rocks of the Irving Formation; 3) macroscopic folding of the Vallecito Conglomerate and underlying Irving Formation occurred during post-1700 Ma deformation and greenschist facies metamorphism; 4) the Irving-Vallecito contact in Vallecito Creek canyon is a zone of ductile and brittle faulting that locally juxtaposes the western limb of a faulted syncline containing rocks of the Irving Formation and basal Vallecito with a stratigraphically higher section of the Vallecito Conglomerate that makes up the eastern limb; and 5) Early Proterozoic juvenile arc basement and continental supracrust of the Precambrian complex in the southeastern Needle Mountains were intruded at about 1435 Ma by the Eolus Granite and related intrusive rocks.

Cumulative Mileage

Interval Mileage

0.0

Entrance to Tamarron Resort. Turn left (south) and continue on U.S. Highway 550 (Figures 1-2).

The route followed today takes us south to the north end of Durango, then east on County Road 240 to the Pine River valley (Figures 1-2). We will then proceed north on County Road 501 to the Vallecito Reservoir area. The distance to the first stop is about 45 road miles (72 kilometers). The first stop is 14 miles (22.4 km) due east of Bakers Bridge in the Animas River valley (Figure 1). Our route down the valley takes us stratigraphically up-section into Upper Cretaceous rocks (Figures 3-4). County

Road 240 follows the contact between the Mancos Shale and the underlying Dakota Sandstone (both Upper Cretaceous). On County Road 501, we travel up the Pine River valley and down-section through the stratigraphy shown in Figure 3.

- 3.5 3.5 Road to Bakers Bridge. Continue south on U.S. Highway 550. Outcrops to the west (right) are Mississippian Leadville Limestone and Devonian Ouray Formation with "lukewarm" springs forming colorful calcareous tufa deposits.
- 6.3 2.8 Knob to the east, with trees and a small house, is a kame that formed during stagnation of the Animas glacier. The red beds at 10 o'clock are in the Permian Cutler Formation (Figures 3-4). The flat floor of the Animas valley reflects lacustrine sedimentation in a glacial lake behind terminal moraines that dammed the valley north of Durango.
- 6.8 0.5 Cross the tracks of the Durango and Silverton Narrowgauge Railroad. Redbeds of the Cutler Formation are exposed in the steep cliffs that flank the Animas River canyon. The redbeds are about 2500 feet (765 m) thick, and are on the Pinkerton Trail Member of the Pennsylvanian Hermosa Group (Figures 3-4). Above the Cutler Formation, are more red beds of the Triassic Dolores Formation. The contact between the two redbed sections is difficult to identify. The Dolores Formation is equivalent to rocks of the Shinarump Conglomerate and Chinle Formation on the Colorado Plateau.
- 8.8 2.0 Note the sign for Trimble Hot Springs. Hot springs discharge sulfurous water (90°-110° F) along a fault at this site.
- View to the southeast at about 10 o'clock gives a cross-section through Missionary Ridge. Above the redbeds of the Dolores Formation is 40 feet (12 m) of pinkish sandstone that forms a vertical cliff. This unit may be equivalent to the Triassic Wingate Sandstone (Figures 3-4). From the bottom to top of the stratigraphic section, cliff-forming units are the Entrada Sandstone, Junction Creek Sandstone, and Dakota Sandstone. Much of Durango is built on the Upper Cretaceous Mancos Shale (Figures 3-4).

- 15.6 6.8 First stop light in Durango. Turn left (east) on 32nd Street.
- 15.7 0.1 Cross the Durango and Silverton Narrowgauge Railroad tracks and bridge over the Animas River. 32nd Street follows a small valley formed between two terminal moraines, probably of Pinedale age. To the north (left) across the moraine, are the most recent glaciofluvial and glaciolacustrine deposits.
- 16.9 1.2 Stop sign. Turn right (south) onto County Road 250.
- 17.1 0.2 Stop sign. Turn left (east) onto County Road 240. Gray rock forming the ridge to the south is the Upper Cretaceous Mancos Shale (Figures 3-4).
- 18.0 0.9 Enter the canyon formed on the contact of the Dakota Sandstone and Mancos Shale. For the next 14 miles (22.5 km), County Road 240 follows a topographic low between the Dakota Sandstone and Mesa Verde/Pictured Cliffs hogbacks (Figures 3-4).
- 18.2 0.2 Dakota Sandstone is exposed in roadcut to the north (left). Note the ripple marks on the bedding plane.
- 18.7 0.5 Mancos Shale is exposed in the road cut to the north (left). The dip of bedding varies from 20°-45° to the south. A relatively thin layer of shale remains on the sandstone on the north (left) side of the road, and the slope is very unstable. Many slumps and slides occur along County Road 240 where the road is cut into the south-dipping shales.
- 20.2 1.5 Mancos Shale is exposed in the road cut to the north (left).
- 20.3 0.1 Copper Belle entrance to Edgemont Ranch. We are now crossing the drainage divide between the Animas River (west) and Florida River (east); elevation 7420 ft (2262 m) (Figure 2).

21.5	1.2	<p>Intersection with County Road 234. Continue east on County Road 240 (Figure 2).</p> <p>The Upper Cretaceous Pictured Cliffs Sandstone forms the rimrock to the south (right) and the Lewis Shale forms the slope (Figures 3-4). Formations of the Mesa Verde Group are thin and non-resistant here. The road is built on the Mancos Shale.</p>
22.8	1.3	Cross first bridge over Florida River.
23.1	0.3	Cross second bridge over Florida River.
23.3	0.2	Road cuts through landslide deposits.
24.3	1.0	<p>Road cut to the north (left) exposes the contact between the Point Lookout Sandstone of the Mesa Verde Group and the Mancos Shale (Figures 3-4). To the south is a section of Lewis Shale about 1200 feet thick (366 m) that is overlain by Pictured Cliffs Sandstone on the skyline. All formations are Upper Cretaceous in age.</p>
27.2	2.9	<p>Valley is in the Mancos Shale. The ridge to the south (right) is the Mesa Verde Group, and the Dakota Sandstone is exposed on the skyline to the north (left).</p>
28.5	1.3	Blue Spruce Trading Post.
29.0	0.5	<p>Landslide deposits are exposed in the roadcut to north (left). The county road department has removed the debris slide exposing the slip surface.</p> <p>Helen's Store, a local landmark. County Road 243 leads to Lemon Reservoir. Turn right and continue on County Road 240 across the bridge over Florida River.</p>
29.5	0.5	<p>Cross the drainage divide between the Florida River (west) and the Pine River (east); elevation 7925 feet (2416 m). For the next 2.3 miles, the road follows</p>

the contact between the Dakota Sandstone and Mancos Shale with the Mesa Verde Group forming the rimrock to the south (right) (Figures 3-4).

- 31.8 2.3 Stop sign; County Road 240 ends (Figure 2).
- Turn left (north) onto County Road 501 and proceed north towards Vallecito Reservoir. We are now going up the Pine River valley and down the stratigraphic section shown in Figures 3-4. Rocks of Mesozoic age are not well exposed in this area.
- 34.1 2.3 Glacial outwash containing boulders of the Early Proterozoic Vallecito Conglomerate. Terminal moraine of the Vallecito glacier (Pinedale).
- 36.3 2.2 Road to the right leads to the dam of Vallecito Reservoir. Continue north on County Road 501.
- 36.7 0.4 Road cut to the west (left) exposes the Permian Cutler Formation. The Cutler crops out on the entire western side of the lake, but only the southern one-third of the eastern shore (right). The geologic map of the Durango Quadrangle (Steven and others, 1974) shows a fault under the lake with a down-thrown western block. Exposures of the Pennsylvanian Hermosa Group can be seen at 2 o'clock across the lake. Vallecito dam is at 4 o'clock.
- 39.0 2.3 At 12 o'clock is a view of 13,218 foot (4030 m) Irving Peak that is comprised of Early Proterozoic metamorphosed volcanic and plutonic rocks of the Irving Formation. From the summit, the western flank of Irving Peak drops about 4000 feet (1225 m) over a distance of roughly 1.3 miles (2.2 km), into the valley of Vallecito Creek. The peaks at 11 o'clock expose the ~1435 Ma Eolus Granite. Early Proterozoic Rocks in the southeastern Needle Mountains are exposed in a N-S trending belt that is bounded to the west and east by batholithic masses of the Eolus Granite (Figure 1).

- 40.2 1.2 North end of boathouse.
- 40.5 0.3 Community of Vallecito (Little Texas).
- 41.6 1.1 Intersection of County Road 501 and County Road 500. Turn left (north) onto County Road 500.
- 42.3 0.7 Road cut to the west (left) exposes rocks of the Pennsylvanian Hermosa Group.
- 42.4 0.1 Wits End Ranch.
- 43.5 1.1 Office of Blue Spruce Trailer Park.

STOP 1 (Figure 6): Begin hike here. Total hike distance is between 2-3 miles (3-5 kilometers). Early Proterozoic Vallecito Conglomerate is exposed in cliffs around the trailer park, and farther north on either side of Vallecito Creek.

Proceed to stop 2. Along the way we will be hiking on metamorphosed fluvial sedimentary rocks of the Early Proterozoic Vallecito Conglomerate.

STOP 2 (Figure 6): Late Proterozoic (?) conglomerates exposed at the base of the Paleozoic section. Discussion of ideas on their origin and possible significance. These conglomerates are one of several that have been identified in the Lower Paleozoic stratigraphic sequences in the San Juan Mountains. Campbell (see pages 50-53) raises the possibility that the conglomerates were deposited during a Late Proterozoic period of erosion, rather than during the Cambrian.

STOP 3 (Figure 6): Eolus Granite.

The ~1435 Ma Eolus Granite (Appendix I, NMGC7) consists of two composite batholithic bodies of very coarse-grained to aplitic calc-alkaline granite to granodiorite. A stock of diorite of about

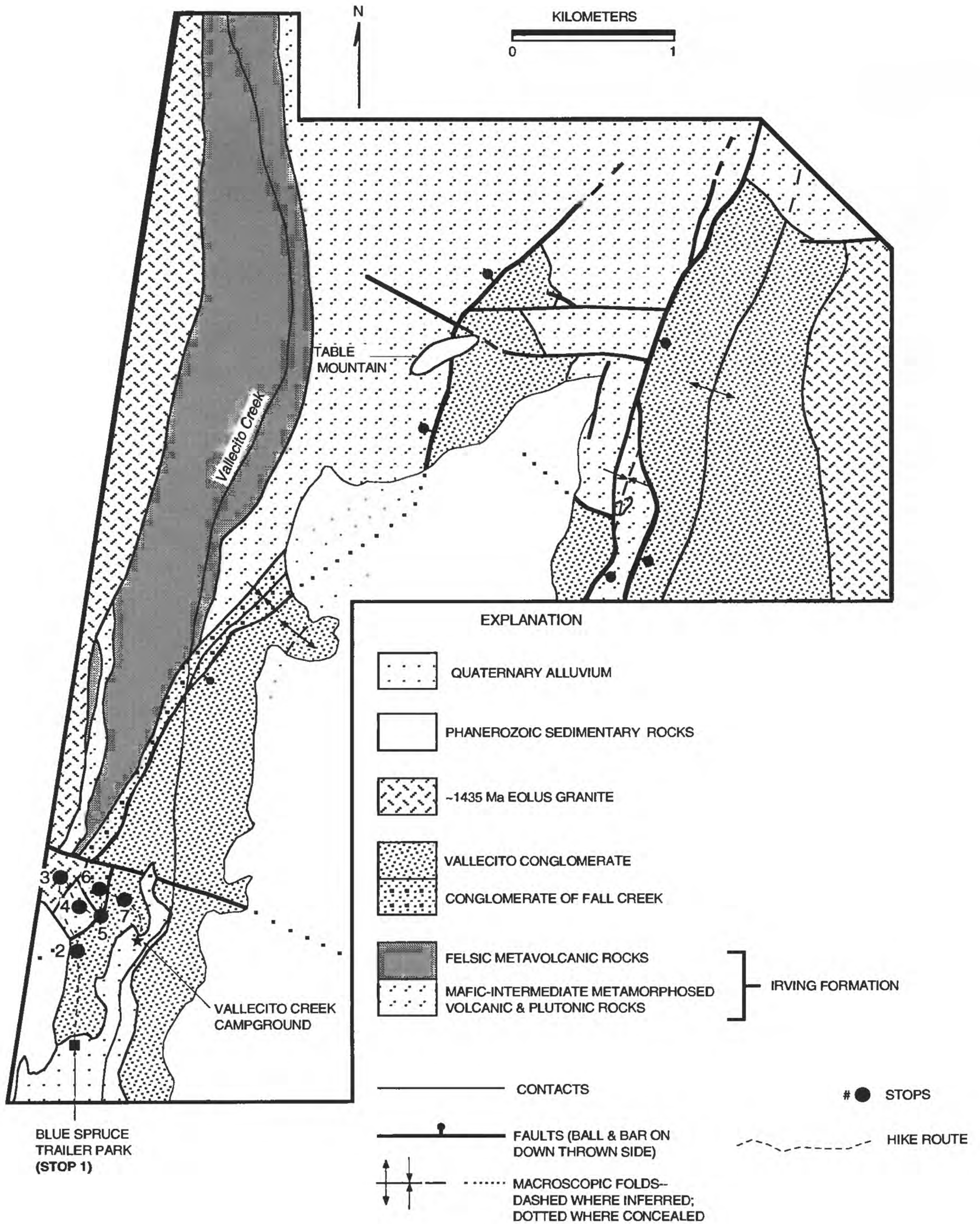


Figure 6: Field trip route map for day 2, stops 1-7.

the same age intrudes granitoids of the Eolus Granite in the Pine River area (Figure 1). The Electra Lake Gabbro, Eolus Granite, and diorite of Pine River form a complete compositional spectrum of Middle Proterozoic intrusive rocks in the Needle Mountains. Partial melting of underplated mantle in a subduction system is suggested by Collier (1989) for the origin of the Eolus Granite. Granite exposed at this locality is typical of much of the Eolus Granite. It contains phenocrysts of perthitic microcline that are set in a coarse-grained groundmass of quartz, perthitic microcline, plagioclase, hornblende, and biotite.

Contacts between the Eolus Granite and Irving Formation here and farther north are commonly marked by zones of intrusive breccia, in which blocks of Irving Formation are set in matrix of undeformed granite. However, locally in the Needle Mountains (e.g., east of Electra Lake, Figure 1) the Eolus Granite shows a weak to strong, east-west penetrative foliation near its contacts. The tectonic controls on the emplacement of the Eolus Granite are poorly constrained.

Walk southeast and examine metamorphosed and deformed mafic igneous rocks in the Early Proterozoic Irving Formation.

STOP 4 (Figure 6): The Irving Formation at this locality is dominated by amphibolite that shows a strong tectonic fabric and three or four generations of mesoscopic folds. Early generations of folds (F_1 and F_2) are isoclinal to tight with the traces of axial surfaces subparallel to compositional layering. These early folds are locally overprinted by F_3 and F_4 (?) tight to open folds with axial traces trending at oblique angles to compositional layering and earlier S_1 and S_2 tectonic foliations. This is similar to what is recorded in rocks of the Irving Formation and Twilight Gneiss in the western and northern Needle Mountains (Figure 1). Some previous workers suggest that F_3 and F_4 folds observed in basement rocks of the Needle Mountains complex are related to post-1700 Ma deformation recorded in the Uncompahgre Formation (Harris and others, 1986, 1987; Gibson, 1987; Harris, 1987; Gibson and Simpson, 1988; Gibson, 1990; Harris, 1990; Gibson and Harris, 1992).

The strong and pervasive tectonic overprint seen here in the Irving Formation is not seen in many parts of this unit in the southeastern Needle Mountains. Locally, and especially in the Table Mountain area (Figures 1, 2, and 6), clues to the origins of these rocks are revealed by well-preserved relict features such as pillow structures, volcanic breccia features, bedding and cross lamination, and porphyritic and trachytic textures. Field, petrographic, and geochemical data for rocks in the Irving Formation in the southeastern Needle Mountains suggest that they are metamorphosed basaltic, andesitic, and rhyolitic flows and tuffs with interbedded immature clastic sedimentary rocks (Barker, 1969; Gonzales, 1988a, 1988b, 1992).

Mineral assemblages in the amphibolite in this area are dominated by hornblende, oligoclase-andesine, epidote, and sphene. This assemblage is consistent with the upper greenschist to lower amphibolite facies metamorphism that is recorded in all rocks of the Irving Formation in the southeastern Needle Mountains (Cross and others, 1905; Barker, 1969; Gonzales, 1988a, 1988b, 1992).

Walk southeast to contacts between the Irving Formation, conglomerate of Fall Creek, and Vallecito Conglomerate.

STOP 5 (Figure 6): In this area the Irving Formation is in contact with fluvial sedimentary rocks of the Vallecito Conglomerate and conglomerate of Fall Creek (Figures 1 and 6). The nature of these contacts, and therefore the stratigraphic relationships of these units, are controversial (Figure 7). The contacts have been interpreted as conformable depositional surfaces, faults or zones of shearing, or a combination of the two (Cross and others, 1905; Cross and Larsen, 1935; Larsen and Cross, 1956; Barker, 1969; Burns and others, 1980; Ethridge and others, 1984; Gonzales and Ruiz, 1982; Gonzales, 1988a, 1988b).

Near stop 5, quartz-rich rocks of the Vallecito Conglomerate are in contact with the Irving Formation along a near vertical fault that strikes northeast-southwest. A pronounced foliation that trends subparallel to bedding is developed in rocks in the Vallecito south and east of the contact. Dextral movement on the fault has deflected bedding and foliation near the contact, producing a drag fold (Plate 2).

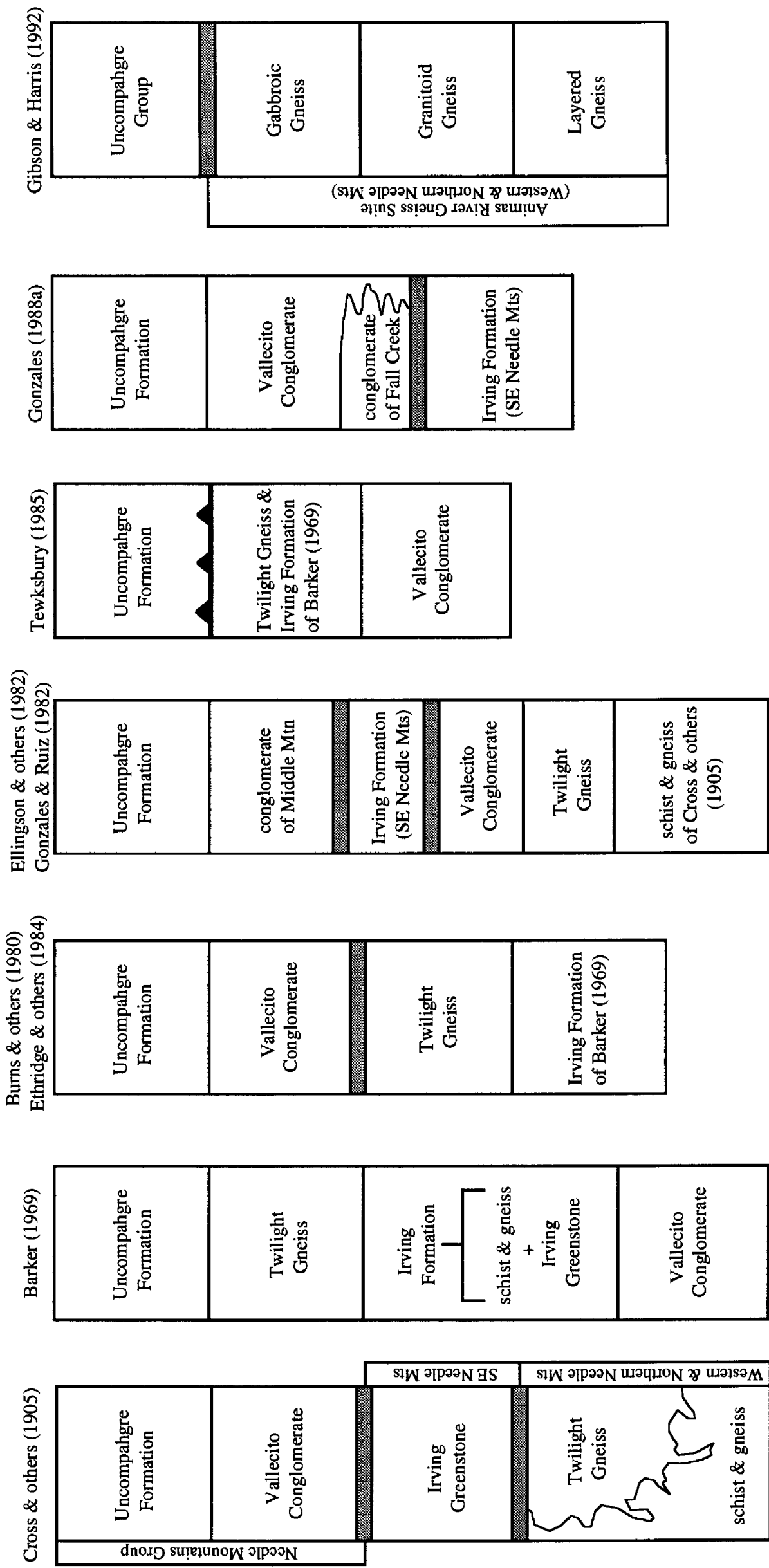


Figure 7: Proposed successions of layered Proterozoic rocks in the Needle Mountains complex. Animas Gneiss Suite of Gibson and Harris (1992) includes rocks of both the Irving Formation and Twilight Gneiss. Shaded areas between units indicate unconformities. Sawtooth symbol denotes that the Uncompahgre Formation is in thrust contact with pre-1700 Ma rocks, and that its stratigraphic position is uncertain.

About 50-100 meters north of stop 5, the Irving Formation and Vallecito Conglomerate are separated by an amphibolite clast-rich conglomerate that makes up the conglomerate of Fall Creek (Gonzales, 1988a, 1988b; Figures 6 and 7). Rocks of this unit appear to rest in pronounced angular unconformity on both the mafic and felsic lithologies in the Irving Formation. Gonzales (1988a, 1988b) interpreted the contact between the Irving Formation and conglomerate of Fall Creek as a sheared unconformable depositional surface. The contact between the Vallecito Conglomerate and the conglomerate of Fall Creek is a major zone of faulting. Ductile fabrics seen along this contact indicate that the west side is up.

Unconformable depositional contacts between the Vallecito Conglomerate and Irving Formation occur locally in the Table Mountain area (Figures 1, 2, and 6). In these locations, stratigraphic top indicators show that the Vallecito Conglomerate was deposited upon the Irving Formation (Burns and others, 1980; Ethridge and others, 1984; Gonzales, 1988a, 1988b).

Trough cross-stratification seen in the steeply west dipping beds in the Vallecito Conglomerate in Vallecito Creek shows stratigraphic tops to the west, while locally in the conglomerate of Fall Creek both tops to the east and west are observed. On the basis of this and other evidence, Gonzales (1988a, 1988b) interpreted the conglomerate of Fall Creek as a basal facies of the Vallecito Conglomerate that is exposed in a faulted syncline. However, the conglomerate of Fall Creek is nowhere in stratigraphic continuity with the main mass of the Vallecito Conglomerate. Macroscopic folds were generated in both the Vallecito Conglomerate and Uncompahgre Formation during deformation between 1700-1400 Ma (Cross and others, 1905; Barker, 1969; Tewksbury, 1982, 1989; Burns and others, 1980; Ethridge and others, 1984; Harris and others, 1986, 1987; Gibson, 1987; Harris, 1987; Gonzales, 1988a, 1988b; Gibson and Simpson, 1988; Gibson, 1990; Harris, 1990; Gibson and Harris, 1992).

STOP 6 (Figure 6): Conglomerate of Fall Creek.

The conglomerate of Fall Creek is a clast- to matrix-supported pebble to cobble conglomerate, that contains abundant clasts of metamorphosed mafic to felsic schist and gneiss. Cross and others (1905) interpreted these conglomerates as a basal facies of the Vallecito Conglomerate. In contrast, Barker (1969) suggested that it was a basal part of the Irving Formation.

Clasts of all principal lithologies found in the Irving Formation in the southeastern Needle Mountains occur in this unit. The conglomerate and interlayered sandstone lenses are interpreted as debris flows and local channel sands that were deposited unconformably upon deformed and metamorphosed rocks of the Irving Formation (Gonzales, 1988a, 1988b). Conglomerate with abundant clasts of Irving-type lithologies also occurs in the basal section of the Vallecito Conglomerate in the Table Mountain area (Figures 1, 2, and 6).

STOP 7 (Figure 6): Vallecito Conglomerate

The Vallecito Conglomerate is dominated by matrix- to clast-supported pebble to boulder conglomerate. Dominant clast lithologies are fine-grained to pebbly quartzite, vein quartz, chert, jasper, and argillite. The quartzite clasts are typically massive, but some show a relict bedding, planar lamination, or cross lamination.

Note the pronounced cross stratification in rocks of the Vallecito Conglomerate, showing stratigraphic tops to the west.

The stratigraphic relationship of the Vallecito Conglomerate and Uncompahgre Formation (Figure 1) is an important unresolved problem (Figure 7). These units share some similarities in depositional histories, and both were involved in multi-phase deformation and greenschist facies metamorphism. Cross and others (1905) placed the Vallecito Conglomerate stratigraphically beneath the Uncompahgre Formation, and assigned both units to their Needle Mountains Group (Figure 7). Barker (1969) placed the Vallecito Conglomerate beneath the Irving Formation, and suggested that rocks of the Uncompahgre Formation were deposited unconformably upon all pre-1700 Ma rocks in the

Needle Mountains (Figure 7). More recent work (Burns and others, 1980; Ethridge and others, 1984; Gonzales, 1988a, 1988b) suggests that the Vallecito Conglomerate is younger than the Irving Formation, and may be in part correlative with the Uncompahgre as originally proposed by Cross and others (1905).

Hike east through section of Vallecito Conglomerate to Vallecito Creek campground.

End hike at Vallecito Creek Campground.

47.8 Retrace route to intersection of County Road 500 and County Road 501 (Figure 2).

OPTIONAL IF TIME PERMITS: Turn left (east) onto County Road 501.

48.3 0.5 Cross bridge over Vallecito Creek.

48.8 0.5 Pass Middle Mountain Road No. 724 on the left (east), and continue on County Road 501 (Figure 2).

50.0 0.2 Pavement ends.

52.1 2.1 Cross cattle guard. End of County Road 501. Continue on Forest Service Road 602 through private land. Pine River enters Vallecito Reservoir to the south (right). Road cuts into glacial gravels.

52.5 0.4 Cross cattle guard. Pine River canyon is to the right.

54.2 1.7 At 1 o'clock is a view of the Pine River valley and Runlett Peak (11,100 ft, 3384 m). The steep cliffs on the flanks of Runlett Peak expose west-dipping beds in the Vallecito Conglomerate that define the western limb of an upright to steeply inclined, south-plunging anticline. This fold continues northward into the Hell Canyon-Dollar Lake area (Plate 2).

54.4 0.2 Road cuts expose rocks of the Hermosa Group.

- 54.7 0.3 Cross cattle guard.
- 55.2 0.5 The Lower Paleozoic section is not well exposed and is probably very thin in this area. Vallecito Conglomerate crops out at 9 o'clock.
- 55.7 0.5 Cross another cattle guard!
- 55.8 0.1 Vallecito Conglomerate outcrops to the north (left).
- 56.0 0.2 **STOP 8 (Figure 1):** End of the road. Trail head for Weminuche Wilderness Area starts here.
- Summary Discussion:** Time- and litho-stratigraphic framework and tectonic history of Needle Mountains Proterozoic complex.
- Retrace route to Tamarron Resort.
- 105.8 49.8 Turn right (east) into Tamarron Resort.
- End of field trip.**

THE NEEDLE MOUNTAINS PROTEROZOIC COMPLEX: A SUMMARY

by

David A. Gonzales and Clay M. Conway

INTRODUCTION

The purpose of this section is to summarize the current understanding of Proterozoic geologic history in the Needle Mountains complex, and attempt to place these events in a regional context. There have been a number of individuals who have contributed to our understanding of the Proterozoic geology in the southwestern Colorado. This includes work done by: Cross and others (1905), Silver and Barker (1968); Barker (1969); Bickford and others (1969); Burns and others (1980); Tewksbury (1981); Ellingson and others (1982); Gibson (1987); Harris (1987); Gonzales (1988a); and ongoing studies by J. Campbell, C. Conway, D. Gonzales, J. Ellingson, G. Siek, and W.R. Van Schmus. Ideas presented in the following discussion lean heavily on the results of recent detailed work, some of which are in conflict with conclusions drawn in earlier studies.

The Needle Mountains complex is one of the best preserved and most diverse Proterozoic assemblages in the Southwest. It contains an Early Proterozoic greenstone-granite complex in which andesitic volcanic rocks are locally abundant, 1735-1715 Ma syn-tectonic granitoids and post-tectonic ~1700 Ma granitoids, a ~1435 Ma granite-gabbro intrusive complex, and multiple episodes of deformation and metamorphism between 1800-1400 Ma. Some of these lithologic associations and events are not common in the Early Proterozoic rocks exposed south of the Archean Wyoming craton. An understanding of the evolution of this complex could provide important clues to the generation and assembly of Early Proterozoic crust in the southwestern United States.

GEOLOGIC FRAMEWORK

Approximately 1100 square kilometers of Early to Middle Proterozoic rocks are exposed in the Needle Mountains and adjacent ranges in southwestern Colorado (Figure 8). The Precambrian complex can be divided into four major groups on the basis of the timing and general nature of events recorded (Figure 1). The oldest rocks in the Needle Mountains complex consist of 1800-1750 Ma (Silver and Barker, 1968; Bickford and others, 1968, 1969; Appendix I) amphibolite facies and multiply deformed volcanic and minor intrusive rocks of the Irving Formation, and trondhjemitic-tonalitic plutonic rocks of the Twilight Gneiss (Figure 9). Rocks of the Irving Formation and Twilight Gneiss are locally intruded by 1735-1695 Ma (Bickford and others, 1968, 1969; Silver and Barker, 1968; Appendix I) syn- or post-orogenic granitoids that make up the Tenmile Granite and Bakers Bridge Granite. Thick successions of deformed and greenschist facies fluvial and marine siliciclastic sedimentary rocks comprise the Vallecito Conglomerate and Uncompahgre Formation (Figures 1 and 9). These sedimentary cover successions are generally faulted against the 1800-1700 Ma crystalline complex, but locally they lie on the older rocks along preserved unconformable depositional surfaces (Burns and others, 1980; Ethridge and others, 1984; Harris and others, 1986, 1987; Gibson, 1987, 1990; Gonzales, 1988a, 1988b; Harris, 1987, 1990). Early to Middle Proterozoic crystalline and siliciclastic assemblages in the Needle Mountains are cut by a host of ~1435 and ~1350 Ma granitic to gabbroic intrusive rocks that make up the Eolus Granite, Electra Lake Gabbro, quartz diorite of Pine River, and Trimble Granite (Figures 1 and 9) (Bickford and others, 1968, 1969; Silver and Barker, 1968; Appendices I and II).

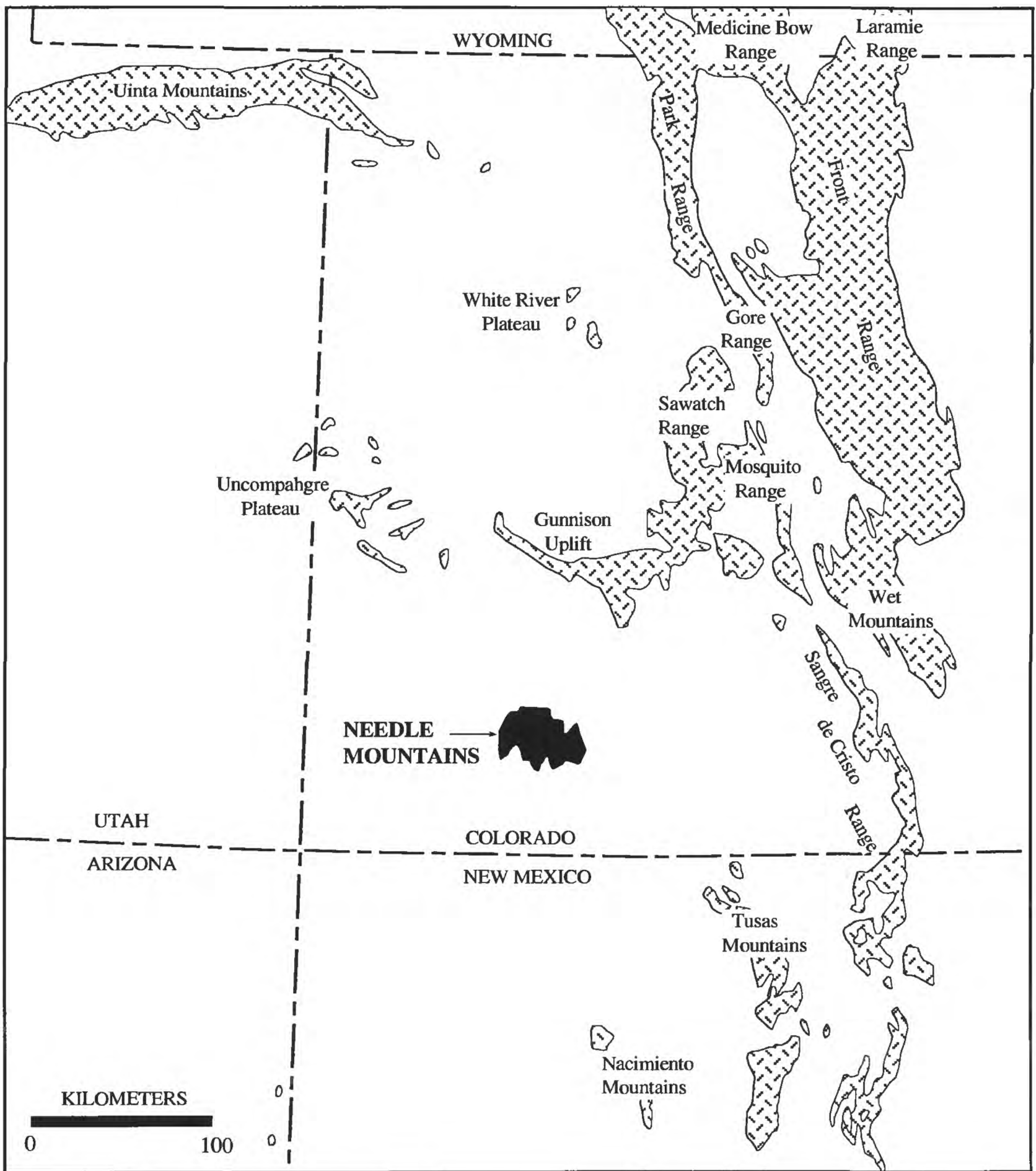


Figure 8: Exposures of Proterozoic rocks in the southern Rocky Mountains.

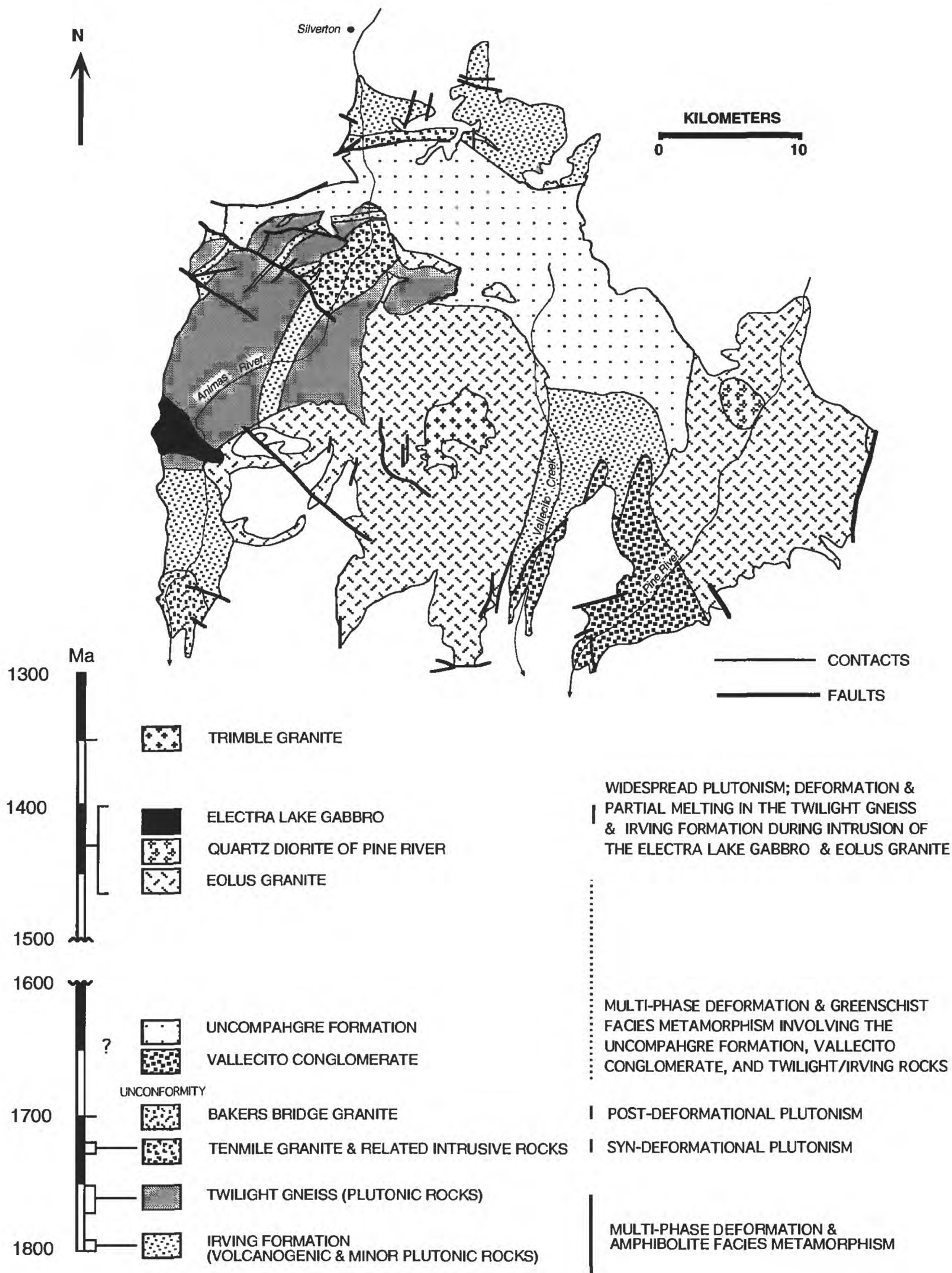


Figure 9: Generalized geologic map showing the principal lithostratigraphic units in the Needle Mountains complex, and a summary of the approximate timing and nature of major events. Dotted lines indicate that the timing of the event is poorly constrained, and gives the possible time range.

LITHOLOGIC UNITS

Irving Formation (metavolcanic suite)

Early Proterozoic metamorphosed volcanic and minor intrusive rocks in the Needle Mountains comprise three separate belts that make up the Irving Formation of Barker (1969) (Figures 1 and 9). Cross and others (1905) originally grouped the western and northern exposures and called them "Archean" schists and gneisses (Figure 7). They interpreted the similar suite of rocks in the southeastern Needle Mountains as a younger unit that they named the Irving Greenstone (Figure 7). On the basis of similarities in protoliths and deformational histories, Barker (1969) combined the "Archean" schist and gneiss complex and Irving Greenstone of Cross and others (1905) into his Irving Formation (Figure 7). Until recently (see Gibson and Harris, 1992 on Figure 7), this nomenclature has been widely accepted and will be used in the following discussion. The correlation of these metavolcanic suites is one of the most controversial issues of Precambrian geology in the Needle Mountains (Figure 7). This has been partly due to the lack of absolute age determinations for these rocks. New age determinations (Appendix I) suggest that volcanogenic rocks in the Irving Formation formed between 1805-1780 Ma. However, the correlation of the different belts of Irving Formation is still uncertain due to variable imprecision in the U-Pb zircon analyses obtained (Appendix I, samples NMGC22 and NMGC25), and lack of other unequivocal evidence to constrain their time-stratigraphic relationship.

All exposures of the Irving Formation are polyphase deformed and metamorphosed at upper-greenschist to lower amphibolite facies. The western and northern exposures are dominated by mafic to felsic gneisses and schists in which clues to protolith types are typically masked by a strong tectonic overprint. However, well-preserved primary features are locally observed. These include relict pillow structures, pillow and volcanic breccia, bedding and lamination, and amygdaloidal and porphyritic textures (Figure 10). A sample of felsic metavolcanic rock of the Irving Formation collected east of Electra Lake (Figures 1, 5, and 9) yields a U-Pb zircon age of ~1800 Ma (Appendix I, NMGC25).

A remarkably well preserved suite of volcanogenic and minor intrusive rocks make up the Irving Formation in the southeastern Needle Mountains (Gonzales, 1988a, 1988b, 1992) (Figures 1, 6, and 9). Strong and pervasive deformation masks the original features in some parts of this suite, but relict features are common and widespread (Figure 11). Rhyolitic schists and gneisses that give a U-Pb zircon age of 1800-1785 Ma are dominant west of Vallecito Creek (Figures 1, 2, 6, and 9). This age suggests that rocks of the Irving Formation in the western and southeastern Needle Mountains may be coeval. East of Vallecito Creek (Figure 1, 2, and 9) the Irving Formation is composed chiefly of massive to pillowed basaltic to andesitic flows, pillow breccias, basaltic tuffs, turbiditic sandstones and siltstones, volcanoclastic conglomerate, hydrothermal chert and jasper deposits, and crosscutting gabbroic and lamprophyric dikes and small intrusive masses (Gonzales, 1988a, 1988b, 1992). Andesitic flows and tuffs in this suite are a rare component of Early Proterozoic complexes in the Southwest (e.g., Condie, 1986; Van Schmus and others, 1993). Volcanic and plutonic rocks of this complex are tholeiitic to calc-alkaline and show strong chemical affinities to Phanerozoic magmatic arc and back-arc assemblages (Barker, 1969; Gonzales, 1988a, 1988b, 1992). Isotopic and geochemical data for Irving rocks in the western and northern Needle Mountains give similar results (Gonzales, unpublished data). If all the Early Proterozoic volcanogenic assemblages in the Needle Mountains complex are time correlative, then rocks in the southeastern Needle Mountains may form a stratigraphically higher part of the succession. This is weakly implied by their better preservation and slightly lower metamorphic grade, occurrence of turbiditic sedimentary rocks and siliceous hydrothermal deposits, and higher proportion of andesitic volcanic rocks (Gonzales 1988a, 1988b, 1992).



Figure 10: Metamorphosed basaltic volcanic breccia in the Irving Formation near Highland Mary Lakes. Note the abundant elongate fragments that are flattened subparallel to coplanar S_1 and S_2 tectonic foliations.

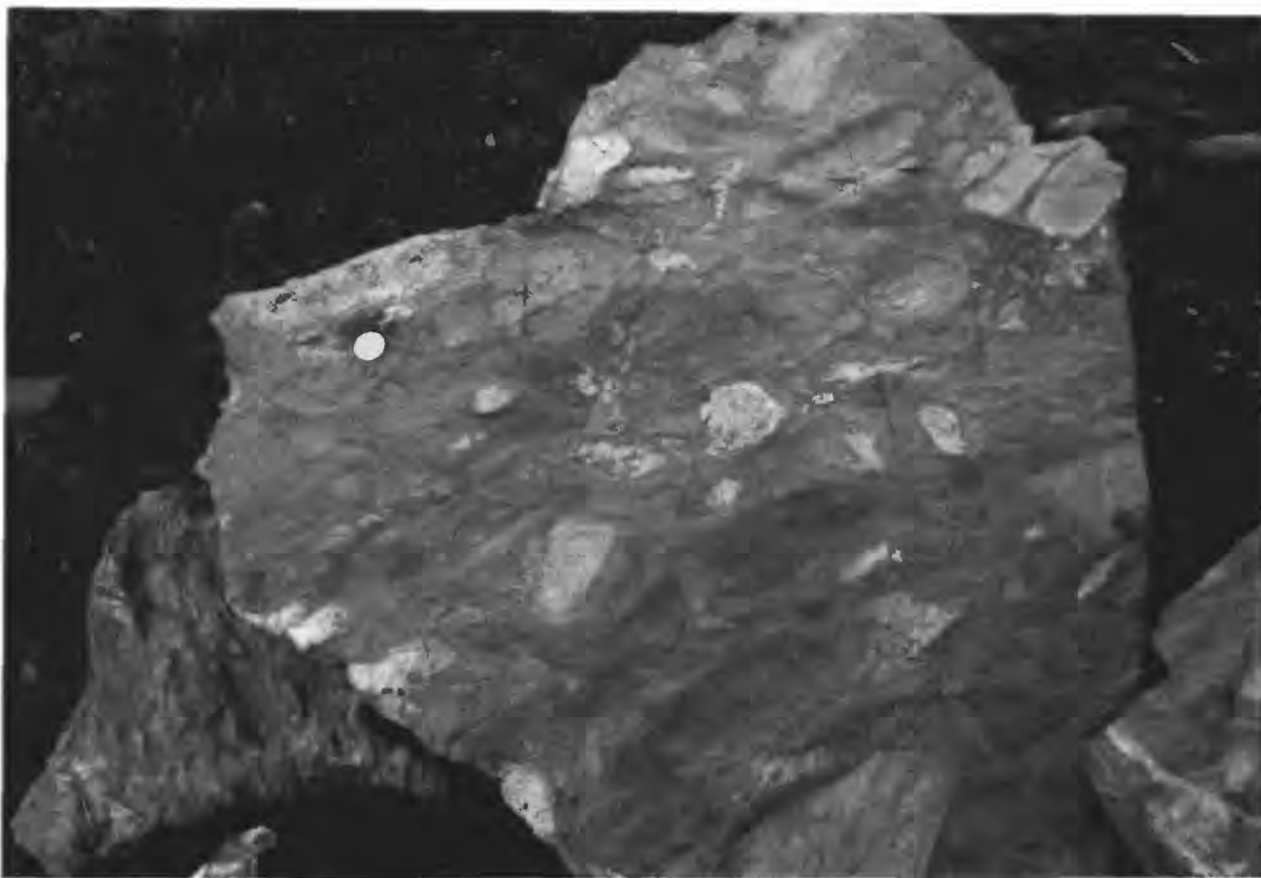


Figure 11: Metamorphosed polymict conglomerate with pebble- and cobble-sized clast of intermediate to mafic volcanic rock. These debris flow deposits, along with turbiditic sandstones and siltstones, occur in the volcanic succession east of Table Mountain in the southeastern Needle Mountains.

Collectively, rocks of the Irving Formation are interpreted as metamorphosed and deformed juvenile magmatic arc and back-arc complex that share similarities in constitution, mode and environment of formation, and tectonic histories with other 1800-1700 Ma suites in the Southwest (e.g., DePaolo, 1981; Condie, 1982, 1986; Nelson and DePaolo, 1984; Reed and others, 1987; Tweto, 1987; Van Schmus and others, 1993). Their history is especially similar to the more extensively studied Early Proterozoic volcano-plutonic rocks in the Gunnison-Salida area, roughly 150 km to the north (e.g., Boardman, 1986; Boardman and Condie, 1986; Bickford and Boardman, 1984; Bickford and others, 1989; Condie and Nuter, 1981; Knoper, 1986; Knoper and Condie, 1988). However, rocks in the Irving Formation are slightly older than most other pre-1700 Ma volcanogenic assemblages in Colorado, Arizona, and New Mexico (e.g., Karlstrom and others, 1987; Reed and others, 1987; Tweto, 1987; Premo and Van Schmus, 1989; Van Schmus and others, 1993).

Twilight Gneiss (metamorphosed trondhjemitic-tonalitic intrusive suite)

Deformed and metamorphosed trondhjemitic to tonalitic gneisses and thin amphibolite sheets exposed in the western and northern Needle Mountains make up the Twilight Gneiss of Barker (1969) (Figures 1 and 9). Cross and others (1905) called these rocks the Twilight Granite (Figure 9), and interpreted the trondhjemitic to tonalitic gneisses as plutonic rocks that intruded the Irving Formation. They also suggested that the amphibolites in the Twilight were "fragments" of amphibolite from the Irving Formation. The intrusive origin for the Twilight Gneiss proposed by Cross and others (1905) was based largely on relationships that they observed in the Electra Lake area (Figures 1, 2, and 5). At this locality, amphibolite layers in the Twilight Gneiss have undergone brittle deformation, and tension fractures resulting from this event are filled with undeformed granitoid that is gradational with adjacent trondhjemitic gneiss (Figure 12). Cross and others (1905) argued that undeformed granitoid in these tension fractures was related to intrusion of Twilight rocks into the Irving Formation. Brittle deformation of amphibolite layers in the Twilight Gneiss was interpreted as intrusive brecciation of "fragments" of the Irving Formation. Recent detailed mapping in this area shows that the brittle deformation and granitoid injection post-dates all tectonic events recorded in the Twilight Gneiss and Irving Formation (Gonzales and others, 1993; Gonzales and others, 1994). Furthermore, these features are concentrated in an aureole of the Electra Lake Gabbro and appear to be closely tied to the emplacement of this body at ~1435 Ma. Gonzales and others (1994) suggest the fractures and associated granitoid stringers are related to deformation and crustal anatexis during Middle Proterozoic plutonism, rather than Early Proterozoic intrusive activity.

Barker and coworkers (Barker, 1969; Barker and others, 1969; Barker and Peterman, 1974; Barker and others, 1976) proposed that the Twilight Gneiss was either a bimodal volcanic complex, or basaltic flows that were intruded by hypabyssal porphyritic dacite to quartz latite sills. Recent work in the Twilight Gneiss suggests that it is composed largely of metamorphosed trondhjemitic, tonalitic, and minor granodioritic intrusive rocks (Harris and others, 1987; Gibson, 1987; Gibson and Simpson, 1988; Gonzales and others, 1993; Gonzales, unpublished field data). An intrusive origin for these rocks is supported by their lithologic association, textural and compositional homogeneity, internal crosscutting relationships (Figure 13), and occurrence of intrusive features such as xenoliths (Figure 14). Most of these rocks are medium- to coarse-grained, but locally in the Lime Creek area (Figure 1) there are small masses of trondhjemitic gneiss that contain 10-50%, 3-10 mm, ellipsoidal crystals of quartz and feldspar that are set in a fine-grained matrix. These quartz-phyrlic lithologies are interpreted as a porphyritic hypabyssal intrusive rocks that are slightly younger than associated coarser-grained rocks in the unit. Barker and others (1969) reported "crudely bipyramidal aggregates of quartz" that they interpreted as relict volcanic quartz



Figure 12: Interlayered amphibolite and trondhjemitic gneiss in the Twilight Gneiss at Electra Lake. Brittle fractures that cut the amphibolite layers (dark rocks) locally become ductile shear zones in adjacent trondhjemitic gneiss. Fractures and shear zones are filled with undeformed granitoid that extends from layers of trondhjemitic gneiss. These undeformed granitoid stringers are interpreted as partial melt fractions that were generated by melting of the gneisses during intrusion of the Electra Lake Gabbro. The photograph shows about 4 meters of outcrop perpendicular to layering.



Figure 13: Metamorphosed gabbro (dark rock) and xenolith-bearing tonalitic gneiss of the Twilight Gneiss in the Lime Creek area. Gabbro intruded the tonalite prior to deformation and amphibolite facies metamorphism. Note that mafic xenoliths in the tonalitic gneiss are cut by the gabbro, and that a strong tectonic foliation (S_1 , S_2) trends across the contacts of these rocks.



Figure 14: Xenolith-rich tonalitic gneiss in the Twilight Gneiss, Lime Creek area. Xenoliths (mafic) are flattened subparallel to tectonic foliation (S_1 , S_2). Similar xenolith-rich zones occur throughout the Twilight Gneiss, and in some outcrops the xenoliths define F_1 and F_2 tight to close folds. Compass for scale is seen in the lower left part of the photo.

phenocrysts. Our petrographic studies of all lithologies in the Twilight Gneiss show that relict quartz phenocrysts are flattened and recrystallized into lenticular polygranular aggregates, however, no bipyramidal crystals were observed.

Thin amphibolite layers of the Twilight Gneiss are interpreted as swarms of fine- to coarse-grained gabbroic sills and dikes that intruded the trondhjemitic-tonalite complex (Gibson, 1987; Gibson and Simpson, 1988; Gonzales and others, 1993), and not as "fragments" of Irving Formation as suggested by Cross and others (1905). These amphibolite layers are typically 1-2 m thick and continue along strike for tens to hundreds of meters, are texturally and compositionally homogeneous, and locally cross cut the contacts of trondhjemitic and tonalitic lithologies. Gabbroic intrusives are also found in volcanogenic sequences of the Irving Formation in the Highland Mary Lakes area (Figure 1), and appear to be equivalent to the metamorphosed mafic intrusives in the Twilight Gneiss. At some localities in the Lime Creek and Electra Lake areas (Figure 1), the Twilight Gneiss contains hundreds of subparallel layers of amphibolite over < 1-2 kilometers across strike. Recent detailed mapping (Gonzales, unpublished) in the Lime Creek area also reveals that along strike for 3-4 kilometers, only local tectonic repetition of these layers occurs.

Until recently (Gonzales and others, 1993) an intrusive relationship of the Twilight Gneiss with the Irving Formation was not documented, other than the one proposed by Cross and others (1905) in the Electra Lake area. In most localities, interlayered gneiss and amphibolite of the Twilight are in contact with thick successions of amphibolite in the Irving Formation. Compositional layering and tectonic fabrics in both units are generally subparallel near the contacts. However, at the Irving-Twilight boundary exposed on the steep western flank of Animas Canyon in the Needleton area (Figure 1), 2-5-m-thick layers of trondhjemitic gneiss are found in the Irving Formation (Gonzales and others, 1993). These layers of trondhjemitic gneiss are generally subparallel to compositional layering and S_1 - S_2 tectonic foliations in the Irving Formation, but in some outcrops they cut compositional layering in the Irving at low angles. Rocks in the Irving Formation at this locality are thinly laminated and resemble metamorphosed bedded tuffs seen in other parts of the unit. No other definitive field evidence regarding the relative age relations of these units is reported. The relationship seen in the Needleton area is supported by U-Pb zircon ages that give crystallization ages for rocks of the Twilight Gneiss of between 1770-1755 Ma (Appendix I). Ages obtained for rocks in the Irving Formation and Twilight Gneiss suggest that rocks in the Irving Formation are roughly 20-30 million years older. Whether the Irving Formation was deformed before intrusion of the Twilight rocks is uncertain. These units share similar structural and metamorphic histories. However, an early tectonic event in the Irving Formation may have been overprinted by later deformation.

Trondhjemitic and tonalitic gneisses occur in layers that are typically tens to hundreds of meters thick, but locally are less than several meters thick. The trend of layering defined by these rocks is subparallel to that of the amphibolite layers in the Twilight Gneiss. South of the Electra Lake Gabbro, layering in the Twilight Gneiss strikes roughly east-west and dips moderately to steeply to the south-southeast. From north of the Electra Lake Gabbro to Silverton (Figures 1 and 9), the layering and fabrics trend north-northeast and dip moderately to steeply southeast. East of Silverton (Figures 1 and 9), layering in rocks mapped as Twilight Gneiss strikes east-west and generally dips south (Harris and others, 1986, 1987; Gibson, 1987; Gibson and Simpson, 1988; Gibson and Harris, 1992). Axial traces of F_1 and F_2 isoclinal to tight folds and corresponding S_1 and S_2 foliation are subparallel to the compositional layering throughout the Twilight. The trend of compositional layering and tectonic fabrics in the Irving Formation in these areas is also similar to what is observed in the Twilight Gneiss. Layering and deformation fabrics seen in the Irving Formation and Twilight Gneiss thus define a regional sigmoidal pattern.

The Twilight Gneiss is interpreted as an intrusive complex composed of numerous concordant bodies of varying thickness (Gonzales and others, 1993). Folding and flattening

of these rocks has produced mesoscopic repetition and alignment of layers, and features such as boudinage and pinch and swell structure. However, there is no strong field evidence to suggest that tectonic repetition and alignment during folding and transposition produced the numerous subparallel layers seen throughout the Twilight Gneiss. In contrast, most observations indicate that the layering is probably a reflection of primary intrusive relationships produced by the widespread emplacement of sills and dikes before deformation and metamorphism.

Gonzales and others (1993) suggest that emplacement of the subparallel intrusives in the Twilight Gneiss occurred during an extensional event. The implications of this are problematic and require further evaluation, particularly regarding the generation of trondhjemitic-tonalitic magmas in this type of tectonic regime. There is a consensus that Early Proterozoic suites throughout the Southwest formed in arc systems (e.g., Reed and others, 1987; Van Schmus and others, 1993). Extension and dike emplacement could have accompanied compressional tectonism in a volcanic arc, or occurred as a separate and distinct event. Emplacement of gabbroic dike swarms into older granitoid gneiss and greenstones during extension is documented in a number of Archean and Proterozoic crystalline complexes (e.g., Tarney and Weaver, 1987; Fahrig, 1987).

Tenmile Granite & related rocks (deformed Early Proterozoic granitoids)

Deformed granitoid intrusive rocks that give U-Pb zircon ages of between 1735-1715 Ma (Appendix I, NMGC21 and NMGC23) intrude the Irving Formation and Twilight Gneiss throughout the western and northern Needle Mountains (Figures 1 and 9). This group consists mostly of medium- to coarse-grained, calc-alkaline granite and monzonite (Barker, 1969) that form the Tenmile Granite, and small stocks exposed about 6 kilometers south of Silverton (Figures 1 and 9). Also included are deformed granitic dikes and sills that cut rocks of the Irving Formation and Twilight Gneiss in the vicinity of Electra Lake, and in the area north of the Uncompahgre Formation between the Animas River and Highland Mary Lakes (Figures 1 and 9). All of these rocks exhibit a weak to strong tectonic foliation, and dikes and sills of this group are locally boudinaged and folded (Gibson, 1987; Gibson and Simpson, 1988; Gonzales, unpublished data).

The granitoid intrusives that occur in the Animas River-Highland Mary Lakes region were originally assigned to Cross and others (1905) Whitehead Granite. As originally defined, the Whitehead Granite apparently included rocks of both the Twilight Gneiss and a younger deformed intrusive suite (Barker, 1969; Bickford and others, 1969). Because of similarities in age (Silver and Barker, 1969; Bickford and others, 1968, 1969), rock types, and general history, Barker (1969) proposed that the younger granitic rocks of the Whitehead Granite be included as part of the Tenmile Granite. This correlation and nomenclature are used in this discussion.

A previous age of about 1700-1690 Ma was obtained for the Tenmile Granite and related rocks in the Whitehead Granite (Cross and others, 1905) from U-Pb zircon analyses (Silver and Barker, 1969), and Rb-Sr whole-rock isochron ages (Bickford and others, 1968, 1969). Recent U-Pb zircon studies indicate that the Tenmile Granite is about 1720-1715 Ma (Appendix I, NMGC21). Age determinations on the granitic rocks from the area between Animas River and Highland Mary Lakes have not been attempted since the work done in the late 1960's. However, a sample of one of the deformed granitic sills and dikes that cuts the Irving Formation in the Electra Lake area yields a U-Pb zircon age of 1731 ± 10 Ma (Appendix I, NMGC23). This new data suggests that older granitoid suite in the Needle Mountains consists of deformed intrusives that were emplaced between about 1735-1715 Ma.

Most previous workers propose that rocks of the Uncompahgre Formation were deposited unconformably upon the Tenmile Granite and related intrusive rocks (Cross and others, 1905; Barker, 1969; Harris and others, 1986, 1987; Gibson, 1987; Harris, 1987;

Gibson and Simpson, 1988; Gibson, 1990; Harris, 1990; Gibson and Harris, 1992). There has also been a consensus that these granitoids were deformed after deposition of the Uncompahgre Formation and Vallecito Conglomerate (Barker, 1969; Bickford and others, 1969; Tewksbury, 1985; Harris and others, 1986, 1987; Gibson, 1987; Harris, 1987; Gibson, 1990; Harris, 1990). Results from recent studies suggest that deformation of "Whitehead" granitoids exposed north of the Uncompahgre Formation occurred during a second episode of folding in the siliciclastic cover assemblage (F_{2C} or F_{3B} of Harris and others, 1986; Harris and others, 1987; Gibson, 1987; Harris, 1987; Gibson, 1990; Harris, 1990; Gibson and Harris, 1992). This is based largely on the observations that a subvertical, east-west striking " S_{3B} " foliation developed in the Tenmile Granite is parallel to " F_{3B} " axial surfaces, and "Whitehead" dikes are folded by " F_{3B} " and boudinaged in the limbs of these structures.

There is no question that the post-1700 Ma deformation event recorded in the Uncompahgre Formation and Vallecito Conglomerate affected the Tenmile Granite and associated intrusives. However, many of the structures observed in the 1730-1715 Ma intrusive suite in the western and northern Needle Mountains could have developed during or shortly after their emplacement. We propose that deformation of these granitoids was pre- or syn-tectonic and preceded intrusion of the post-tectonic Bakers Bridge Granite, and deposition of siliciclastic sedimentary assemblages in the Needle Mountains complex. This is supported by the close spatial occurrence of deformed ~1730 Ma dikes and undeformed ~1700 Ma Bakers Bridge Granite, at similar crustal levels.

Magmatism between 1730-1720 Ma that accompanied or shortly followed a major deformational event in the Needle Mountains complex, closely parallels similar events at other places in the Southwest. Syntectonic plutons and related intrusives of this age are common in north-central Colorado (e.g., Premo and Van Schmus, 1989; Tweto, 1987; Reed and others, 1987; Reed and others, 1993), the 1730-1720 Ma Gunnison plutonic complex in west-central Colorado (Bickford and others, 1989), and Sangre de Cristo Range about 200 kilometers to the east (Figure 8) (T. Sabin, personal communication). In central Arizona the East Verde River Formation with tuffs as young as 1720 Ma (Karlstrom and Bowring, 1993) were isoclinally folded, then unconformably overlain by the Tonto Basin Supergroup at about 1700 Ma (Wrucke and Conway, 1987, 1993; Conway and others, 1987). Histories appear to be similar at other sites in western Arizona and northern New Mexico. In the Yavapai province in northern New Mexico and southern Colorado late magmatism and deformation were followed by cratonic magmatism and sedimentation of the Mazatzal province at 1700-1680 Ma (Conway and others, 1994). In the Needle Mountains, this cratonic magmatism and sedimentation are represented by the Bakers Bridge Granite and siliciclastic sedimentary rocks of the Vallecito Conglomerate and Uncompahgre Formation.

Bakers Bridge Granite & related rocks (undeformed Early Proterozoic granitoids)

A pluton of undeformed medium- to coarse-grained granite and "alaskite" with minor quartz monzonite make up the Bakers Bridge Granite (Barker, 1969). Bickford and others (1969) also mapped a small mass of biotite-muscovite granite on the southern edge of this body. These rocks intrude the Irving Formation at the southernmost extent of Precambrian exposures in the western Needle Mountains (Figures 1 and 9), and the contact of these units is marked by a zone of intrusive breccia that contains abundant angular fragments of amphibolite. A sample of potassium feldspar-phyric magnetite-biotite-hornblende granite exposed at Bakers Bridge yields a U-Pb zircon age of 1699 ± 7 Ma. This suggests the Bakers Bridge Granite is roughly 15-30 million years younger than the older deformed granitoids in the Needle Mountains. The Bakers Bridge Granite is similar in many respects to other post-tectonic ~1700 Ma granitoids that occur throughout the Southwest (Van Schmus and others, 1993).

The Bakers Bridge Granite differs markedly from the Tenmile Granite and related deformed intrusive rocks. The Tenmile suite is composed largely of strongly foliated, grayish biotite-rich granite to diorite that have complex internal intrusive relations and contain abundant xenoliths. In contrast, the Bakers Bridge Granite is almost entirely a homogeneous reddish granite with no discernible tectonic fabrics. A few geochemical analyses reported for the Bakers Bridge Granite (Barker, 1969) show that these rocks are low in Ca and Mg, and high in Na and K. These signatures are similar to red(oxidized) high-crustal-level ~1700 Ma granitoids that are widespread in central Arizona, and that occur in some places in northern New Mexico and southern Colorado. This suite of post-orogenic granitic intrusive and related volcanic rocks have A-type affinities and share some characteristics with the 1500-1300 Ma transcontinental anorogenic magmatic suites (Conway, 1976, 1991; Conway and others, 1994). Rocks of this generation, especially the supracrustal rocks, have been extensively affected by foreland folding and thrusting of the Mazatzal orogeny at about 1650 Ma. However, as in the case of the Bakers Bridge Granite, they locally are unaffected by this deformational event, possibly because they lie below levels of generally thin-skinned thrusting, or are otherwise sheltered from later deformation.

Vallecito Conglomerate & Uncompahgre Formation (siliciclastic sedimentary successions)

Deformed greenschist facies siliciclastic sedimentary rocks of the Vallecito Conglomerate and Uncompahgre Formation are exposed in an arcuate belt that extends from the western to the southeastern Needle Mountains (Figures 1 and 9). Marine and fluvial sandstone, shale, and mudstone comprise the Uncompahgre Formation while the Vallecito Conglomerate consists of a thick succession of fluvial pebble- to cobble-conglomerate, quartz-rich sandstone, and subordinate mudstone and siltstone.

There are no absolute ages for rocks in either the Vallecito Conglomerate or Uncompahgre Formation. Most workers have concluded that the Vallecito was deposited unconformably upon the Irving Formation (Cross and others, 1905; Burns and others, 1980; Ethridge and others, 1984; and Gonzales, 1988a, 1988b) (Figure 7). In addition, field studies in the western and northern parts of the Needle Mountains complex show that Uncompahgre Formation was deposited unconformably upon the Irving Formation, Twilight Gneiss, and 1720-1715 Ma granitoids (Barker, 1969; Harris and others, 1986, 1987; Gibson, 1987; Harris, 1987; Gibson, 1990; Harris, 1990). Recent U-Pb analyses (Aleinikoff and others, 1993) of detrital zircons from a sample of Uncompahgre quartzite yield $^{207}\text{Pb}/^{206}\text{Pb}$ ages of between 1735-1655 Ma, and four of these five fractions give a co-linear trend with an upper intercept age of about 1690 Ma. This data suggests that the Uncompahgre Formation is post-1690 Ma, and that pre-1695 Ma crystalline rocks in the Needle Mountains were probably a source of detrital zircons in the Uncompahgre. Both the Uncompahgre Formation and Vallecito Conglomerate are cut by the Eolus Granite, which places a lower age bracket of 1435 Ma for deposition and deformation in these units. However, given the similarities of these rocks to other 1700-1650 Ma siliciclastic sedimentary rocks in central Arizona and northern New Mexico, they are most likely part of this group.

The Vallecito Conglomerate consists of siliciclastic fluvial successions that attain a maximum thickness of at least 1000 meters. This unit is composed mostly of matrix- to clast-supported pebble to boulder conglomerate and fine- to coarse-grained sandstone that are locally interbedded with thinly laminated siltstone. Conglomerates in this unit contain subangular to subrounded fragments of massive or laminated quartzite, vein quartz, chert, jasper, banded-iron formation, argillite, and metamorphosed felsic to mafic schist and gneiss that typically have relict igneous textures (Cross and others, 1905; Barker, 1969; Burns and others, 1980; Ethridge and others, 1984; Gonzales, 1988a, 1988b). Quartzite clasts are generally dominant but clasts of mafic to felsic schist and gneiss comprise between 10-90% of basal conglomeratic deposits in the Table Mountain area (Figure 1). These incompetent

clast lithologies are also dominant in the conglomerate of Fall Creek which Gonzales (1988a, Figure 7) interprets as a basalt facies of the Vallecito Conglomerate. Rocks in the Vallecito Conglomerate were deposited in a high energy fluvial system, primarily as proximal braided stream and debris flow deposits (Burns and others, 1980; Ethridge and others, 1984; Gonzales, 1988a, 1988b).

A strong tectonic overprint is generally not seen in the Vallecito Conglomerate. It consists mostly of well-preserved sedimentary successions that are unfoliated or only weakly foliated. However, rocks in the basal sections exhibit a strong foliation, mineral and pebble tectonic lineations, and multiple episodes of mesoscopic folding and ductile shearing (Gonzales, 1988a, 1988b). Deformation recorded in the Vallecito Conglomerate involved the generation of a series of macroscopic folds whose axial surfaces trend roughly north-south. The most prominent structure seen is an upright to steeply inclined, gently to moderately south-plunging anticline that is exposed in the Hell Canyon-Dollar Lake area (Figure 6 and Plate 2). Gonzales (1988a, 1988b) argues that the conglomerate of Fall Creek is exposed in a faulted macroscopic syncline in the Vallecito Creek area and infers several other major folds in the Vallecito Conglomerate (Figures 1, 6, 9, and Plate 2). Due to the lack detailed of studies, however, the structural record in the Vallecito Conglomerate is still poorly constrained.

The Uncompahgre Formation consists of metamorphosed successions of quartz-rich sandstones, shales, mudstones, and minor conglomerates that are up to 2500 meters thick. The tectonic and depositional histories of these rocks have been the subject of several recent detailed studies (Tewksbury, 1981, 1982, 1984, 1985, 1986; Harris, 1987; Harris and Eriksson, 1987, 1990; Harris, 1990). A transitional alluvial to shallow marine shelf depositional environment for the Uncompahgre Formation is suggested by Harris (1987), Harris and Eriksson (1990), and Harris (1990). This agrees with earlier conclusions by Cross and others (1905) and Barker (1969) regarding the general depositional history of these rocks. Deformation in the Uncompahgre involved multiple episodes of folding (Tewksbury, 1981, 1985; Harris and others, 1986, 1987; Harris, 1987; Harris, 1990), and an early episode of north-directed thrusting (Harris and others, 1986, 1987; Harris, 1987; Harris, 1990).

Though the Vallecito Conglomerate and Uncompahgre Formation share some similarities in depositional and structural records, their stratigraphic relationship remains uncertain. Both units are exposed in the area east of Table Mountain (Figure 1), but they are nowhere in direct contact. Most previous workers have considered the Uncompahgre Formation to be younger than the Vallecito Conglomerate (Cross and others, 1905; Barker, 1969; Burns and others, 1980; Ethridge and others, 1984). Burns and others (1980) and Ethridge and others (1984) suggested that these units may be partly time correlative. This is supported by the overall compositional maturity of rocks in the Vallecito and Uncompahgre, and stratigraphic position of both units relative to pre-1695 Ma crystalline complex in the Needle Mountains.

Eolus Granite, Electra Lake Gabbro, Trimble Granite, & related rocks (Middle Proterozoic intrusive suite)

Early Proterozoic crystalline and siliciclastic assemblages in the Needle Mountains (Figure 1) are cut by ~1435 and ~1350 Ma calc-alkaline plutonic rocks of the Electra Lake Gabbro, Eolus Granite, quartz diorite of Pine River, and Trimble Granite (Figure 9) (Bickford and others, 1968, 1969; Silver and Barker, 1968; Gonzales and others, 1994). Emplacement of this spectrum of Middle Proterozoic intrusive rocks marks the final episode in the Precambrian record of the Needle Mountains. New and previous geochemical and isotopic data suggest that these plutonic rocks are genetically related, and that some were derived by partial melting of depleted mantle or fractionation of such melts (Bickford and others, 1969; Collier, 1989; Gonzales and others, 1994).

New U-Pb zircon ages indicate that both the Electra Lake Gabbro and Eolus Granite are ~1435 Ma (Gonzales and others, 1994; Appendix I, NMGC7 and NMGC27). The ~1435 Ma age for the Electra Lake Gabbro is supported by Sm-Nd whole rock and mineral separate ages of 1430 ± 25 Ma and 1451 ± 41 Ma (Gonzales and others, 1994; Appendix II). These data are consistent with previous U-Pb zircon analyses (Silver and Barker, 1968), and Rb-Sr whole-rock and mineral isochron data (Bickford and others, 1968, 1969), that yield ages of about 1450-1440 Ma for these units. A close temporal association of these rocks is supported by their cross-cutting relationships (Barker, 1969). Granitic dikes related to the Eolus Granite locally cut the Electra Lake Gabbro (Gonzales and others, 1994) (Figures 1 and 9), and part of the western mass of the Eolus Granite is cut by the Electra Lake Gabbro (Figure 5 and Plate 1).

Medium- to coarse-grained, porphyritic or equigranular, granitic to granodioritic rocks of the Eolus Granite comprise batholithic masses in the central and eastern parts of the complex (Figures 1 and 9). The eastern mass is intruded by a stock of diorite which Barker (1969) calls the quartz diorite of Pine River, and the western body of the Eolus Granite is cut by a small pluton of biotite monzogranite and granite (Barker, 1969; Collier, 1989) that make up the ~1350 Ma Trimble Granite (Silver and Barker, 1968; Bickford and others, 1968, 1969) (Figure 9). Intrusion of these plutons was accompanied by the widespread emplacement of aplite, granitic pegmatite, and medium- to coarse grained granitoid dikes.

Collier (1989) shows that rocks of the Eolus Granite share some mineralogic and chemical signatures with A-type anorogenic granites, but also have chemical traits of I-type calc-alkaline arc magmas. His data indicate that these rocks are metaluminous to peraluminous, and are characterized by LREE enriched and HREE depleted chondrite-normalized patterns with moderate to strong negative Eu anomalies. On the basis of geochemical data, Collier (1989) proposes that the Eolus Granite and related rocks formed by fractionation of magmas generated by melting of an underplated mantle wedge in a subduction system, possibly during the transition from compressional to extensional tectonism. He also suggests that the ~1350 Ma Trimble Granite (Silver and Barker, 1968; Bickford and others, 1968, 1969) formed by similar processes, calling on partial melting of a single melt reservoir or multiple source areas to produce the 1435-1350 Ma intrusive suite.

Five samples of the Eolus Granite yield $\epsilon_{Nd(t)}$ values of 0.86-1.77 with corresponding crust-formation ages (T_{DM}) of 1804-1709 Ma (Gonzales, unpublished data). Initial $^{87}Sr/^{86}Sr$ ratios of 0.7043-0.7050 were obtained by Bickford and others (1969) for several samples of Eolus Granite from Rb-Sr whole-rock and mineral separate isochrons. These Sm-Nd and Rb-Sr isotopic data are consistent with the generation of Eolus Granite by fractionation of magmas formed by melting of a slightly depleted (relative to CHUR) mantle reservoir or primitive crust. The positive $\epsilon_{Nd(t)}$ values for samples of Eolus Granite contrast with the negative epsilon signatures typical of most ~1400 granitoids in the Southwest. Other granitoids with positive $\epsilon_{Nd(t)}$ values include the Dells Granite, Lawler Peak Granite, and Oracle Granite in Arizona, and Rana Granite in New Mexico (Bickford and Anderson, 1993).

The Electra Lake Gabbro is a rare mafic component of 1470-1360 Ma "anorogenic" plutonic suite that extends NE-SW across the United States (e.g., Reed and others, 1993; Bickford and Anderson, 1993). It is composed of medium- to coarse-grained hypersthene-augite ophitic gabbro with minor diorite, granodiorite, and pegmatitic gabbro (Cross and others, 1905; Barker, 1969; Tweto, 1987; Gonzales and others, 1994) (Figures 1, 5, 9, and Plate 1). These rocks are generally equigranular and massive, but locally show a pronounced E-W trending magmatic foliation. They also show a ubiquitous late-stage deuteritic recrystallization that is reflected in amphibole and biotite rims around pyroxenes.

The exposed parts of the Electra Lake Gabbro are dominated by a pear-shaped main mass that is roughly 5 km long and up to 3 km wide (Figure 9 and Plate 1). It is located in the core of a steep to upright, open to gentle, pre-1700 Ma fold that plunges steeply to the southeast. This fold forms the southern bend of a regional sigmoidal structure defined by

subparallel aligned compositional layering and tectonic fabrics in the Twilight Gneiss and Irving Formation (i.e., S_1 and S_2 tectonic foliations related to F_1 and F_2 isoclinal to tight folds). In addition to the main mass of the gabbro there is a smaller satellite body exposed farther to the south (Figure 5 and Plate 1), and numerous dikes and sheets that extend from these larger masses.

Sm-Nd whole-rock data for 15 samples of the Electra Lake Gabbro give $\epsilon_{Nd(t)}$ values of 0.92-2.90 with crust-formation ages (T_{DM}) between 1842-1618 Ma (Gonzales and others, 1994; Appendix II). The highest $\epsilon_{Nd(t)}$ value obtained falls about 2-3 epsilon below the depleted mantle curve of Depaolo (1981) at $t = 1435$ Ma. These data suggest that the parent magma of the Electra Lake Gabbro was generated by partial melting of a slightly depleted mantle reservoir or high degrees of melting of primordial mafic crust. Because the second option requires nearly complete melting of only mafic crustal rocks, it is not preferred. The range of $\epsilon_{Nd(t)}$ values observed in the Electra Lake Gabbro might be attributed to crustal contamination of a mantle-derived melt, but there is no petrologic or geochemical evidence for crustal contamination in these rocks. Extensive contamination by an evolved crustal component would be necessary if the melt was derived from a depleted mantle with an evolution curve similar to that of Depaolo (1981). Further geochemical studies are needed to fully evaluate the petrogenesis of mafic rocks of the Electra Lake Gabbro.

Multiply deformed, amphibolite facies, trondhjemitic to tonalitic gneisses and interlayered amphibolite sheets in the Twilight Gneiss bound the main mass of the Electra Lake Gabbro to the north and south (Figure 5 and Plate 1). Brittle deformation of amphibolite layers in the Twilight Gneiss and locally in the Irving Formation occurs within an aureole of the Electra Lake Gabbro. The deformation is manifested in a profusion of cross-cutting and anastomosing fractures that are commonly filled with undeformed granitoid dikelets and stringers (Figures 12, 15, and 16). In most outcrops the undeformed dikelets consist of graphically intergrown or massive equigranular assemblages dominated by quartz and plagioclase with minor biotite, and are gradational into adjacent trondhjemitic gneiss layers. As mentioned previously, Cross and others (1905) argued that the Twilight Gneiss was intrusive in origin, and that the brittle deformation and granitoid stringers seen in it in the Electra Lake area were formed by intrusive brecciation of amphibolite fragments from the Irving Formation (Figures 1 and 9). Barker (1969) proposed that partial melting of trondhjemitic gneisses in the Twilight Gneiss during high-grade metamorphism produced the undeformed granitoids that were then injected into tensional fractures. The close temporal relationship implied by Cross and others (1905) for the undeformed granitoids and trondhjemitic gneiss was based largely on their gradational contacts. However, Barker (1969) correctly recognized that the granitoid stringers were undeformed and that they cut structural fabrics in Twilight Gneiss.

Our work demonstrates that brittle deformation and related granitoid injection around the Electra Lake Gabbro post-dates pre-1435 Ma tectonic events (Figures 15 and 16) recorded in the Twilight Gneiss and Irving Formation (Gonzales and others, 1993; Gonzales and others, 1994), but are not recorded in the Electra Lake Gabbro. This event is reflected in ductile and brittle deformation that is concentrated in an aureole of the Electra Lake Gabbro suggesting a close tie to its emplacement, and is locally recorded in rocks of the Eolus Granite. Contrary to the conclusions of Cross and others (1905) and Barker (1969), we conclude that the deformation and anatexis recorded in Early Proterozoic rocks in the western Needle Mountains accompanied the emplacement of mantle-derived melts at mid- to upper-crustal levels during N-S shortening at ~ 1435 Ma. Contraction accompanied by extension and disruption of surrounding crystalline basement may have provided a pathway for intrusion of basaltic magma. Thermal effects of this event are reflected in partial melting trondhjemitic gneisses in an aureole of the gabbro with injection of partial melt fractions into brittle fractures and associated shear zones. Softening of the crust during intrusion of the Electra Lake Gabbro probably facilitated movement of the pluton to middle to upper crustal

levels. Heat necessary for melting of country rocks was provided by the main mass and satellite bodies of the Electra Lake Gabbro, and heat and fluids associated with the nearby Eolus Granite. Brittle deformation associated with Middle Proterozoic mafic magmatism in the Needle Mountains agrees with existing evidence for relatively shallow levels of emplacement for many of the 1470-1360 Ma intrusive bodies at depths of 10-16 km (see discussion in Bickford and Anderson, 1993).

Melting of trondhjemitic gneisses of the Twilight Gneiss during emplacement of the Electra Lake Gabbro is reflected in melt-filled fractures and breccia zones within 1-1.5 kilometers of the pluton margins. There is a gradual increase in degree of thermal softening toward the main mass of the Electra Lake Gabbro. Zones composed of variably rotated angular blocks of amphibolite in a matrix of unfoliated to weakly foliated trondhjemitic gneiss are common within ~0.5 kilometers of the pluton. These zones resemble intrusive breccia and within them there is a transition from strongly foliated gneiss to massive granitoid that has undergone nearly complete recrystallization and fabric annealing. In many outcrops only vestiges of the tectonic fabrics of the gneiss are preserved. In addition to these melt breccias, undeformed granitoid dikelets and stringers inject brittle fractures and ductile shear zones in the country rocks within 1-1.5 kilometers of the main mass of the Electra Lake Gabbro. These dikelets and stringers generally extend from trondhjemitic gneiss layers that record multiple generations of folds and related ductile fabrics produced during pre-1435 Ma metamorphism and deformation (Gonzales and others, 1994). Although melt-filled fractures and shear zones are typically concentrated in more competent amphibolite layers they also locally cut tonalitic and trondhjemitic gneiss layers in the Twilight Gneiss. Partial-melt injections and breccia zones in the contact aureole are locally cut by ~1435 Ma granitic dikes that are related to the Eolus Granite (Silver and Barker, 1968; Barker, 1969). Similar dikes also cut the Electra Lake Gabbro. Locally, stringers from these granitic dikes fill brittle fractures in amphibolite layers within the contact aureole of the gabbro. In some melt breccia zones, dike material is intimately mixed with partial melt and shows a pronounced tectonic foliation. The involvement of Eolus Granite intrusives in this melting and deformation provides additional constraint on the timing of this event.

Tension fractures in an aureole of the Electra Lake Gabbro are typically planar or curvilinear, subvertical, and millimeters to tens of centimeters thick. Conjugate to en-echelon fracture arrays are common. However, networks composed of interconnected branching and splaying fractures occur in many outcrops, and are dominant within ~0.5 kilometers of the main mass of the pluton. Brittle fractures in the amphibolites locally become ductile shear zones in adjacent layers of trondhjemitic and tonalitic gneiss. These shear zones deflect foliation in the gneisses, commonly form conjugate sets, and provide local pathways for partial melt injection. Brittle fractures and mesoscopic shear zones in an aureole of the Electra Lake Gabbro are dominated by arrays trending 50°-80° northwest and 10°-50° northeast. This conjugate pattern is commonly reflected in mesoscopic fractures and shear bands in which northeast and northwest trending sets typically show sinistral and dextral offset, respectively. These data are consistent with the development of a regional conjugate fracture system under a maximum principal stress oriented between 10° NE to 30° NW. Extension related to this N-S compression is indicated by boudinage in amphibolite layers, E-W and NW-SE tectonic foliation in ~1435 Ma dikes and margins of the western Eolus Granite batholith, and possibly by NW-SE primary magmatic foliation in the Electra Lake Gabbro. Boudinage attributed to this event is reflected in brittle detachment of melt-injected amphibolite layers, and necking that both deforms and is cut by partial melt injections.

The only other 1470-1360 Ma plutonic complex in the Southwest that contains a high proportion of mafic rocks is the Laramie anorthosite complex in Wyoming. This complex contains anorthosite and anorthositic gabbro and genetically related plutons of pyroxene or hornblende monzonite and syenite (Fountain and others, 1981; Goldberg, 1984; Snyder and



Figure 15: Folded layers of amphibolite and trondhjemitic gneiss in the Twilight Gneiss about 0.75 kilometers northeast of its contact with the Electra Lake Gabbro. Enechelon fractures cut the compositional layering, and all tectonic fabrics in these rocks. The fractures are filled with undeformed granitoid that was generated by partial melting of the gneiss layers.



Figure 16: An F_2 fold defined by interlayered trondhjemitic gneiss and amphibolite, and S_2 tectonic foliation. Stringers of undeformed granitoid extend from the upper part of the fold and cut the foliation in the surrounding amphibolite.

others, 1988; Frost and others, 1990; Kolker and others, 1990). Some of the models (Fountain and others, 1981; Snyder and others, 1988) proposed for the generation of these rocks involve partial melting of a mantle reservoir, ponding of this mafic melt at the base of thick continental crust accompanied by crystal fractionation to produce anorthosite, and anatectic melting of crustal rocks to generate more evolved granitoids. Anorthositic magmas are then emplaced diapirically at crustal levels of between 8-15 kilometers (Snyder and others, 1988), and both the anorthosites and granitoids undergo fractional crystallization after emplacement. Fountain and others (1981) suggest that there was partial melting of metamorphic country rocks (e.g., granitoid gneisses) during intrusion of monzonitic intrusives, and that these magmas assimilated variable amounts of this partial melt fraction (Fountain and others, 1981).

Magmatic processes similar to those proposed for the Laramie anorthosite complex may be applicable to the ~1435 Ma granitic to gabbroic intrusive rocks in the Needle Mountains complex. These models are particularly appealing because they provide adequate mechanisms for producing a range of compositions with varying geochemical signatures, as noted by Collier (1989) for rocks of the Eolus Granite. Ponding of a mantle derived melt at the base of thickened crust might also explain the apparent late-stage emplacement of mafic intrusive rocks in the Needle Mountains, after the generation of large volumes of granitoid rocks by fractionation of mantle- and minor crustal-derived melts. Intrusion accompanied by partial melting of older country rocks is an interesting feature documented for both the Electra Lake Gabbro and Laramie anorthosite complex. However, contamination of the Electra Lake Gabbro by partial melt fractions appears to have been minor. Though there are some similarities in these two suites of rocks, they have contrasting isotopic signatures. Samples from the Electra Lake Gabbro and Eolus Granite are characterized by initial $^{87}\text{Sr}/^{86}\text{Sr}$ ratios of less than 0.7052 and positive $\epsilon_{\text{Nd}(t)}$ signatures (Appendix II). Anorthositic to granitic rocks in the Laramie anorthosite complex have negative $\epsilon_{\text{Nd}(t)}$ values (-1.7 to -4.8) and a wider range of initial $^{87}\text{Sr}/^{86}\text{Sr}$ ratios (0.7028 to 0.7130; Subburayuda, 1975; compilation of data in Bickford and Anderson, 1993). The age, lithologic variety, and general histories of 1440-1430 Ma intrusive suites in the Needle Mountains and Laramie anorthosite complex may imply regional similarities in crust-forming processes at ~1400 Ma. Contrasting isotopic signatures probably reflect differences in melt sources and magmatic processes. All evidence for the Needle Mountain suite suggests a genetic tie to mantle-derived melts with minor involvement of S-type melts and contamination by evolved crust.

GENERAL TECTONIC HISTORY OF THE NEEDLE MOUNTAINS COMPLEX

All exposures of Irving Formation and Twilight Gneiss (Figures 1 and 9) record upper-greenschist to amphibolite facies metamorphism, and three or four phases of macroscopic to mesoscopic folding (Cross and others, 1905a, 1905; Barker, 1969; Gibson and others, 1986, 1987; Gibson, 1987; Gibson and Simpson, 1988; Gonzales and others, 1993). Early fold generations consist of F_1 to F_2 (F_{1B} and F_{2B} of Harris and others, 1987, b = basement) tight to isoclinal folds in which the axial traces of the folds and associated S_1 and S_2 tectonic foliations are generally subparallel to primary compositional layering (Harris and others, 1986, 1987; Gibson, 1987; Gibson and Simpson, 1988; Gonzales and others, 1993; Gonzales, unpublished field studies). These early structures are deformed by at least two later generations of folds. Detailed structural studies in the Highland Mary Lakes area (Figure 1) show that F_1 - S_1 and F_2 - S_2 structures in the Irving Formation and Twilight Gneiss are overprinted by macroscopic to mesoscopic tight to open folds and related axial planar foliations. These younger structures are considered a third generation of "basement" folds (F_{3B} of Harris and others, 1987) that were produced during F_{2C} in the Uncompahgre Formation (c = cover assemblage; Harris and others, 1986, 1987; Gibson, 1987; Harris, 1987; Gibson and Simpson, 1988). Locally in the Lime Creek and Electra Lake areas (Figure 1) we

have observed mesoscopic close to open folds whose axial traces are oblique to basement F_1 - S_1 and F_2 - S_2 structures. In some cases, these late structures appear to be due simply to progressive ductile deformation in the Twilight Gneiss and Irving Formation, and not a distinct event that occurred during deformation of the Uncompahgre Formation. In the Lime Creek area, a fourth episode of "basement" folding is recognized (Harris and others, 1986, 1987; Gibson, 1987; Gibson and Simpson, 1988). These F_{4B} (Harris and others, 1987) structures are defined by pegmatitic dikes that cut F_{2B} , and tight to open folds with north-northeast or east-striking axial surfaces that deform F_{2B} . This fourth fold generation is described as steeply plunging folds that are not coaxial with F_{1B} and F_{2B} (Gibson, 1987; Gibson and Simpson, 1988).

As mentioned previously, the deformational history of the Vallecito Conglomerate is poorly constrained. The most conspicuous structures are south-plunging macroscopic folds whose axial traces trend roughly north-south. Limbs of folds documented in the Vallecito Conglomerate are cut by north-northeast trending faults that have experienced several episodes of movement accompanied by ductile and brittle deformation (Barker, 1969; Burns and others, 1980; Ethridge and others, 1984; Gonzales, 1988a, 1988b). In contrast, detailed structural studies in the Uncompahgre Formation reveal a complex sequence of events. Different interpretations of the structural history have been proposed (Tewksbury, 1981, 1985; Harris and others, 1987; Harris, 1990). Tewksbury (1981, 1985) suggested that the Uncompahgre was an allochthonous sheet that was emplaced during south-directed thrusting with related polyphase folding. In contrast, more recent work suggests that the Uncompahgre Formation is parautochthonous (Figures 1 and 9) and its deformation involved early north-directed, thin-skinned thrusting that was followed by "cusped" infolding into pre-1695 Ma crystalline rocks (Harris and others, 1986, 1987; Harris, 1987, 1990; Gibson and Harris, 1992). This infolding is thought to have been accompanied by intense shearing on an unconformity at the base of the Uncompahgre Formation with upward movement occurring on both its southern and northern contacts. This second model agrees with the work of Barker (1969). He suggested that erosion of pre-1695 Ma crystalline rocks was followed by deposition of the Uncompahgre Formation that was then folded into the older complex to form the "Uncompahgre synclinorium."

Though there are different models for the tectonic processes in the Uncompahgre, there is general agreement in the style and sequence of folding events and related deformation (see Tewksbury, 1989, Figure 3). Using the designations of Harris and others (1987; b = basement, c = cover) the different deformation events reported are (oldest to youngest): D_{1C} : mesoscopic F_{1C} folds and S_{1C} axial planar slaty cleavage; $D_{2C} = D_{3B}$: macroscopic tight to open F_{3B} folds with axial planar S_{3B} foliation, and macroscopic to mesoscopic tight to open F_{2C} folds with axial planar S_{2C} spaced cleavage; $D_{3C} = D_{4B}$: mesoscopic F_{4B} with axial traces oblique to F_{1B} and F_{2B} and related structures, and mesoscopic to macroscopic F_{3C} folds and S_{3C} spaced cleavages. The D_{3B} event is thought to be responsible for deformation of the Tenmile Granite and related intrusives, but as mentioned previously, we suggest that deformation of these granitoids occurred during or shortly after their emplacement.

Deformation in the Middle Proterozoic intrusive complex in the Needle Mountains is not widely observed. Deformation and partial melting in the Twilight Gneiss occurred during emplacement of the ~1435 Ma Electra Lake Gabbro (Gonzales and others, 1994), and ~1435 Ma dikes and pluton margins of the Eolus Granite locally show an E-W tectonic foliation. Whether this deformation reflects a regional or subregional tectonic event is uncertain. It could have been generated by crustal movements associated with pluton emplacement, rather than a widespread tectonic event.

SUMMARY

On the basis of our recent detailed work, we suggest the following sequence of events in the Needle Mountains Proterozoic complex (Figure 9):

~1805-1780 Ma: Calc-alkaline to tholeiitic magmatism in an arc system producing thick successions of basaltic-andesitic-rhyolitic volcanic rocks and minor mafic intrusives of the Irving Formation.

~1770-1755 Ma: Emplacement of trondhjemitic-tonalitic-granodioritic sill-like bodies. This was followed by the intrusion of numerous gabbroic sheets, probably during extensional tectonism. These rocks collectively make up the Twilight Gneiss.

multi-phase deformation and upper greenschist to lower amphibolite facies metamorphism

~1735-1715 Ma: Granitoid plutonism producing the Tenmile Granite and related granitoid intrusive rocks.

ductile deformation during or shortly after emplacement of the granitoids

~1700 Ma: Post-tectonic granitoid plutonism forming the Bakers Bridge Granite.

extensive erosion

< 1695 Ma: Deposition of the fluvial and marine siliciclastic sedimentary rocks of the Vallecito Conglomerate and Uncompahgre Formation.

multi-phase deformation and greenschist facies metamorphism

~1435 Ma: Calc-alkaline magmatism generating mostly I-type granitic to gabbroic intrusive rocks of the Eolus Granite, Electra Lake Gabbro, and related rocks.

Emplacement of the Electra Lake Gabbro and Eolus Granite during N-S contraction and E-W extension. This event involved deformation and anatexis in the Twilight Gneiss, and local ductile deformation of ~1435 Ma dikes and pluton margins of the Eolus Granite.

~1350 Ma: intrusion of the Trimble Granite and associated dikes and sills.

extensive erosion

Late Proterozoic (?): deposition of quartzite-clast conglomerates as proximal braided stream deposits in channels eroded into older Precambrian rocks. See discussion by Campbell on pages 50-53.

ARE THERE OTHER PRECAMBRIAN CONGLOMERATES IN THE SAN JUAN MOUNTAINS?

BY
JOHN A. CAMPBELL
FORT LEWIS COLLEGE
DURANGO, COLORADO

Cross and Hole (1910) noted in the Engineer Mountain area that the Ignacio Formation as they defined it contained two different kinds of conglomerate. A basal conglomerate that consists of well rounded pebbles, cobbles and boulders of quartzite that was noted in low areas or "hollows" in the underlying Precambrian rocks. The clasts in this conglomerate were derived from the Precambrian Uncompahgre Formation. Lying above this conglomerate in the coarse grained well-bedded sandstones of the Ignacio they noted other conglomerate zones of white, gray or pink pebbles. In this study it has been found that this second type of conglomerate may be a basal conglomerate where the well rounded quartzite clast conglomerate is not present. Baars and Knight (1957) also noted two different kinds of conglomerates in their measured sections of the Ignacio Formation.

Baars (1966) and Baars and See (1968), in developing the paleotectonic framework for the San Juan Mountains, considered the basal well rounded quartzite clast conglomerate, the first type of Cross and Hole, to be a lateral facies of the coarse grained sandstones of the Ignacio Formation.

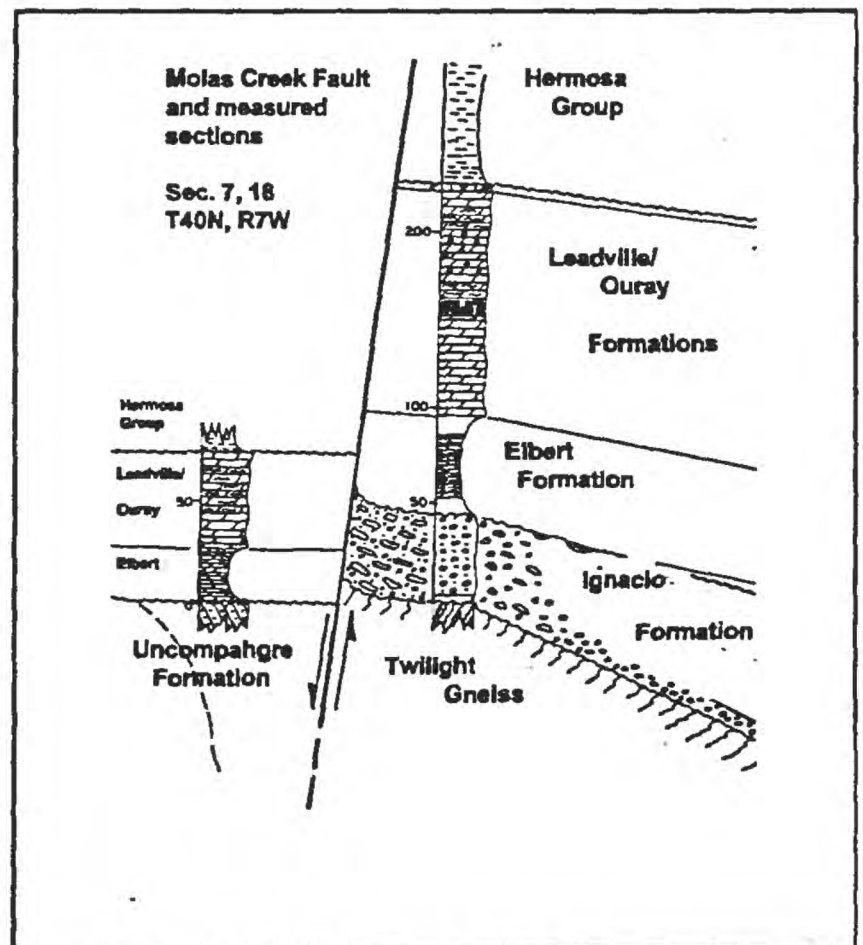


Figure 1: Modified from Baars and See, 1968

It was observed these conglomerates were found near major faults and concluded that they were the result of Cambrian movement on the faults with the development of "talus-like" deposits at the base of the faults. Normal, shallow marine, deposition occurred around these conglomerates at the base of cliffs. Figure 1 shows these relationships as conceived by Baars and See. In addition to suggesting that these conglomerates were lateral facies of Ignacio sandstones they imply that they are Cambrian in age.

In studying the Lower Paleozoic stratigraphic sequences in the San Juan Mountains these basal, well rounded quartzite clast conglomerates have been found in a number of locations (fig. 2). These locations include places that are near faults as well as away from faults, on top of horsts or in grabens as delineated by Baars and See(1968), and on both sides of a fault that was thought to have moved during the Cambrian. In addition major faults were examined in other places that could have had conglomerate associated with them but no conglomerates have been found. These results, or lack thereof, have forced a reexamination of the model for formation as well as age of these deposits.

These conglomerates occur as lenses that fill channels cut in a variety of Precambrian rocks including the Twilight

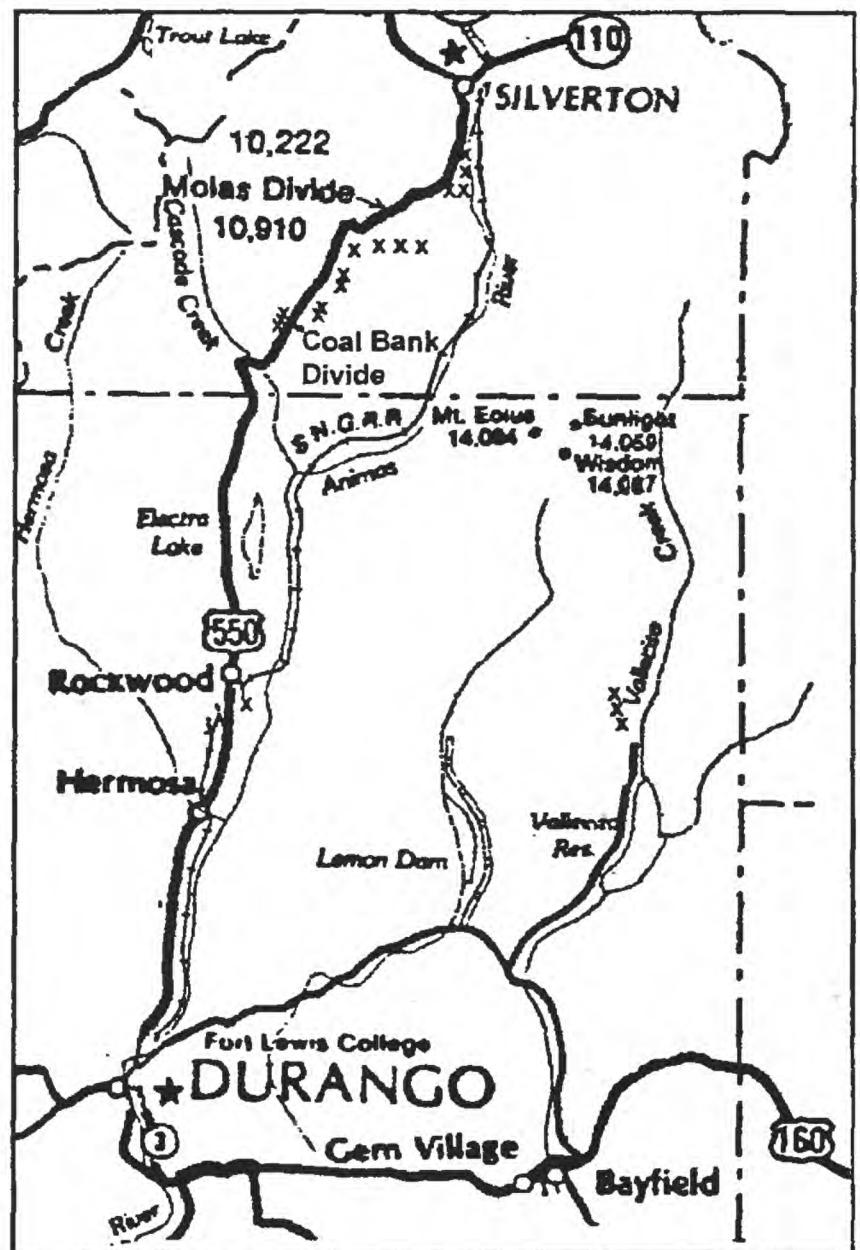


Figure 2: Location Map showing locations of outcrops of quartzite clast conglomerates as shown by an x.

Gneiss, Bakers Bridge Granite, Uncompahgre Formation and Vallecito Conglomerate. The lenses are flat-topped often fining upward in grain size with coarse grained sandstone lenses toward the top. These sandstone lenses are roughly parallel with the tops of the conglomerate lenses and in turn are roughly parallel with the overlying deposits. The overlying deposits are usually the marine sandstones of the remainder of the Ignacio Formation, however, at several locations along the west side of the San Juans the overlying rocks are limestones of the Hermosa Group and at other locations the shales of the Elbert Formation. The size of the conglomerate lenses ranges from a few cms thick up to 30 meters thick and from a few tens of cms wide up to hundreds of meters wide. The length of these channels often cannot be determined, however, one above Vallecito Creek can be traced for several kilometers north to south.

Clast size ranges from a few inches up to three feet in diameter and the clasts are typically well to very well rounded. The clast composition is 100% quartzite. The Uncompahgre Formation is the source for the clasts along the west side of the San Juan Mountains and the Vallecito Conglomerate is the source along Vallecito Creek. A coarse sand matrix is common between clasts at a number of locations however the deposits are clast supported. At several locations along the west side of the San Juan Mountains the clasts show a discoloration rind that is 1 to 3 cm thick measured from the surface of the quartzite clast. These look like weathering rinds that completely encircle the clast.

No sedimentary structures have been found in these conglomerates other than the coarse sandstone lenses near the tops of the deposits. Imbrication is poorly developed, however, imbrication studies have been attempted to get some idea of current directions. Along the west side of the San Juan Mountains the current directions were to the west and to the west-southwest.

A depositional model for these deposits will have to include their composition, roundness, geometry, texture, stratigraphic position, relationship (or lack of) to contemporary structures and approximate age. Two depositional models are shown in figure 3. They seem to be older than the marine, dated portion of the Ignacio Formation, but younger than the youngest source for the clasts, the Precambrian Uncompahgre Formation. Erosionally they have responded as if part of the "basement". Their roundness and compositional maturity along with the weathering rinds suggests antiquity.

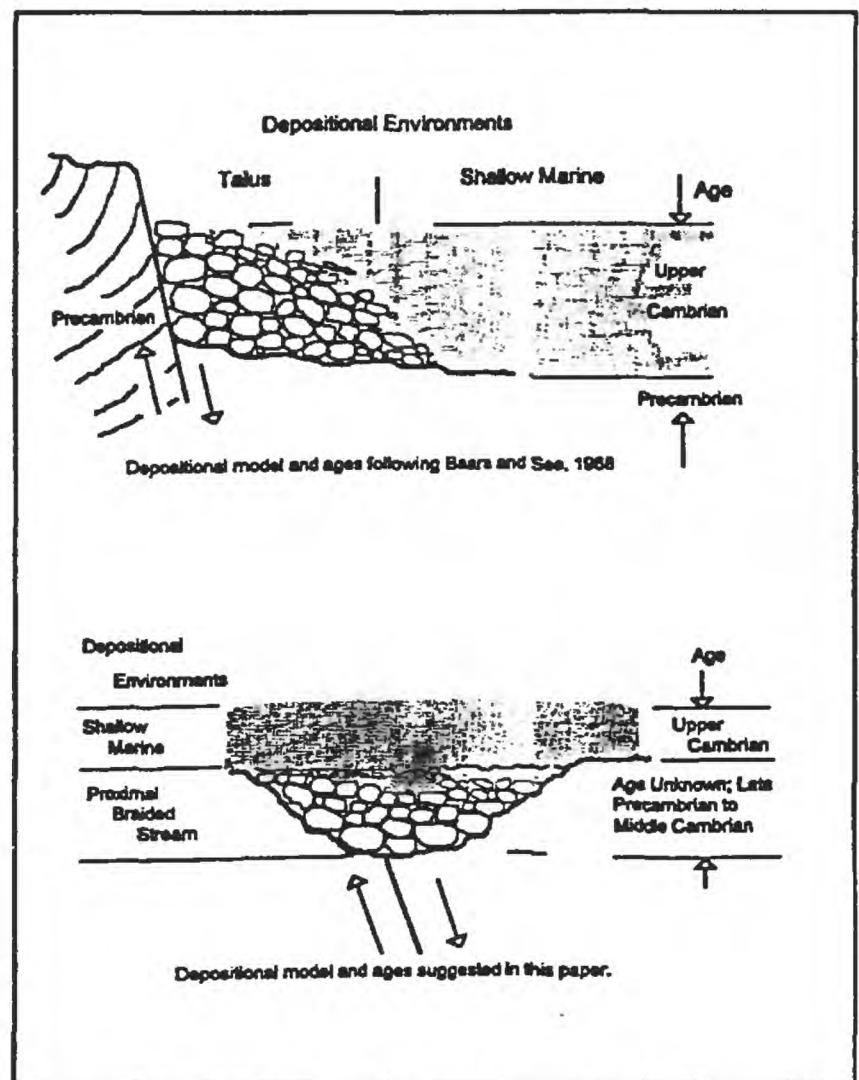


Figure 3: Two depositional models for the quartzite-clast conglomerates and the age relationships.

Source for the clasts is essentially local, no more than a few kilometers away, however, clast size and roundness suggests high energy levels and long transport. The shape of the deposits suggests channels and the deposits appear as proximal braided stream deposits. The occurrence of the outcrops suggests more than one braided stream channel draining to the west, southwest and to the south. A series of braided streams draining a highly weathered Precambrian terrain, the Transcontinental Arch, during late Precambrian or early Cambrian time is suggested. These streams may have followed preexisting faults in the western portion of the area.

APPENDIX I

U-PB ISOTOPIC DATA FOR SAMPLES OF PROTEROZOIC ROCKS IN THE NEEDLE MOUNTAINS

All analyses were performed by D.A. Gonzales at the University of Kansas, Isotope Geochemistry Laboratory.

Note: All data listed are for zircon fractions. NM(#) = nonmagnetic split collected on a Franz L-1 isodynamic magnetic separator set at angle of side tilt # of degrees and 1.5 amps. Sieve sizes are in microns; aa = air abraded fraction using the method described by Krogh (1982). Zircon dissolution followed the methods of Krogh (1973) and Parrish (1987). Elemental separation was accomplished using HBr anion column chemistry for lead and HCl column chemistry for uranium. Samples were spiked with either a mixed $^{205}\text{Pb}/^{235}\text{U}$ or $^{208}\text{Pb}/^{235}\text{U}$ spike.

Isotopic analyses were determined on a VG Sector multicollector thermal ionization mass spectrometer. Lead samples were loaded on rhenium filaments with silica gel and 0.25 M phosphoric acid (Cameron and others, 1969). Uranium samples were loaded on rhenium filaments with 0.25 M phosphoric acid and colloidal graphite. Errors on $^{206}\text{Pb}/^{204}\text{Pb}$ atomic ratios were minimized by using a Daly multiplier and are typically on the order of 1% or less. Errors for $^{206}\text{Pb}/^{204}\text{Pb}$ atomic ratios were reduced further on samples spiked with ^{205}Pb by using a dynamic Daly calibration after the technique of Roddick and others (1987, p. 115). Ages calculated using the decay constants recommended by Steiger and Jager (1977): $^{235}\lambda = 9.8485 \times 10^{-9} \text{ yr}^{-1}$, $^{238}\lambda = 1.55125 \times 10^{-9} \text{ yr}^{-1}$, and $^{238} \text{U}/^{235} \text{U} = 137.88$.

* Measured atomic ratio corrected for spike and mass fractionation only. Pb mass fractionation correction is $0.12\% \pm 0.05\%$ per amu.

† Measured atomic ratios corrected for mass fractionation, U and Pb blanks, spike, and initial common Pb. Measured analytical blanks are $< 0.1 \text{ ng}$ of Pb and $< 0.01 \text{ ng}$ for U. Initial common Pb composition is calculated from the model growth-curve of Stacey and Kramers (1975) using an interpreted age for the sample.

Ages were determined using the regression and error analysis methods of Ludwig (1980, 1993). Model 1 solutions were used if the probability of fit was greater than 20%, and Model 2 solutions were used if the probability of fit was less than 20%.

Sample Number: NMGC3

Unit: Twilight Gneiss

Lithology: trondhjemitic gneiss with quartz "eyes" (relict phenocrysts)
Location:

General Area: Lime Creek area, approximately 250 m southwest of Scout Lake

County: San Juan

7.5 Minute Topographic Quadrangle: Engineer Mountain

Longitude: 107° 46' 33"

Latitude: 37° 39' 01"

Fraction Analyzed	Weight (mg)	U (ppm)	Pb (ppm)	* 206Pb/ Pb204	Atomic Ratios				Apparent Ages (Ma)		
					†207Pb/ 206Pb	†208Pb/ 206Pb	†206Pb/ 238U	†207Pb/ 235U	206Pb/ 238U	207Pb/ 235U	207Pb/ 206Pb
1) NM(-1), -200, aa	0.090	354.9	94.2	814.9	0.107366	0.07669	0.25949	3.8413	1487.2	1601.4	1755.2
2) NM(-1), +200, aa	0.029	410.8	111.1	1057.4	0.107194	0.07437	0.26468	3.9119	1513.7	1616.2	1752.3
3) NM(0), -200, aa	0.093	558.0	132.2	3432.9	0.1073	0.07835	0.23137	3.4228	1341.6	1509.6	1754.1
4) NM(0), +200, aa	0.384	521.9	127.3	5931.8	0.107407	0.07803	0.23828	3.5288	1377.8	1533.7	1755.9
5) NM(1), -200, aa	0.175	578.6	133.3	7160	0.107234	0.08015	0.22492	3.3254	1307.8	1487	1752.9
6) NM(1), +200, aa	0.352	543.4	131.2	11263	0.107508	0.07928	0.23598	3.4980	1365.8	1526.8	1757.6
7) NM(2), -200, aa	0.2292	615.6	136.6	8793	0.107305	0.08134	0.21642	3.202	1262.9/	1457.6	1754.2

Concordia Intercepts (Ma):

REGRESSION
MODEL

LOWER

MSWD

UPPER

12.2

2

All Fractions:

1754 ± 7

5 ± 42

Sample Number: NMGC6
Unit: Bakers Bridge Granite
Lithology: potassium-feldspar phyrlic hornblende-biotite-magnetite granite
Location:
General Area: Bakers Bridge (collected fresh pieces from blasting site)
County: LaPlata
7.5 Minute Topographic Quadrangle: Hermosa
Longitude: 107° 47' 55"
Latitude: 37° 27' 31"

Fraction Analyzed	Weight (mg)	U (ppm)	Pb (ppm)	* 206Pb/ Pb204	Atomic Ratios				Apparent Ages (Ma)			
					†207Pb/ 206Pb	†208Pb/ 206Pb	†206Pb/ 238U	†207Pb/ 235U	206Pb/ 238U	207Pb/ 235U	207Pb/ 206Pb	207Pb/ 206Pb
1) NM (-1), -200, aa	0.044	189.78	72.3	159.9	0.104181	0.13412	0.29125	4.1836	1647.8	1670.8	1699.9	1699.9
2) NM (-1), +200, aa	0.678	216.4	68.1	435.8	0.103057	0.08452	0.27371	3.8893	1559.6	1611.5	1679.9	1679.9
3) NM (0), -200, aa	0.160	211.26	55.7	968.4	0.103058	0.07489	0.25432	3.6138	1460.7	1552.6	1679.9	1679.9
4) NM (0), +200, aa	2.206	269.51	83.1	350.5	0.103384	0.091585	0.25322	3.6680	1476.1	1564.4	1684.7	1684.7
5) NM (-1), +200, aa	0.152	186.6	53.9	1034.5	0.103589	0.07448	0.27820	3.9735	1582.3	1628.8	1689.4	1689.4
6) NM (0), -200, aa	0.106	242.9	63.4	1189.1	0.103169	0.07827	0.25419	3.6149	1461.3	1553.8	1681.9	1681.9
7) NM (0), +200, aa	0.330	261.4	71.2	1225.4	0.103507	0.07369	0.25924	3.6998	1486	1571.3	1687.9	1687.9
8) NM (1), -200, aa	0.055	392.5	90.1	560	0.102071	0.07534	0.21482	3.0233	1254.4	1413.5	1662.1	1662.1
9) NM (2), -200, aa	0.124	494.0	109.6	689.9	0.10161	0.09461	0.20225	2.8336	1187.4	1364.5	1653.7	1653.7

Concordia Intercepts (Ma):

	UPPER	LOWER	MSWD	REGRESSION MODEL
All Fractions:	1699 ± 7	162 ± 51	15.1	2
Fractions 2, 4, 5-9:	1696 ± 9	147 ± 63	20.7	2
Fractions 2-9:	1696 ± 8	147 ± 55	18.2	2
Fractions 1-2, 4-9:	1699 ± 8	162 ± 57	17.6	2

Sample Number: NMGC7

Unit: Eolus Granite

Lithology: potassium-feldspar phyrlic hornblende-biotite granite

Location:

General Area: Endlich Mesa; approximately 1.6 km East of Stump Lakes

County: LaPlata

7.5 Minute Topographic Quadrangle: Vallecito Reservoir

Longitude: 107° 36' 56"

Latitude: 37° 29' 40"

<u>Fraction Analyzed</u>	<u>Weight (mg)</u>	<u>U (ppm)</u>	<u>Pb (ppm)</u>	<u>*206Pb/ Pb204</u>	<u>Atomic Ratios</u>				<u>Apparent Ages (Ma)</u>			
					<u>†207Pb/ 206Pb</u>	<u>†208Pb/ 206Pb</u>	<u>†206Pb/ 238U</u>	<u>†207Pb/ 235U</u>	<u>206Pb/ 238U</u>	<u>207Pb/ 235U</u>	<u>207Pb/ 206Pb</u>	<u>206Pb/ 206Pb</u>
1) NM(0), -100, aa	0.022	378.5	91.9	2451	0.090395	0.06405	0.24004	2.9918	1386.9	1405.5	1433.9	1433.9
2) NM(1), -100, aa	0.071	611.9	136.4	3678.4	0.090397	0.06399	0.22121	2.7572	1288.3	1344	1433.9	1433.9
3) NM(1), -100, aa	0.042	597.1	132.5	6353.1	0.092527	0.06265	0.22215	2.7644	1293.2	1346	1430.9	1430.9
4) NM(1), -100, aa	0.027	609.2	141.8	4794.6	0.090397	0.06476	0.23209	2.8927	1345.4	1380	1433.9	1433.9
5) NM(2), -200, aa	0.027	468.3	106.1	7432.5	0.090391	0.06537	0.22696	2.8285	1318.5	1363.1	1433.8	1433.8
6) NM(2), +200, aa	0.073	698.4	179.9	749.9	0.090408	0.1221	0.22941	2.8597	1331.4	1371.4	1434.2	1434.2
7) NM(3), -200, aa	0.018	497.5	110.8	7335.5	0.090647	0.06387	0.22364	2.7952	1301.1	1354.3	1439.2	1439.2
8) NM(3), +200, aa	0.047	712.7	174.1	454.1	0.090293	0.06954	0.21589	2.6878	1260.2	1325.1	1431.7	1431.7

U
∞

Concordia Intercepts (Ma):

<u>UPPER</u>	<u>LOWER</u>	<u>MSWD</u>	<u>REGRESSION MODEL</u>
1435 ± 7	23 ± 112	9	2

All Fractions:

Sample Number: NMGC13
Unit: Twilight Gneiss
Lithology: tonalitic gneiss
Location:

General Area: East of Electra Lake, approximately 500 m north of Edison public parking area
County: LaPlata
7.5 Minute Topographic Quadrangle: Electra Lake
Longitude: 107° 48" 01"
Latitude: 37° 33' 29"

Fraction Analyzed	Weight (mg)	U (ppm)	Pb (ppm)	*206Pb/ Pb204	Atomic Ratios				Apparent Ages (Ma)		
					†207Pb/ 206Pb	†208Pb/ 206Pb	†206Pb/ 238U	†207Pb/ 235U	206Pb/ 238U	207Pb/ 235U	207Pb/ 206Pb
NM(-1), -100, aa	0.224	402.6	113.2	3698.9	0.107095	0.09827	0.27048	3.9939	1543.2	1633	1750.6
NM(0), - 200, aa	0.112	466.4	130.6	3671.8	0.107314	0.1022	0.26755	3.9586	1528.3	1625.7	1754.2
NM(0), + 200, aa	0.703	431.7	118.8	3010.2	0.106838	0.1048	0.26009	3.8313	1490.3	1599.3	1746.2
NM(1), - 200, aa	0.443	552.5	126.1	2325.8	0.106263	0.1116	0.21381	3.1326	1249.1	1440.7	1736.3
NM(1), + 200, aa	0.701	531.7	122.1	2444.9	0.106469	0.1085	0.21563	3.1655	1258.7	1448.8	1739.8
NM(2), - 200, aa	0.300	524.3	127.3	3840.6	0.106638	0.1079	0.23059	3.3904	1337.6	1502.2	1742.7
NM(2), + 200, aa	0.265	549.6	125.6	1973.2	0.106236	0.1109	0.21386	3.1325	1249.3	1440.7	1735.8

Concordia Intercepts (Ma):

UPPER	LOWER	MSWD	REGRESSION MODEL
1759 ± 6	88 ± 33	5.2	2

All Fractions:

Sample Number: NMGC14
Unit: Twilight Gneiss
Lithology: trondhjemitic gneiss
Location:

General Area: On "Old" Lime Creek Road approximately 1.6 km west of Scout Lake
County: San Juan
7.5 Minute Topographic Quadrangle: Engineer Mountain
Longitude: 107° 47' 05"
Latitude: 37° 39' 14"

Fraction Analyzed	Weight (mg)	U (ppm)	Pb (ppm)	* 206Pb/ Pb204	Atomic Ratios			Apparent Ages (Ma)			
					†207Pb/ 206Pb	†208Pb/ 206Pb	†206Pb/ 238U	†207Pb/ 235U	206Pb/ 238U	207Pb/ 235U	207Pb/ 206Pb
1) NM(0), - 200, aa	0.189	447.7	128.8	7009.8	0.107898	0.07975	0.28079	4.1774	1595.4	1669.6	1764.2
2) NM(0), + 200, aa	0.304	442.6	119.9	7651.9	0.107701	0.07896	0.26475	3.9315	1514.1	1620.2	1760.9
3) NM(1), - 200, aa	0.387	530.8	138.3	8019.2	0.107671	0.08347	0.25504	3.7863	1464.4	1589.8	1760.4
4) NM(1), + 200, aa	0.633	479.1	124.2	8870.8	0.107553	0.08073	0.25255	3.7452	1451.6	1581.1	1758.4
5) NM(2), - 200, aa	0.162	587.7	141.8	4320.7	0.107249	0.08423	0.23376	3.4567	1354.2	1517.4	1753.2
6) NM(2), + 200, aa	0.491	525.3	133.2	6865.8	0.107484	0.08259	0.24618	3.6483	1418.7	1560.1	1757.2

Concordia Intercepts (Ma):

UPPER	LOWER	MSWD	REGRESSION MODEL
1771 ± 3	89 ± 21	2.1	2

All Fractions:

Sample Number: NMGC16

Unit: Twilight Gneiss

Lithology: tonalitic gneiss layer (metamorphosed tonalitic sill)

Location:

General Area: Approximately 200 m north of "Old" Lime Creek Road at start of Potato Lake hiking trail

County: San Juan

7.5 Minute Topographic Quadrangle: Engineer Mountain

Longitude: 107° 46' 18"

Latitude: 37° 39' 15"

Fraction Analyzed	Weight (mg)	U (ppm)	Pb (ppm)	* 206Pb/ Pb204	Atomic Ratios			Apparent Ages (Ma)			
					†207Pb/ 206Pb	†208Pb/ 206Pb	†206Pb/ 238U	†207Pb/ 235U	206Pb/ 238U	207Pb 235U	207Pb/ 206Pb
1) NM(-2), aa	0.005	388.3	101.2	4328.3	0.106896	0.09159	0.25169	3.7096	1447.2	1573.4	1747.2
2) NM(1), aa	0.011	339.9	93.1	8254.5	0.106908	0.09458	0.26455	3.8996	1513.1	1613.6	1747.4
3) NM(3), aa	0.006	465.9	118.4	1858.1	0.1066	0.08553	0.24357	3.5797	1405.2	1545.1	1742.1

Concordia Intercepts (Ma):

UPPER	LOWER	MSWD	REGRESSION MODEL
1757 ± 7	96 ± 48	1.06	1

All Fractions:

Sample Number: NMGC17

Unit: Twilight Gneiss

Lithology: granodioritic gneiss layer (metamorphosed granodioritic dike)

Location:

General Area: Approximately 250 m north of "Old" Lime Creek Road at start of Potato Lake hiking trail

County: San Juan

7.5 Minute Topographic Quadrangle: Engineer Mountain

Longitude: 107° 46' 15"

Latitude: 37° 39' 16"

<u>Fraction Analyzed</u>	<u>Weight (mg)</u>	<u>U (ppm)</u>	<u>Pb (ppm)</u>	<u>*206Pb/ Pb204</u>	<u>Atomic Ratios</u>				<u>Apparent Ages (Ma)</u>		
					<u>t207Pb/ 206Pb</u>	<u>t208Pb/ 206Pb</u>	<u>t206Pb/ 238U</u>	<u>t207Pb/ 235U</u>	<u>206Pb/ 238U</u>	<u>207Pb/ 235U</u>	<u>207Pb/ 206Pb</u>
1) NM(0), -200, aa	0.031	738.3	187.2	976.1	0.106753	0.1056	0.23559	3.4677	1363.7	1519.9	1744.7
2) NM(0), +200, aa	0.076	580.9	154.4	2160.3	0.107161	0.09392	0.25376	3.7495	1457.9	1582	1751.7
3) NM(1), -200, aa	0.032	953.5	229.9	1017.7	0.105925	0.1259	0.21971	3.2088	1280.3	1459.3	1730.4
4) NM(1), +200, aa	0.094	597.1	157.4	1799.6	0.10756	0.09825	0.24849	3.6853	1430.7	1568.2	1758.5
5) NM(2), -200, aa	0.059	1085.9	212.2	1369.4	0.105514	0.1226	0.17972	2.6146	1065.4	1304.8	1723.3
6) NM(2), +200, aa	0.119	1061.2	206.2	1719.4	0.105172	0.1127	0.1807	2.6203	1070.8	1306.4	1717.3
7) NM(3), -200, aa	0.054	1087	188.4	936.8	0.104998	0.1308	0.15591	2.2571	933.9	1199	1714.3

Concordia Intercepts (Ma):

<u>UPPER</u>	<u>LOWER</u>	<u>MSWD</u>	<u>REGRESSION MODEL</u>
1766 ± 15	115 ± 47	108	2

All Fractions:

Sample Number: NMGC21

Unit: Tenmile Granite

Lithology: potassium feldspar phyrlic biotite-hornblende granite

Location:

General Area: west side of Animas Canyon about 400 m northwest of Ruby Creek-Animas River Confluence

County: San Juan

7.5 Minute Topographic Quadrangle: Snowden Peak

Longitude: 107° 40' 58"

Latitude: 37° 39' 20"

<u>Fraction Analyzed</u>	<u>Weight (mg)</u>	<u>U (ppm)</u>	<u>Pb (ppm)</u>	<u>* 206Pb/ Pb204</u>	<u>Atomic Ratios</u>				<u>Apparent Ages (Ma)</u>		
					<u>†207Pb/ 206Pb</u>	<u>†208Pb/ 206Pb</u>	<u>†206Pb/ 238U</u>	<u>†207Pb 235U</u>	<u>206Pb/ 238U</u>	<u>207Pb 235U</u>	<u>207Pb/ 206Pb</u>
1) NM(0), -100, aa	0.032	604.3	158.2	1080.2	0.104398	0.05124	0.26075	3.7533	1493.7	1582.8	1703.7
2) NM(1), -200, aa	0.025	782.5	186.8	811	0.103799	0.05576	0.23416	3.3513	1356.3	1493.1	1693.1
3) NM(1), +200, aa	0.053	775.5	157.4	1088.4	0.10354	0.05770	0.19795	2.8259	1164.3	1362.4	1688.5
4) NM(2), -100, aa	0.082	934.6	191.5	1259.3	0.10258	0.05386	0.19969	2.8244	1173.7	1362	1671.3
5) NM(3), -200, aa	0.049	1324.2	213.1	693.7	0.100387	0.05451	0.15276	2.1144	916.4	1153.5	1631.3
6) NM(3), +200, aa	0.062	986.3	155.8	676.8	0.101285	0.05863	0.14916	2.0830	896.2	1143.2	1647.8
7) NM(4), -200, aa	0.025	1133	189.6	422.1	0.102641	0.05104	0.15524	2.1969	930.3	1180.1	1672.4
8) NM(4), -200, aa	0.026	1085.6	179.1	440.4	0.101301	0.05352	0.15363	2.1458	921.3	1163.7	1648.1

Concordia Intercepts (Ma):

	<u>UPPER</u>	<u>LOWER</u>	<u>MSWD</u>	<u>REGRESSION MODEL</u>
Fractions 1, 2, 4:	1720 ± 3	163 ± 10	1.1	1
Fraction 1, 2, 4, 5:	1719 ± 5	156 ± 15	2.2	2
Fractions 1, 2, 4, 5, 8:	1716 ± 14	140 ± 40	49.9	2
Fractions 1, 2, 4, 5, 6, 8:	1714 ± 13	130 ± 35	89.4	2
Fractions 1, 2, 4-8:	1712 ± 20	116 ± 49	196	2
Fractions 1-8:	1714 ± 18	116 ± 47	196	2

Sample Number: NMGC22

Unit: Irving Formation, southeastern Needle Mountains

Lithology: felsic schist & gneiss

Location:

General Area: Approximately 600 m northwest of first footbridge at Vallecito Creek

County: LaPlata

7.5 Minute Topographic Quadrangle: Columbine Pass

Longitude: 107° 32' 12"

Latitude: 37° 30' 56"

Fraction Analyzed	Weight (mg)	U (ppm)	Pb (ppm)	* 206Pb/ Pb204	Atomic Ratios				Apparent Ages (Ma)			
					†207Pb/ 206Pb	†208Pb/ 206Pb	†206Pb/ 238U	†207Pb/ 235U	206Pb/ 238U	207Pb/ 235U	207Pb/ 206Pb	207Pb/ 206Pb
1) NM(-1), aa	0.007	179.3	39.6	805.0	0.10765	0.002814	0.22312	3.3117	1298.3	1483.8	1760	1760
2) NM(-1), aa	0.011	220.4	38.3	937.2	0.105329	0.01021	0.17387	2.5251	1033.6	1279.3	1720.1	1720.1
3) NM(0), aa	0.004	237.2	38.6	1034.8	0.105609	0.006405	0.16547	2.4094	987.1	1245.4	1724.9	1724.9
4) NM(1), aa	0.004	139.7	37.7	415.5	0.10818	0.006732	0.25937	3.8687	1486.6	1607.2	1769	1769
5) NM(0), aa	0.001	364	108.4	613.9	0.10795	0.005621	0.30608	4.5573	1721.4	1741.2	1765.1	1765.1
6) NM(-1), aa	0.007	40.2	11.8	389.9	0.111604	0.008575	0.29169	4.4866	1650	1728.5	1824.9	1824.9

Concordia Intercepts (Ma):

	UPPER	LOWER	MSWD	REGRESSION MODEL
Fractions 1, 3, 4:	1786 ± 10	120 ± 29	0.5	1
Fractions 1, 3, 4, 5:	1785 ± 10	116 ± 28	0.9	1
Fractions 1-4:	1787 ± 26	132 ± 76	4.9	2
All Fractions:	1797 ± 48	153 ± 193	6.9	2

Sample Number: NMGC23

Unit: Irving Formation

Lithology: strongly foliated granitic sill that cuts metamorphosed basaltic rocks in the Irving Formation
Location:

General Area: West side of Forebay Lake

County: LaPlata

7.5 Minute Topographic Quadrangle: Electra Lake

Longitude: 107° 47' 27"

Latitude: 37° 31' 40"

Fraction Analyzed	Weight (mg)	U (ppm)	Pb (ppm)	* 206Pb/ Pb204	Atomic Ratios			Apparent Ages (Ma)			
					†207Pb/ 206Pb	†208Pb/ 206Pb	†206Pb/ 238U	†207Pb/ 235U	206Pb/ 238U	207Pb/ 235U	207Pb/ 206Pb
1) NM(-1), aa	0.021	1206.9	254.2	1550.7	0.105126	0.02011	0.20984	3.0416	1228	1418.1	1716.5
2) NM(0), -200, aa	0.032	1050	180.7	3710.9	0.104241	0.02008	0.17545	2.5217	1042.1	1278.3	1701
3) NM(0), +200, aa	0.077	1341	268.2	3791.2	0.104879	0.02081	0.20355	2.9435	1194.1	1392.2	1712.2
4) NM(1), -200, aa	0.056	1105.4	169.8	2282.5	0.10426	0.02007	0.15497	2.2278	928.7	1189.8	1701.3
5) NM(1), +200, aa	0.085	1222	185.6	3038.1	0.103661	0.01948	0.15434	2.2059	925.2	1182.9	1690.7
6) NM(2), -200, aa	0.055	1223.7	160.4	1322.9	0.103205	0.02073	0.12985	1.8477	786.9	1062.6	1682.6
7) NM(2), +200, aa	0.088	1234.5	167.9	1430	0.103439	0.02237	0.13483	1.9229	815.4	1089.1	1686.7

Concordia Intercepts (Ma):

	UPPER	LOWER	MSWD	REGRESSION MODEL
All Fractions:	1731 ± 10	66 ± 20	1.83	2
Fractions 1-4 & 6-7:	1731 ± 9	62 ± 7	1.83	2

Sample Number: NMGC25

Unit: Irving Formation

Lithology: felsic gneiss & schist

Location:

General Area: Head of Sawmill Canyon, east of Electra Lake

County: LaPlata

7.5 Minute Topographic Quadrangle: Electra Lake

Longitude: 107° 47' 49"

Latitude: 37° 33' 08"

Fraction Analyzed	Weight (mg)	U (ppm)	Pb (ppm)	*206Pb/ Pb204	Atomic Ratios				Apparent Ages (Ma)		
					†207Pb/ 206Pb	†208Pb/ 206Pb	†206Pb/ 238U	†207Pb/ 235U	206Pb/ 238U	207Pb/ 235U	207Pb/ 206Pb
1) NM(0), aa	0.009	476.4	96.1	2697.4	0.0984597	0.02779	0.20647	2.8029	1210	1356.3	1595.2
2) NM(1), aa	0.002	3624.6	1067.5	2033	0.108225	0.04839	0.29397	4.3866	1661.3	1709.8	1769.7
3) NM(2), aa	0.003	2304.2	680.9	997	0.108093	0.04381	0.2941	4.3832	1662	1709.2	1767.5
4) NM(2), aa	0.004	3289.5	883.6	1376.3	0.104552	0.1027	0.25486	3.6740	1463.5	1565.7	1706.4
5) NM(0), aa	0.005	1039.7	234.8	498.7	0.101267	0.06054	0.21732	3.0343	1267.7	1416.3	1647.5
6) NM(3), aa	0.001	6908.7	1705.9	1563.4	0.104031	0.04072	0.24813	3.5591	1428.8	1540.5	1697.3
7) NM(3), aa	0.096	2498	680.6	2472	0.10689	0.05120	0.26801	3.9499	1530.7	1624	1747.1

Concordia Intercepts (Ma):

UPPER	LOWER	MSWD	REGRESSION MODEL
1801 ± 6	578 ± 22	0.265	1
1803 ± 20	555 ± 71	19	2

Fractions 1-4:

All Fractions:

Sample Number: NMGC27
Unit: Electra Lake Gabbro
Lithology: Pegmatitic Gabbro
Location:

General Area: Electra Lake, Approximately 300 m SW of Ignacio Lake
County: LaPlata
7.5 Minute Topographic Quadrangle: Electra Lake, CO
Longitude: 107° 47' 55"
Latitude: 37° 34' 50"

Fraction Analyzed	Weight (mg)	U (ppm)	Pb (ppm)	*206Pb/ Pb204	Atomic Ratios				Apparent Ages (Ma)			
					†207Pb/ 206Pb	†208Pb/ 206Pb	†206Pb/ 238U	†207Pb/ 235U	206Pb/ 238U	207Pb/ 235U	207Pb/ 206Pb	207Pb/ 206Pb
					MSWD	REGRESSION MODEL	UPPER	LOWER	MSWD	REGRESSION MODEL	UPPER	LOWER
1) NM (-1), +200, aa	0.066	260.2	65.9	7451.1	0.090385	0.1314	0.23969	2.9871	1385.1	1404.3	1433.7	1433.7
2) NM (0), -200, aa	0.013	235.2	61.8	810.9	0.090478	0.1186	0.23831	2.9729	1377.9	1400.7	1435.6	1435.6
3) NM (0), +200, aa	0.061	300.4	72.8	2542	0.090239	0.1203	0.22806	2.8376	1324.3	1365.5	1430.6	1430.6
4) NM (1), +200, aa	0.047	306.2	78.7	9830.9	0.090401	0.1332	0.24337	3.0335	1404.2	1416.1	1434	1434
5) NM (-1), -200, aa	0.014	312.4	76.5	11608	0.090535	0.1018	0.23855	2.9778	1379.1	1402	1436.8	1436.8
6) NM (-1), +200, aa	0.060	276.3	70.5	41651	0.090355	0.1289	0.243	3.0273	1402.3	1414.5	1433	1433
7) NM (0), -200, aa	0.048	353.2	85.7	11508	0.090336	0.1109	0.23429	2.9182	1356.9	1386.6	1432.7	1432.7
8) NM (0), +200, aa	0.103	277.8	70.7	22847	0.090418	0.1194	0.24415	3.0437	1408.2	1418.7	1434.4	1434.4
9) NM (-1), -200, aa	0.059	300.2	75.7	23465	0.090400	0.1203	0.24402	3.0416	1407.6	1418.1	1434	1434
10) NM (0), -200, aa	0.019	347.9	87.9	3755.1	0.090431	0.1223	0.23996	2.9919	1386.5	1405.6	1434.7	1434.7
11) NM (1), -200, aa	0.009	326.5	80.7	3822.9	0.090383	0.1232	0.23637	2.9456	1367.8	1393.7	1433.6	1433.6
12) NM (2), -200, aa	0.022	437.6	95.7	2892.1	0.090312	0.1201	0.20681	2.5753	1211.8	1293.6	1431.1	1431.1
13) NM (2), +200, aa	0.088	314.6	70.7	6259.8	0.090249	0.1266	0.21323	2.6533	1246	1315.6	1430.8	1430.8

Concordia Intercepts (Ma):

UPPER	LOWER	MSWD	REGRESSION MODEL
1435 ± 2	31 ± 35	2.12	2

All Fractions:

Sample Number: NMGC28
Unit: Twilight Gneiss
Lithology: Tonalitic Gneiss
Location:

General Area: At Hairpin Turn on "Old" Lime Creek Road
County: San Juan
7.5 Minute Topographic Quadrangle: Engineer Mountain, CO
Longitude: 107° 45' 44"
Latitude: 37° 38' 35"

Fraction Analyzed	Weight (mg)	U (ppm)	Pb (ppm)	* 206Pb/ Pb204	Atomic Ratios				Apparent Ages (Ma)		
					†207Pb/ 206Pb	†208Pb/ 206Pb	†206Pb/ 238U	†207Pb/ 235U	206Pb/ 238U	207Pb/ 235U	207Pb/ 206Pb
1) NM(0), aa	0.081	372.1	104.8	19797	0.108021	0.09532	0.27161	4.0454	1549	1643.4	1766.3
2) NM(1), aa	0.025	529.9	140.4	10068	0.107945	0.09891	0.25444	3.7869	1461.3	1590	1765
3) NM(1), aa	0.016	494.7	140.4	3524.4	0.108053	0.10052	0.26980	4.0196	1539.8	1638.2	1766.8
4) NM(2), -200, aa	0.041	595.8	145.1	20554	0.107638	0.09669	0.23484	3.4853	1359.8	1523.9	1759.8
5) NM(2), +200, aa	0.042	513.9	132.4	18109	0.10795	0.09478	0.24869	3.7016	1431.7	1571.7	1765.1
6) NM(3), -200, aa	0.028	573.0	138.1	8113.3	0.107662	0.10201	0.23058	3.4228	1337.5	1509.6	1760.2

∞

Concordia Upper & Lower Intercepts (Ma):

UPPER	LOWER	MSDW	REGRESSION MODEL
1772 ± 4	3 ± 29	3.75	2

All Fractions:

APPENDIX II

Sm-Nd ISOTOPIC DATA FOR SAMPLES OF THE ELECTRA LAKE GABBRO

Analyses were performed by D.A. Gonzales and G.S. Siek at the University of Kansas, Isotope Geochemistry Laboratory.

Note: NM(#) or M(#) = non-magnetic or magnetic splits that were collected on a Franz L-1 isodynamic magnetic separator set at an amperage of # and side tilt of +10°. Dissolution of samples was accomplished using an HF/HNO₃ mixture in a sealed teflon bomb kept at approximately 180°C for 5-7 days. Separation of the REE group from Sr and Rb was done using standard HCl cation exchange procedures. Samarium and neodymium were separated using HDEHP-on-Teflon (Patchett and Ruiz, 1987; White and Patchett, 1984). Samples were spiked with a mixed ¹⁵⁰Nd-¹⁴⁹Sm tracer.

Isotopic analyses were determined on a VG Sector multi-collector thermal ionization mass spectrometer. Neodymium samples were loaded on single rhenium filaments with AG50W-X8 resin and 0.25M phosphoric acid; samarium samples were loaded on single Ta filaments with 0.25M phosphoric acid. Neodymium was analyzed as Nd+ using dynamic-multicollector mode with ¹⁴⁴Nd = 0.5V or 1.0V, and samarium was analyzed using static-multicollector mode at a preset voltage. Neodymium isotopic compositions are normalized to ¹⁴⁶Nd/¹⁴⁴Nd = 0.7219 and referenced to LaJolla ¹⁴³Nd/¹⁴⁴Nd = 0.511850. Epsilon values for neodymium at the time of crystallization are calculated using (¹⁴³Nd/¹⁴⁴Nd) (CHUR, 0 Ma) = 0.512638 and a (¹⁴⁷Sm/¹⁴⁴Nd) (CHUR, 0 Ma) = 0.1967.

Ages were determined using the regression and error analysis methods of Ludwig (1980, 1993). MSWD for the whole-rock and mineral separate isochron data are 1.6, and the probability of fit is between 18-20%. Ages were calculated using Model 1 solutions.

Reported ratios are corrected for spike, mass fractionation, and blanks.

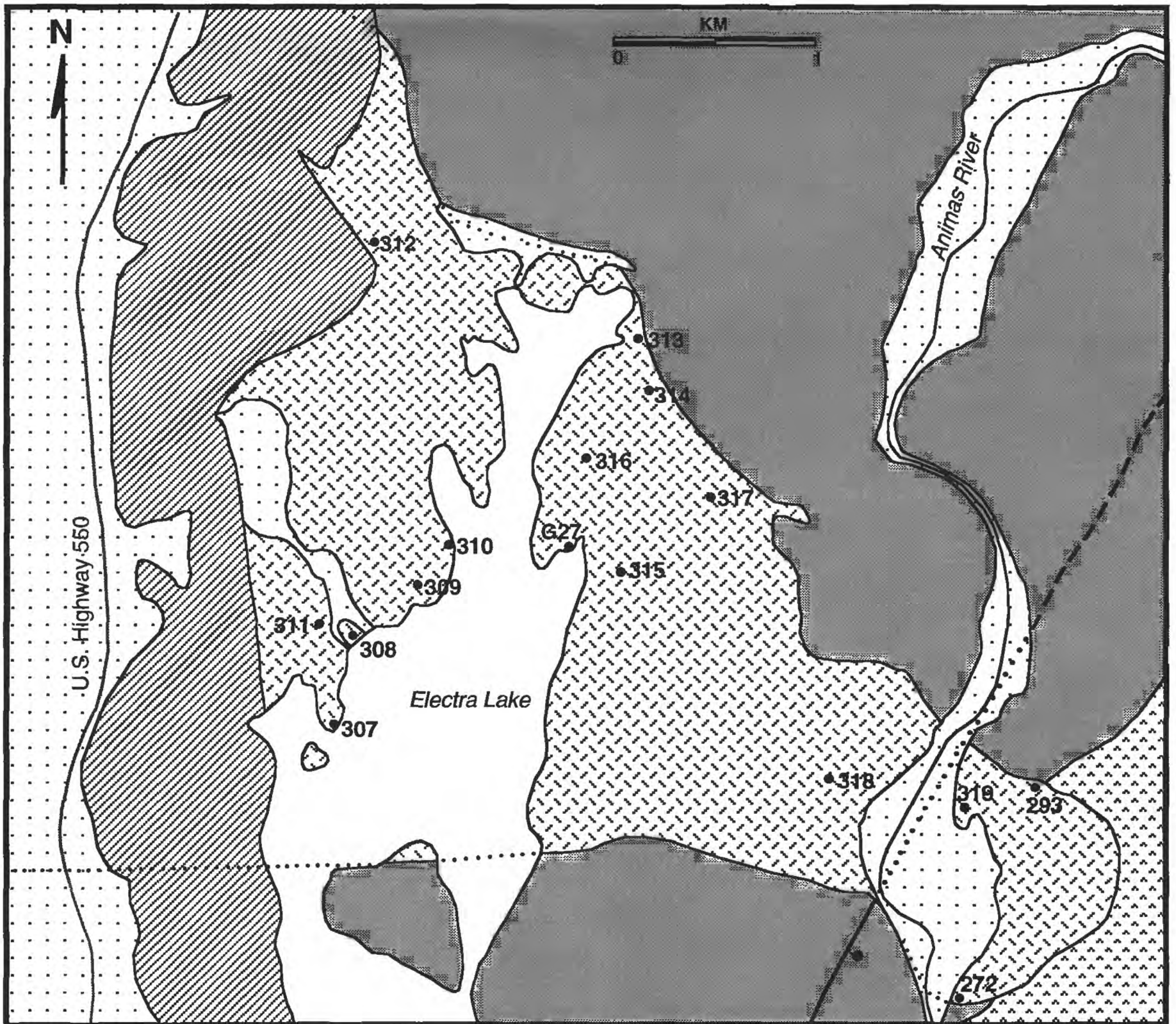
Measured analytical Nd and Sm blanks are <100 picograms.

TABLE 1
MINERAL SEPARATE Sm-Nd ISOTOPE DATA

	Sm (ppm)	Nd (ppm)	$\frac{147\text{Sm}}{144\text{Nd}}$	% 2 σ error	$\frac{143\text{Nd}}{144\text{Nd}}$	% 2 σ error
SAMPLE 316						
M(0.3) Pyroxene	1.64	4.90	0.20219	1.10	0.512810	0.0020
M(0.4) Pyroxene	1.11	3.32	0.20200	1.09	0.512824	0.0023
M(0.5) Pyroxene	2.76	8.33	0.20048	1.07	0.512774	0.0020
NM(1.5) Plagioclase	0.50	3.69	0.08144	1.10	0.511658	0.0066
Mineral Separate & Whole-Rock Age: $t = 1450 \pm 41$ Ma						
Initial $^{143}\text{Nd}/^{144}\text{Nd} = 0.510879$ ($\epsilon_{\text{Nd}(t)}$ relative to CHUR = 2.3)						
SAMPLE 318						
M(0.1) Pyroxene	4.07	14.52	0.16950	1.03	0.512501	0.0018
M(0.3) Pyroxene	3.37	11.14	0.18275	1.14	0.512646	0.0014
M(0.5) Pyroxene	12.59	46.23	0.16468	1.06	0.512442	0.0020
NM(1.5) Plagioclase	1.10	7.87	0.08480	2.11	0.511724	0.0024
Mineral Separate & Whole-Rock Age: $t = 1425 \pm 30$ Ma						
Initial $^{143}\text{Nd}/^{144}\text{Nd} = 0.510920$ ($\epsilon_{\text{Nd}(t)}$ relative to CHUR = 2.5)						

TABLE 2
WHOLE ROCK Sm-Nd ISOTOPE DATA

<u>Sample</u>	<u>Sm</u> (ppm)	<u>Nd</u> (ppm)	$^{147}\text{Sm}/$ ^{144}Nd	$\% 2 \sigma$ <u>error</u>	$^{143}\text{Nd}/$ ^{144}Nd	$\% 2 \sigma$ <u>error</u>	$\epsilon_{\text{Nd}(t)}$ ($t = 1435 \text{ Ma}$)	<u>T_{DM}</u> (Ma)
272	2.77	11.02	0.15132	1.06	0.512362	0.0052	2.89	1672
293	3.43	13.16	0.15757	1.06	0.512362	0.0020	1.95	1842
307	5.92	26.99	0.13262	1.03	0.512109	0.0018	1.51	1751
308	5.76	24.35	0.14304	1.02	0.512240	0.0024	2.15	1726
309	10.41	47.05	0.13372	1.02	0.512125	0.0020	1.62	1745
310	10.60	52.78	0.12140	1.05	0.511989	0.0022	1.25	1736
311	6.29	28.44	0.13367	1.03	0.512088	0.0018	0.92	1813
312	0.50	2.26	0.132690	1.11	0.512180	0.0043	2.90	1618
313	3.17	12.80	0.14987	1.03	0.512277	0.0030	1.61	1822
314	2.73	11.67	0.14144	1.06	0.512221	0.0020	2.08	1727
315	2.21	9.79	0.13657	1.11	0.512179	0.0018	2.15	1702
316	1.17	4.75	0.149110	1.09	0.512299	0.0023	2.30	1749
317	0.95	4.28	0.13487	1.06	0.512151	0.0105	1.91	1720
318	3.07	13.94	0.13323	1.06	0.512171	0.0018	2.61	1647
319	1.73	6.83	0.15281	1.10	0.512334	0.0022	2.18	1768



EXPLANATION

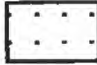

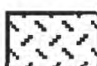
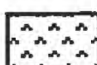


-  QUATERNARY ALLUVIUM
-  PALEOZOIC SEDIMENTARY ROCKS
-  ELECTRA LAKE GABBRO
-  EOLUS GRANITE
-  TWILIGHT GNEISS
-  318 SAMPLE LOCATIONS

Figure 17: Generalized geologic map showing the locations of samples listed in Appendix II, Tables 1 and 2.

References Cited

- Aleinikoff, J.N., Reed, J.C., Jr., and Wooden, J.L., 1993, Lead isotopic evidence for the origin of Paleo- and Mesoproterozoic rocks of the Colorado Province, U.S.A.: *Precambrian Research*, v. 63, p. 97-122.
- Baars, D.L., and Knight, 1957, Pre-Pennsylvanian Stratigraphy of the San Juan Mountains, Colorado, *in* Brewster, Baldwin., ed., *Guidebook of southwestern San Juan Mountains*, New Mexico Geological Society Eight Field Conference, 258 p.
- Baars, D.L., 1966, Pre-Pennsylvanian paleotectonics, Paradox Basin, *American Association of Petroleum Geologists Bulletin*, v. 50, no. 10, p. 2082-2111.
- Baars, D.L., and See, P.D., 1968, Pre-Pennsylvanian stratigraphy and paleotectonics of the San Juan Mountains, southwestern Colorado, *Geological Society of America Bulletin*, v. 79, no. 3, p. 333-350.
- Barker, F., 1969, Precambrian geology of the Needle Mountains: U.S. Geological Survey Professional Paper 644-A, 35 p.
- Barker, F., Peterman, Z.E., and Hildreth, R.A., 1969, A Rb/Sr study of the Twilight Gneiss, West Needle Mountains, Colorado: *Contributions to Mineralogy and Petrology*, v. 23, p. 271-282.
- Barker, F., and Peterman, Z.E., 1974, Bimodal tholeiitic-dacitic magmatism and the Early Precambrian crust: *Precambrian Research*, v. 1, p. 1-12.
- Barker, F., Peterman, Z.E., and Friedman, I., 1976, The 1.7-1.8 b.y. old trondhjemites of southwestern Colorado and northern New Mexico; geochemistry and depth of genesis: *Geological Society of America Bulletin*, v. 87, p. 189-198.
- Bickford, M.E., Barker, F., Wetherill, G.W., and Lee-Hu, C., 1968, Geochronology of Precambrian rocks of the Needle Mountains, southwestern Colorado: Part II: Rb-Sr results: *Geological Society of America Special Paper 115-Abstracts for 1967*, p. 14.
- Bickford, M.E., Wetherill, G.W., Barker, F., and Lee-Hu, C., 1969, Precambrian Rb-Sr chronology in the Needle Mountains, southwestern Colorado: *Journal of Geophysical Research*, v. 74, no. 6, p. 1660-1676.
- Bickford, M.E., and Boardman, S.J., 1984, A Proterozoic volcano-plutonic terrane, Gunnison and Salida areas, Colorado: *Journal of Geology* v. 92, no. 6, p. 657-666.
- Bickford, M.E., Shuster, R.D., and Boardman, S.J., 1989, U-Pb geochronology of the Proterozoic volcano-plutonic terrane in the Gunnison and Salida areas, Colorado, *in* Grambling, J.A., and Tewksbury, B.J., *Proterozoic geology of the southern Rocky Mountains: Geological Society of America Special Paper 235*, p. 33-48.
- Bickford, M.E., and Anderson, J.L., 1993, Middle Proterozoic magmatism, *in* Reed and others, eds., *Precambrian: Conterminous U.S.*; Geological Society of America, Inc., *The Geology of North America*, Boulder, Colorado, volume C-2, p. 281-292.

- Boardman, S.J., and Condie, K.C., 1986, Early Proterozoic bimodal volcanic rocks in central Colorado, U.S.A., Part II: Geochemistry, petrogenesis, and tectonic setting: *Precambrian Research*, v. 34, p. 37-68.
- Boardman, S.J., 1986, Early Proterozoic bimodal volcanic rocks in central Colorado, U.S.A., Part I: Petrography, stratigraphy and depositional history: *Precambrian Research*, v. 34, p. 1-36.
- Burns, L.K., Ethridge, F.G., Tyler, N., Gross, A.S., and Campo, A.M., 1980, Geology and uranium evaluation of the Precambrian quartz pebble conglomerates of the Needle Mountain, southwest Colorado: National Uranium Evaluation, U.S. Department of Energy Report GJBX-118 (80), 161 p.
- Cameron, A.E., Smith, D.H., and Walker, R.L., 1969, Mass spectrometry of nanogram-size samples of lead: *Analytical Chemistry*, v. 41, p. 525-526.
- Condie, K.C., and Nuter, J.A., 1981, Geochemistry of the Dubois Greenstone succession: An early Proterozoic bimodal volcanic association in west-central Colorado: *Precambrian Research*, v. 15, p. 131-155.
- Condie, K.C., 1982, Plate-tectonics model for Proterozoic continental accretion in the southwestern United States: *Geology*, v. 10, p. 37-42.
- Condie, K.C., 1986, Geochemistry and tectonic setting of Early Proterozoic supracrustal rocks in the southwestern United States: *Journal of Geology*, v. 94, p. 845-864.
- Condie, K.C., and Knoper, M.W., 1986, Geology and origin of Early Proterozoic rocks from the Gunnison area, central Colorado, *in* Van Schmus, W.R., ed., *Proterozoic geology and geochemistry*, Guidebook for International Field Conference on Proterozoic Geology and Geochemistry: University of Kansas, p. 3-16.
- Conway, C.M., 1976, Petrology, structure, and evolution of a Precambrian volcanic and plutonic complex, Tonto Basin, Gila County, Arizona: Pasadena, California Institute of Technology, Ph.D. thesis, 460 p.
- Conway, C.M., 1991, Tectonomagmatic settings of Proterozoic metallogenic provinces in the southwestern United States, *in* Good, E.E., Slack, J.F., and Kotra, R.K., eds., *U.S.G.S. Research on Mineral Resources - 1991 Programs with Abstracts*, Seventh Annual V.E. McKelvey Forum on Mineral and Energy Resources: U.S. Geological Survey Circular 1062, p. 9-10.
- Conway, C.M., Karlstrom, K.E., Wrucke, C.T., and Silver, L.T., 1987, Tectonic and magmatic contrasts across a two-province boundary in central Arizona, *in* Davis, G.H., and VandenDolder, E.M., eds., *Geologic diversity of Arizona and its margins: Excursions to choice areas (Field Trip Guidebook, 100th Annual Meeting, Geological Society of America)*: Arizona Bureau of Geology and Mineral Technology Special Paper 5, p. 158-175.
- Conway, C.M., Silver, L.T., Wrucke, C.T., and Gonzales, D.A., 1994, Progress in understanding the boundary between the Yavapai and Mazatzal provinces, southwestern U.S.A.: *Geological Society of America Abstracts with Programs*, v. 26, no. 6, p. 9.

- Cross, W., Howe, E., Irving, J.D., and Emmons, W., 1905, Description of the Needle Mountains quadrangle, Colorado: U.S.G.S. Atlas of the United States, Folio 131, 14 p.
- Cross, W., and Hole, A.D., 1910, Description of the Engineer Mountain quadrangle, Colorado: U.S.G.S. Atlas of the United States, Folio 171, 14 p.
- Collier, J.D., 1989, Mid-Proterozoic postorogenic granites, and associated uranium mineralization of the Needle Mountains, southwestern Colorado, *in* Grambling, J.A., and Tewksbury, B.J., Proterozoic geology of the southern Rocky Mountains: Geological Society of America Special Paper 235, p. 75-85.
- DePaulo, D.J., 1981, Neodymium isotopes in the Colorado Front Range and crust-mantle evolution in the Proterozoic: *Nature*, v. 291, p. 193-196.
- Ellingson, J.A., Gonzales, D.A., and Ruiz, L.N., 1982, The Irving Formation and the Proterozoic sequence in the Needle Mountains, southwestern Colorado: Geological Society of America Abstracts with Programs, v. 14, no. 6, p. 311.
- Ethridge, F.G., Noel, N., and Burns, L.K., 1984, Sedimentology of a Precambrian quartz-pebble conglomerate, southwest Colorado, *in* Koster, E.H., and Steel, R.J., eds., Sedimentology of gravels and conglomerates: Canadian Society of Petroleum Geologists, Memoir 10, p. 165-174.
- Fahrig, W.F., 1987, The tectonic settings of continental mafic dyke swarms: Failed arm and early passive margin, *in* Halls, H.C., and Fahrig, W.F., eds., Mafic dyke swarms: Geological Association of Canada Special Paper 34, p. 331-348.
- Fountain, J.C., Hodge, D.S., and Hills, F.A., 1981, Geochemistry and petrogenesis of the Laramie anorthosite complex, Wyoming: *Lithos*, v. 14, p. 113-132.
- Frost, C.D., Meier, M., and Oberli, F., 1990, Single crystal U-Pb zircon age determinations for the Red Mountain pluton, Laramie Anorthosite Complex, Wyoming: *American Mineralogist*, v. 75, p. 21-26.
- Gibson, R.G., 1987, Structural studies in a Proterozoic gneiss complex and adjacent cover rocks, West Needle Mountains, Colorado: Ph.D. Dissertation, Virginia Polytechnic Institute and State University, Blacksburg, Virginia, 154 p.
- Gibson, R.G., and Simpson, C., 1988, Proterozoic polydeformation in basement rocks of the Needle Mountains, Colorado: *Geological Society of America Bulletin*, v. 100, p. 1957-1970.
- Gibson, R.G., 1990, Proterozoic contact relationships between gneissic basement and metasedimentary cover in the Needle Mountains, Colorado, U.S.A.: *Journal of Structural Geology*, v. 12, no. 1, p. 99-111.
- Gibson, R.G., and Harris, C.W., 1992, Geologic map of Proterozoic rocks in the northwestern Needle Mountains, Colorado: Geological Society of America Map and Chart Series MCH075 (Map and Pamphlet), scale 1:12,000.

- Goldberg, S.A., 1984, Geochemical relationships between anorthosite and associated iron-rich rocks, Laramie Range, Wyoming: *Contributions to Mineralogy and Petrology*, v. 87, p. 376-387.
- Gonzales, D.A., and Ruiz, L.N., 1982, Proterozoic geology of the Middle Mountain area, Needle Mountains, Colorado: *Geological Society of America Abstracts with Programs*, v. 14, no. 6, p. 312.
- Gonzales, D.A., 1988a, A geological investigation of the Early Proterozoic Irving Formation, southeastern Needle Mountains, Colorado: M.S. Thesis, Northern Arizona University, Flagstaff, Arizona, 151 p.
- Gonzales, D.A., 1988b, A geological investigation of the Early Proterozoic Irving Formation, southeastern Needle Mountains, Colorado: U.S. Geological Survey, Open-File Report No. 88-660, 119 p.
- Gonzales, D.A., 1992, Geology and geochemistry of Early Proterozoic volcano-plutonic basement, southeastern Needle Mountains, Colorado: *Geological Society of America Abstracts with Programs*, v. 24, no. 6, p. 15.
- Gonzales, D.A., Van Schmus, W.R, and Conway, C.M., 1993, Interlayered granitoid gneiss and amphibolite of the Twilight Gneiss: an Early Proterozoic intrusive complex in the western Needle Mountains, southwestern Colorado: *Geological Society of America Abstracts with Programs*, v. 25, no. 1, p. 11.
- Gonzales, D.A., Siek, G.S., and Conway, C.M., 1994, The Electra Lake Gabbro: Timing and nature of Middle Proterozoic mafic plutonism in the Needle Mountains, southwestern Colorado: *Geological Society of America Abstracts with Programs*, v. 26, no. 6, p. 15.
- Harris, C.W., Gibson, R.G., Simpson, C., and Eriksson, K.A., 1986, Early to Middle Proterozoic polyphase deformation, West Needle Mountains, SW Colorado: Preliminary results: *Geological Society of America Abstracts with Programs*, v. 18, no. 5, p. 360.
- Harris, C.W., 1987, Sedimentological and structural analysis of the Proterozoic Uncompahgre Group: Ph.D. Dissertation, Virginia Polytechnic Institute and State University, Blacksburg, VA., 231 p.
- Harris, C.W., Gibson, R.G., Simpson, C., and Eriksson, K.A., 1987, Proterozoic cusped basement-cover structure, Needle Mountains, Colorado: *Geology*, v. 15, p. 950-953.
- Harris, C.W., and Eriksson, K.A., 1987, Tide-, storm-, and wave-influenced shelf sedimentation in a tectonically active intracratonic basin: the Proterozoic Uncompahgre Group, southwest Colorado: *Geological Society of America Abstracts with Programs*, v. 19, no. 5, p. 277.
- Harris, C.W., and Erickson, K.A., 1989, Allogenic controls on the evolution of storm and tidal shelf sequences in the Early Proterozoic Uncompahgre Group, southwest Colorado, USA: *Sedimentology*, v. 30, p. 189-213.
- Harris, C.W., 1990, Polyphase suprastructure deformation in metasedimentary rocks of the Uncompahgre Group: Remnant of an Early Proterozoic fold belt in southwest Colorado: *Geological Society of America Bulletin*, v. 102, p. 664-678.

- Karlstrom, K.E., Bowring, S.A., and Conway, C.M., 1987, Tectonic significance of an Early Proterozoic two-province boundary in central Arizona: *Geological Society of America Bulletin*, v. 99, p. 529-538.
- Karlstrom, K.E., and Bowring, S.A., 1993, Proterozoic orogeny of Arizona, *in* Reed and others, eds., *Precambrian: Conterminous U.S.*; Geological Society of America, Inc., Boulder, Colorado, *The Geology of North America*, volume C-2, p. 188-211.
- Knoper, M.W., and Condie, K.C., 1988, Geochemistry and petrogenesis of Early Proterozoic amphibolites, west-central Colorado, U.S.A.: *Chemical Geology*, v. 67, p. 209-225.
- Kolker, A., Lindsley, D.H., and Hanson, G.N., 1990, Geochemical evolution of the Maloin Ranch pluton, Laramie Anorthosite Complex, Wyoming: Trace elements and petrogenetic models: *American Mineralogist*, v. 75, p. 572-588.
- Krogh, T. E., 1973, A low contamination method for hydrothermal decomposition of zircon and extraction of U and Pb for isotopic age determinations: *Geochimica et Cosmochimica Acta*, v. 37, p. 485-494.
- Krogh, T.E., 1982, Improved accuracy of U-Pb ages by the creation of more concordant systems using an air abrasion technique: *Geochimica et Cosmochimica Acta*, v. 46, p. 637-649.
- Lee, K., Epis, R.C., Baars, D.L., Knapper, D.H., and Summer, R.M., 1976, Road log: Paleozoic tectonics and sedimentation and Tertiary volcanism in the western San Juan Mountains, Colorado, *in* Epis, R.C., and Weimer, R.J., eds., *Studies in Colorado field geology: Professional Contributions of Colorado School of Mines*, no. 8, p. 139-158.
- Ludwig, K.R., 1980, Calculation of uncertainties of U-Pb isotope data: *Earth and Planetary Science Letters*, v. 46, p. 212-220.
- Ludwig, K.R., 1993, ISOPLOT - A plotting and regression program for radiogenic-isotope data: version 2.70: United States Geological Survey Open-File Report 91-445, 42 p.
- Nelson, B. K., and DePaolo, D. J., 1984, 1700-Myr greenstone volcanic successions in southwestern North America and isotopic evolution of the Proterozoic mantle. *Nature*, v. 312, p. 143-146.
- Patchett, P.J., and Ruiz, J., 1987, Nd isotopic ages of crust formation and metamorphism in the Precambrian of eastern and southern Mexico: *Contributions to Mineralogy and Petrology*, v. 96, p. 523-528.
- Parrish, R.R., 1987, An improved micro-capsule for zircon dissolution in U-Pb geochronology: *Isotope Geoscience*, v. 66, p. 99-102.
- Premo, W.R., and Van Schmus, W.R., 1989, Zircon geochronology of Precambrian rocks in southeastern Wyoming and northern Colorado, *in* Grambling, J.A., and Tewksbury, B.J., *Proterozoic geology of the southern Rocky Mountains: Geological Society of America Special Paper 235*, p. 13-32.

- Reed, J.C., Jr., Bickford, M.E., Premo, W.R., Aleinikoff, J.N., and Pallister, J.S., 1987, Evolution of the Early Proterozoic Colorado province: Constraints from U-Pb geochronology: *Geology*, v. 15, p. 861-865.
- Reed, J.C. Jr., Bickford, M.E., and Tweto, O., 1993, Proterozoic accretionary terranes of Colorado and southern Wyoming, *in* Reed and others, eds., *Precambrian: Conterminous U.S.: Geological Society of America, Inc., Boulder, Colorado, The Geology of North America*, volume C-2, p. 211-228.
- Roddick, J.C., Loweridge, W.D., and Parrish, R.R., 1987, Precise U/Pb dating of zircon at sub-nanogram Pb level: *Chemical Geology*, v. 66, p. 111-121.
- Silver, L.T., and Barker, F., 1968, Geochronology of Precambrian rocks of the Needle Mountains, southwestern Colorado-Part 1, U-Pb zircon results (abs): *Geological Society of America Special Paper 115*, p. 204-205.
- Silver, L.T., Conway, C.M., and Ludwig, K.R., 1986, Implications of a precise chronology for Early Proterozoic crustal evolution and caldera formation in the Tonto Basin-Mazatzal Mountains region, Arizona: *Geological Society of America Abstracts with Programs*, v. 18, p. 413.
- Snyder, G.L., Peterman, Z.E., Frost, B.R., Grant, J.A., and Lindsley, D.H., 1988, The crust of the young earth; Guide to the Precambrian continental core in southeast Wyoming, *in* Holden, G.S., ed., *Geological Society of America Field Trip Guidebook: Colorado School of Mines Professional Contributions*, no. 12, p. 1-33.
- Stacey, J.S., and Kramers, J.D., 1975, Approximation of terrestrial lead isotope evolution by a two-stage model: *Earth and Planetary Science Letters*, v. 26, p. 207-221.
- Steiger, R.H., and Jager, E., 1977, Subcommittee on Geochronology: Convention on the use of decay constants in geo- and cosmochemistry: *Earth and Planetary Science Letters*, v. 36, p. 359-362.
- Steven, T.A., Lipman, P.W., Hail, J.W. Jr., Barker, F., and Luedke, R.G., 1974, Geologic map of the Durango quadrangle, southwestern Colorado: U.S. Geological Survey Miscellaneous Investigations Map I-764, scale 1:250,000.
- Subburayudu, G.V., 1975, The Rb-Sr isotopic composition and the origin of the Laramie anorthosite-mangerite complex, Laramie Range, Wyoming: Ph.D. Dissertation, State University of New York, 109 p.
- Tarney, J., and Weaver, B.L., 1987, Geochemistry and petrogenesis of Early Proterozoic dyke swarms, *in* Halls, H.C., and Fahrig, W.F., eds., *Mafic dyke swarms: Geological Association of Canada Special Paper 34*, p. 81-93.
- Tewksbury, B.J., 1981, Polyphase deformation and contact relationships of the Precambrian Uncompahgre Formation, Needle Mountains, southwestern Colorado: Ph.D. Dissertation, University of Colorado, 392 p.
- Tewksbury, B.J., 1982, Polyphase deformation in allochthonous rocks of the Uncompahgre Formation, Needle Mountains, southwestern Colorado: *Geological Society of America Abstracts with Programs*, v. 14, no. 6, p. 351-352.

- Tewksbury, B.J., 1984, Proterozoic Geology of the Needle Mountains, Colorado: Geological Society of America Abstracts with Programs, v. 16, no. 4, p. 257-258.
- Tewksbury, B.J., 1985, Revised interpretation of the age of allochthonous rocks of the Uncompahgre Formation, Needle Mountains, Colorado: Geological Society of America Bulletin, v. 96, p. 224-232.
- Tewksbury, 1986, Conjugate crenulation cleavages in the Uncompahgre Formation, Needle Mountains, Colorado: Journal of Structural Geology, v. 8, no. 2, p. 145-155.
- Tewksbury, B.J., 1989, Proterozoic geology of the Needle Mountains: A summary, *in* Grambling, J.A., and Tewksbury, B.J., Proterozoic geology of the southern Rocky Mountains: Geological Society of America Special Paper 235, p. 65-75.
- Tweto, O., 1987, Rock units of the Precambrian basement in Colorado: U.S. Geological Survey Professional Paper 1321-A, 54 p.
- White, W.M., and Patchett, P.J., 1984, Hf-Nd-Sr isotopes and incompatible element abundances in island arcs: Implications for magma origins and crust-mantle evolution: Earth and Planetary Science Letters, v. 67, p. 167-185.
- Wrucke, C.T., and Conway, C.M., 1987, Geologic map of the Mazatzal Wilderness and contiguous roadless areas, Gila, Maricopa, and Yavapai Counties, Arizona: U.S. Geological Survey Open-File Report 87-664, scale 1:48000.
- Wrucke, C.T., and Conway, C.M., 1993, Early Proterozoic unconformity and contrasting regional suites in central Arizona: Geological Society of America Abstracts with Programs, v. 25, p. A-48.
- Van Schmus, W.R., and others, 1993, Transcontinental Proterozoic provinces, *in* Reed and others, eds., Precambrian: Conterminous U.S.; Geological Society of America, Inc., Boulder, Colorado, The Geology of North America, volume C-2, Chapter 4, p. 171-334.